EFFECTS OF CHRONIC MORPHINE TREATMENT ON TUMOR ANGIOGENESIS AND GROWTH

A THESIS SUBMITTED TO THE FACULTY OF THE GRADUATE SCHOOL OF

THE UNIVERSITY OF MINNESOTA BY:

Lisa Koodie

IN PARTIAL FULFILLMENT OF THE REQUIREMENTS FOR THE

DEGREE OF DOCTOR OF PHILOSOPHY

Dr. Sabita Roy, PhD
Advisor

Dr. S. Ramakrishnan, PhD
Co-advisor

June 2009

Acknowledgements

I would like to express my sincere gratitude to my advisor, Dr. Sabita Roy and my co-advisor Dr. S. Ramakrishnan for all their valuable discussions, advice, patience and encouragement throughout my graduate studies which have made this work possible.

I would also like to thank my Graduate Thesis committee: Dr. Stan Thayer and Dr. Chris Pennell for their input and advice on the development of this thesis.

I am grateful to Dr. C. Campbell and Dr. R. Romero for their valuable instruction, discussions and guidance in the graduate curriculum.

I am also grateful to Dr. S. Ramakrishnan's laboratory personnel for their help and assistance with protocols and reagents. I am thankful for such a dynamic working team, my lab members. I am also very grateful to the students, office staff and other faculty members for all the discussions and advice along the way.

I also thank John Oja and Jerry Sedgewick for their assistance in imaging capturing and Dr I. Balsubramanian for her assistance and guidance.

I am also grateful for a supportive family. I extend a huge and special thank you to: my husband, mother, father and brothers, for their patience, encouragement and support during this time.

I especially thank my mother for her belief in me; her devotion and for most of all caring for my beautiful daughter, Hailey Phaedra.

Finally, I am grateful for all the financial assistance during the course of my graduate education provided by the Community of Scholars Program at the University of Minnesota, and National Institute of Drug Abuse, NIH, MD.

Abstract

Morphine is one of the most effective analgesics commonly prescribed for the treatment of severe to moderate cancer pain. To date very little is known regarding the effect of long-term morphine treatment on tumor angiogenesis. Even today, morphine is still commonly prescribed for cancer pain management as pain increases in relation to tumor size, the degree of metastasis, the type of tumor and its location. Effective morphine doses and routes of administration do vary between cancer patients. However, it is important to note that morphine is dose titrated against either analgesia or opioid related side effects. The literature reports that the daily doses used in pain management ranged from 25-2000 mg with an average of between 100-250 mg. In most cases, dose titration is frequent with both instant release and modified release morphine products. Even though adverse effects have been reported, only 4% of patients actually discontinued treatment because of intolerable adverse effects. A review of the literature indicated that the effect of morphine on tumor growth is contradictory and still inconclusive. It is therefore important to understand the effects morphine has in cancer growth and progression.

Tumor growth depends on the dynamic interplay between tumor cells, inflammatory cells, fibroblasts, endothelial cells and many other accessory cells within the tumor microenvironment. As the tumor grows, the formation of a blood supply or angiogenesis is essential. In previous studies, morphine has been shown to inhibit vascular endothelial growth factor (VEGF) secretion from mice cardiomyocytes and human umbilical vein endothelial cells. VEGF is a highly potent pro-angiogeneic molecule and we therefore predicted that morphine would also inhibit angiogenesis

associated with tumor growth. There are many sources of VEGF from within the tumor microenvironment. In the first part of these studies we investigated the effect of chronic morphine treatment on the hypoxic-angiogenic response of tumor cells. These studies show that morphine inhibits the hypoxia-induced tumor cell expression of VEGF to significantly reduce angiogenesis, and suppress tumor growth *in vivo*. Additional investigations supported the view that the effect of morphine was not due to a direct effect on tumor cell apoptosis, but instead indirectly through angiogenesis.

Angiogenesis is a complex and tightly regulated process. Tumor, stromal and inflammatory cells within the tumor microenvironment all contribute to a large pool of chemoattractants that increase the recruitment of myeloid cells from peripheral blood circulation into the tumor tissues. These cells then mature and differentiate into neutrophils, and macrophages that eventually result in a pro-inflammatory-like environment to support and maintain tumor growth. Considering that morphine is highly immuno-suppressive, that is, shown to inhibit numerous immune cell functions we hypothesized that morphine will also inhibit immune cell recruitment and thus angiogenesis. In an *in vivo* model of cell migration and recruitment we found that morphine inhibited not only CD11b+ progenitors of inflammatory cells but also the recruitment of Tie2+/CD14+ endothelial cell precursors known to actively participate in vessel formation.

Finally, when taken together our results suggest that morphine treatment can inhibit tumor cell expression of VEGF; inhibit the recruitment of bone marrow derived endothelial and inflammatory cells to the tumor microenvironment to suppress angiogenesis required for tumor growth. These studies have allowed us to further

understand the effects of a potent analgesic such as morphine in cancer growth. Although many questions remain as to the exact molecular and cellular mechanisms of morphine's actions, our data support the use of morphine for pain associated with cancer. Our results support the view that morphine may not cause any further detriment in the cancer patients' quality of life but further suppress angiogenesis associated with tumor growth and progression.

TABLE OF CONTENTS **PAGE**

TABLE OF CONTENTS

CHAPTER 1

BACKGROUND – LITERATURE REVIEW

LIST OF FIGURES PAGE

CHAPTER 1: Background – Literature Review

CHAPTER 2: Chronic morphine inhibits tumor angiogenesis and growth by suppressing HIF-1alpha and p38 MAPK activity

Chapter 1

BACKGROUND – LITERATURE OVERVIEW

I. Morphine and Tumor Growth

A. The Role of Morphine in the Cancer Pain

Management of pain is a serious problem in patients with cancer. Morphine is considered the "gold standard" for relieving pain and has been used since ancient times for pain relief (Wiffen PJ, 2007). Morphine is still being used today, and is currently one of the most effective drugs available clinically for the management of severe to moderate pain associated with cancer. Management of cancer pain may be important not only to the quality of the patients' lives but also to the cancer treatment itself. In the United States, 30-40% of newly diagnosed cancer patients and 67-90% of patients with advanced cancer report moderate to severe pain which progresses in relation to tumor size, the degree of metastasis, the type of tumor and its location (Cain DM, 2001). Relief for approximately 90% of patients with cancer-related pain involves progressing from non-opioids such as acetaminophen or ibuprofen, to weak opioids like codeine or even to stronger opioids such as morphine (World Health Organization, 1983).

Opioids modulate numerous physiological functions, including hormone secretion, neurotransmitter release, nutrition, gastrointestinal motility and respiratory depression. Effective morphine doses and routes of administration vary between cancer patients, since the dose is titrated against either analgesia or opioid-related side effects (Walsh D, 2006). In surveying the literature for morphine use in cancer pain management, the daily doses used ranges from 25-2000 mg with an average of between

100-250 mg. In most cases, the authors reported that dose titration was frequent with both instant release and modified release morphine products. Even though adverse effects were commonly reported, only 4% of patients discontinued treatment because of intolerable adverse effects (Wiffen PJ, 2007).

In order to study morphine for cancer pain management, it is important to understand cancer growth, which itself is a highly complex process involving many "players". Although cancer growth has been studied for decades, researchers worldwide still do not know the exact causes of many cancers. Research does support that the development of cancer involves the malfunction of genes governing cell growth and division. Environmental insults and genetic changes both can contribute significantly to the development of highly proliferative cancer cells. Cells that divide uncontrollably accumulate to form a solid tumor, or neoplasm. The developing tumor mass often compresses, invades and destroys the surrounding normal tissue. Generally, tumors are benign or malignant. Unlike malignant tumors, benign tumors do not metastasize. Once cancer cells begin dividing, it only takes about a seven-cell distance away from a blood supply for the actively dividing cancer cell to experience a low nutrient and reduced oxygen supply, or hypoxia. The formation of new blood vessels is an essential step required for the tumor mass to grow beyond $1mm^3$. Tumor cells deeper within the center of the developing tumor mass often experience varying levels of hypoxia, with the center-most cells experiencing anoxia, or a complete lack of oxygen (**Figure 1**). In response to hypoxia, tumor cells secrete proangiogenic factors that orchestrate blood vessel development within the tumor microenvironment (**Figure 2**). The formation of new blood

vessels from the endothelium of the preexisting vasculature is called angiogenesis (D'Amore PA, 1996)

Proangiogenic vascular endothelial growth factor (VEGF) stimulates capillary endothelial cell sprouting and tube formation (Cameron IL, 2005). Through the interaction with tumor stromal cells, new blood vessels provide the developing tumor with enough nutrients and oxygen increasing tumor cell survival and thus tumor size. Blood vessel formation also provides a route for tumor cells to escape and metastasize **(Figure 1).** Dr. Judah Folkman (1971) was first to hypothesize that tumor regression should occur once angiogenesis is inhibited. Naturally, any reduction in the tumor cells' source of nutrition should result in tumor cell starvation and death (Folkman J, 1971). Blood vessel formation, or the lack of it, is essential in both physiological processes and various pathological disease states. Therefore understanding and controlling angiogenesis in disorders such as tumor growth will be beneficial, especially to the treatment outcome.

B. Effects of Morphine on Vascular Endothelial Growth Factor and Angiogenesis

In normal human breast tissue the partial pressure of oxygen is approximately 50mmHg. The partial pressure of oxygen in breast cancer tissue is much lower and has been reported to be within the range or 3-10mmHg (Vaupel P, 2006). While anoxic cells within the tumor core may undergo necrosis, hypoxic cells initiate programmed cell death or apoptosis as they are slowly depleted of their ATP stores (Eguchi Y, 1997) Hypoxic regions within the tumor result in increased tumor cell activation of hypoxia inducible transcription factor (HIF-1). In response to hypoxia, tumor cells under the control of HIF-

1 increases the expression of one of the most potent pro-angiogenic molecule, VEGF. HIF-1 controls the hypoxia-induced transcription of VEGF resulting in increased protein translation, and secretion for new blood vessel development (D'Amore PM, 1996; Brekken RA, 2001; Semenza GL, 2001).

VEGF is one of the major pro-angiogenic growth factors known to induce vessel permeability, endothelial cell proliferation, and migration and sprouting, resulting in tumor growth, local tumor cell invasion and metastasis (**Figure 2**) (Folkman J, 1996; Ryan HE, 1998). Chronic morphine treatment inhibits hypoxia-induced VEGF secretion from mouse cardiac and human umbilical vein endothelial cells (Roy S, 2003; Balsubramanian S, 2001). To date very few studies have investigated the effects of opioids on angiogenesis—an essential process mediating tumor growth.

In a chicken chorio-allantoic model of angiogenesis, treatment with the natural opioid ligand, β-endorphin (10ug) or with morphine sulfate (5ug) was shown to independently inhibit blood vessel proliferation. These treatments on average produced shorter vessels that measured less than 50% of those in the placebo treated controls (Pasi A, 1991; Blebea J, 2000). Naltrexone, a non-specific opioid receptor antagonist was suggested as an effective cancer therapeutic (Singleton PA, 2006); therefore it is important to know whether morphine given to cancer patients for pain relief can cause any further detriment to these patients by increasing tumor angiogenesis associated with tumor growth.

C. Effects of Morphine on Tumor Growth

To date, studies investigating the effect of morphine on tumor growth have shown conflicting results. In one study, morphine sulfate administered in mice at 0.714 mg/kg per day for 15 days, followed by 1.43 mg/kg per day for up to 21 days promoted tumor growth using a breast cancer model in mice (Gupta K, 2002). In another study also using breast cancer cells, morphine administered at 10, 20, and 30 mg/kg in the first, second, and third week respectively, inhibited tumor growth through a p53 dependent mechanism (Tegeder I, 2003). Of interest, both studies used the steroid-dependent breast cancer cell line, MCF-7. This is particularly relevant since estrogen has been shown to internalize and reduce the function of the μ-opioid receptor (Micevych PE, 2003). Thus, it is difficult to determine if the effect of morphine in these studies resulted from either a direct effect of morphine or was a consequence of μ-opioid receptor down regulation. In addition, the drug dosages (sub-analgesic) and routes of administration (subcutaneous versus intra-peritoneal) varied between these studies and such factors may have contributed to the observed contradictory results.

Studies conducted on the tumor cell line, Jurkat-cells, indicate morphine can act to directly induce tumor cell apoptosis. More specifically, the apoptotic effects of morphine were attributed to effects through the FADD/p53 and anti-apoptotic PI3K/Akt pathways as well as NF-kappaB pathways (Yin D, 2006). In other studies, morphine at non-toxic concentrations (below 10nM), attenuated matrix metalloprotease (MMP-2) activity in the mouse fibrosarcoma cell line, WEHI 164 (Shariftabrizi A, 2005). Matrix metalloproteases contribute to matrix degradation and extracellular matrix remodeling during physiological and pathological angiogenesis. Chemotactic factors released from

the extracellular matrix provide an additional mechanism for the recruitment of bone marrow-derived myeloid progenitors that further exaggerate tumor growth. A remodeled matrix also facilitates endothelial cell migration and tube formation—events equally essential for successful angiogenesis (**Figure 2**).

As the tumor mass increases, the cancer patient experiences moderate to severe pain associated with for example nerve growth into the tumor. In studies conducted in mice, sciatic neurectomy reduces pain signaling from tumoral tissues, to significantly lower tumor growth and metastasis (Kurashi Y, 2001). Bone pain is another one of the most severe and common of the chronic pains that accompany breast, prostate and even lung cancers. In randomized and controlled trials, sustained-release oral morphine significantly reduced chronic lung cancer-related pain, and this was comparable to the analgesic efficacy of trans-dermal fentanyl. The frequency of nausea, vomiting, urinary retention and urticaria were insignificant between treatments and none of the patients developed hypoventilation (Oztürk T, 2008). In humans, pain-related behaviors can be significantly reduced through the administration of systemic morphine and this has been shown to be naloxone reversible (Luger NM, 2005). In another study, B16-BL6 melanoma cells were inoculated into the hind paw of B16BL/6 mice. This model successfully produced hyperalgesia and spontaneous pain-like behavior in experimental animals. Animals experienced moderate hyperalgesia around day 7 post-inoculation, and this became more severe at about day 14 post-inoculation. In these experiments, the investigators also reported morphine inhibited the moderate to severe hyperalgesia but at higher doses were often necessary to overcome the severe hyperalgesia (Kurashi Y, 2001). This is classical of morphine administration as it is a

drug where human patients often develop tolerance to morphine, requiring higher doses to produce the same effect. The high levels of morphine administered in these studies resulted in a suppression of tumor growth and metastasis. Additional studies employing repeated administration of morphine at 5-10 mg/kg daily for 6 days also showed a marked reduction in tumor growth and lung metastasis (Sasamura T, 2001). However, none of these studies investigated the effects of morphine on angiogenesis within the tumor microenvironment. Considering that morphine can inhibit VEGF secretion, which is essential for the development of angiogenesis, the major focus of the investigations presented herein, was to investigate the effect of morphine at physiologically relevant levels, such as those used in cancer pain management, on angiogenesis.

II. Role of VEGF in Angiogenesis and Tumor Growth

A. The Family of VEGF Proteins and Isoforms

Humans have a single *VEGFA* gene that contains eight exons separated by seven introns. Alternative exon splicing results in the expression of four major splice variants, called VEGF-121, VEGF165, VEGF189 and VEGF206 (Ferrara N, 2003). VEGF is described as a heparin-binding homodimeric glycoprotein of 45 kDa. VEGF121 is an acidic polypeptide, which does not bind heparin and is freely diffusible. Unlike VEGF121, the VEGF189 and 206 isoforms are quite basic and as a result bind tightly to heparin, resulting in their sequestration in the extracellular matrix. VEGF165 has both acidic and basic components and can therefore remain attached to the cell surface or

interact with the extracellular matrix (Ferrara N, 2003). Any disruptions in VEGF's heparin-binding domain can reduce its mitogenic potential. Transgenic mice with deficits in the heparin-binding domain die shortly after birth due to reduced endothelial cell distribution and filopodia formation, suggesting that the heparin binding regions are essential in vascular network formation (Ferrara N, 2003).

In addition to VEGF-A, other members of the VEGF gene family include: placental growth factor, VEGF-B, VEGF-C and VEGF-D. Of the entire family of VEGF proteins VEGF-A is the key regulator involved in blood vessel formation (**Figure 3**). However, VEGF-C and VEGF-D can regulate lymphatic angiogenesis. Decades of research support a unique role for the VEGF family of proteins in controlling the growth and differentiation of multiple anatomic components of the vascular system (**Figure 3**). In the first part of these studies we focused on the potential of hypoxia induced VEGFA expression and its contribution to tumor cell induced angiogenesis using the Lewis Lung carcinoma tumor model in Athymic mice.

B. Localization of VEGF in Tumor Growth

The clinical importance of VEGF for tumor growth is supported by the fact that most tumors secrete vascular endothelial growth factor. The inhibition of VEGF-induced angiogenesis significantly inhibits tumor growth *in vivo* (Brekken RA, 2001). The formation of new blood vessels within the tumor mass is initiated partly through the stresses of nutrient deprivation and hypoxia that are forced on the rapidly growing tumor cells. Tumor cells themselves secrete a host of factors that initiate the tube formation process. However, this is insufficient to support the developing vessels. Stromal cells

together with recruited pro-inflammatory cells further contribute to the large pool of VEGF observed within the tumor microenvironment.

VEGF supports endothelial cell proliferation and survival derived from arteries, veins and even lymphatic vessels. In 3-dimensional *in vitro* models, VEGF alone can orchestrate sprouting and tube formation of endothelial cells. In models consisting of micro-vascular endothelial cells or rat aortic rings, exposure to VEGF results in endothelial cell invasion of collagen gels and the formation of capillary-like structures similar to the formation of lumen *in vivo.* VEGF also prevents the induction of apoptosis in endothelial cells increasing their survival (Ferrara N, 2004). Hypoxia and the local concentration of VEGF secreted from tumor and stromal cells result in the up-regulation of its receptors on vascular endothelial cells within the tumor microenvironment, promoting angiogenesis and tumor growth (Brekken RA, 2001). Lee and colleagues have shown that the switching of tumor cells from the 189-isoform of VEGF-A to secretion of the 165-isoform produces larger tumors with more elaborate vessel networks. The secretion of the diffusible VEGF-165 isoform results in the recruitment of bone marrow-derived stems cells that further potentiate tumor growth (Lee TH, 2006). These results suggest that regulation of VEGF receptors on endothelial and bone marrow derived cells can further, promote tumor angiogenesis and growth (**Figure 3**).

C. Regulation of VEGF under Hypoxia

The regulation of VEGF can occur at multiple levels including, transcription, translation and post-translational protein modification. Under varying levels of oxygen, VEGF mRNA expression is rapidly and reversibly induced in both normal and

transformed cell lines. This hypoxia-induced transcription occurs mainly through the binding of an activated hypoxia-inducible transcription factor-1 (HIF-1) complex to a site-specific hypoxia response element (HRE) located in the VEGF promoter. In addition to regulation at the transcriptional level, hypoxia has also been shown to regulate a distinct subset of proteins capable of binding to the 3' un-translated region of VEGF mRNA to increase its stability (Gardner LB, 2008; Brekken RA, 2001; Ferrara N, 2004).

D. Regulation of HIF-1 under nomoxic and hypoxic conditions

Hypoxia-inducible transcription factors (HIF) are members of the family of basic helix loop-Per Arnt Sim domain-containing proteins involved in the pathophysiology of many disease states including cancer tumorigenesis and malignancy (Semenza GL, 2002). The regulatory subunits of HIF-1 are the α-subunits, HIF1α and HIF2α. Both proteins are similar in their ability to bind to the constitutively expressed β-subunit (ARNT) and form a functional HIF-1 complex with transcriptional activity (**Figure 4**). The induction of HIF-1α by hypoxia has been well studied. HIF-1 has been shown to regulate the transcription of over 70 downstream target genes. The most popular of these genes, include: glycolytic enzymes, glucose transporters (Glut1-4) and VEGF (Semenza GL, 2002).

HIF-1α regulation although complex, is tightly regulated on multiple levels: at the level of protein degradation; protein stabilization; nuclear translocation; as well as transcriptional activation. Stimulation by hypoxia results in a synergistic increase in the mechanisms activating HIF-1α, to induce maximal HIF-1 activation. Within normal physiological levels of oxygen or under normal oxygen tensions, several oxygen sensing

enzymes have been identified to regulate HIF-1α through hydroxylation at specific proline and asparagine residues located with the oxygen dependent degradation domain, the N-terminal transactivation domain and the C-terminal transactivation domains (**Figure 4**). The hydroxylation of Prolines 402/564 by the Prolyl hydroxylases 1-2 (PHDs) is required for interaction with an E3 ligase, von Hippel Landau (pVHL). PHDs require oxygen, iron and 2-oxoglutarate as co-factors for optimal enzyme function (Epstein AC, 2001). Under normal oxygen tensions, PHDs are the primary regulators of HIF degradation through the hydroxylation of the HIF-α subunits. Regions within HIF-1α's inhibitory domain have been shown to be important for the interaction of HIF-1α with another hydroxylase, specifically factor inhibiting HIF-1 (FIH-1) or aspargine hydroxylase.VHL is part of a large complex of proteins that eventually target HIF-1α for ubiquitin-mediated proteosomal degradation (**Figure 5**). The degradation of HIF-1α occurs after initiation by prolyl hydroxylases (PHDs). The VHL/E3 ligase complex recognizes this hydroxylated HIF-1α and through polyubiquitylation by the ubiquitin-conjugating enzyme E2, translocates HIF-1α to the proteasome for degradation. Studies also show this degradation of HIF-α can be inhibited at any of the aforementioned steps; either by various pharmacological inhibitors or from inactivation of genes whose products regulate the HIF system (Kaluz S, 2008).

This E3 ligase, von Hippel−Lindau (VHL) was first identified as a tumor suppressor gene involved in HIF-1-dependent hypoxic responses. In fact, HIF-1 is constitutively activated in VHL-deficient renal carcinoma cell lines due to constitutive stabilization of HIF-1α proteins. In studies where expression of pVHL is restored, constitutively stabilized HIF-1α is lost (Maxwell PH, 1999). VHL-HIF complexes form

in normoxic cells and this is essential in the regulation of the oxygen-dependent degradation of HIF-1α. During hypoxia, degradation is suppressed despite complex formation. Experts in this field contend that critical "targeting-modifications" of HIF-1α within the ODD domain cannot occur without oxygen. Interestingly, the hypoxia mimetics cobalt chloride and desferrioxamine, prevent formation of the VHL complex, suggesting that a different mechanism exists for their stabilization of HIF-1 that is seen under normoxic conditions (Maxwell PH, 1999). Ubiquitin-mediated proteosomal degradation prevents the accumulation and thus stabilization of HIF-1α seen under hypoxic conditions (**Figure 5-6**).

Oxygen is an essential cofactor for prolyl hydroxylases' activity and thus hydroxylation of HIF-1α. Naturally, in conditions where oxygen becomes rate limiting, the activity of these enzymes is reduced, resulting in marked reduction in hydroxylation of HIF-1α subunits. Un-hydroxylated HIF-1 escapes proteosomal degradation and under low oxygen tensions accumulates within the cytoplasm (**Figure 6**). The degree of observable HIF-1α protein stability or transcriptional activation varies with either the stimulus and or cell-type being examined (Bilton R, 2003). The receptor-mediated HIF-1α regulation has been well studied for the past decade. Two well characterized signaling pathways, the Ras/MEK/MAPK and PI3K/Akt/FRAP kinase cascades enhances HIF-1α protein levels and or transcriptional activation under normoxic conditions. Additionally, it has also been shown that under hypoxia, activation of the MAPK and Akt pathways synergistically enhances HIF-1α activity, suggesting that the molecular mechanisms involved must differ from those of hypoxia. The hypoxic generation of reactive oxygen

species enhances kinase activity and this can activate HIF-1α in some systems but not in others (Bilton R, 2003).

Protein detection techniques such as polyacrylamide gel electrophoresis allow HIF-1α protein visualization as it migrates as a diffuse band. This is consistent with an approximate 20kDa increase in molecular mass from its predicted size of 104kDa (Bilton R, 2003). The consensus from the scientific literature is that this broad band contains several species of phosphorylated HIF1α or species bound to VHL (Bilton R, 2003; Maxwell PH, 1999) . In supporting experiments it has been shown that phosphatase treatment can return this protein to its predicted molecular size (Richard DE, 1999).

E. Hypoxia induced MAPKs regulation of HIF-1

To date, several deletion studies have yet to identify site-specific residues, which when phosphorylated are capable of altering the hypoxic induction of HIF-1α. However, early studies showed that the phosphorylation at specific residues facilitates the binding of other co-activators for DNA transactivation in a mammalian two-hybrid system (Gradin K, 2002). Several in vitro assays have successfully demonstrated the capability of MAPK to directly phosphorylate HIF-1α. Activated recombinant or endogenous MAPK can phosphorylate either full-length HIF-1α or a C-TAD fusion product (Minet E, 2000; Richard DE, 1999; Sodhi A, 2000). One proposed function for the phosphorylation of HIF-1α is to increase its transcriptional activation (Bilton R, 2003). Another theoretical explanation for the requirement of phosphorylation during HIF-1 activation is that the phosphorylation of residues on HIF-1α, specifically within the inhibitory domain may prevent the docking of the FIH enzymes and thus hydroxylation and subsequent

protein degradation. The escape from degradation allows HIF-1α nuclear translocation for DNA binding and transactivation (Bilton R, 2003).

Many other kinases have been identified in the signaling of HIF-1 in several cell types; these include the stress kinases p38α, p38γ and JNK (Sodhi A, 2000). Depending on the cell type, the up-regulation of HIF transcriptional activity via MAPK activity can lead to increases in HIF-1α protein synthesis, protein stability and/or transcriptional activation (Bilton R, 2003). In mammalian systems, a wide range of cellular stresses and inflammatory cytokines activate the p38 mitogen-activated protein kinases (MAPKs) family. In the p38MAPK family of kinases, four members have been identified: p38α, p38β, p38γ and p38δ. These kinases have about 60% homology in their amino acid sequence but differ in their expression patterns, substrate specificities and reaction to chemical inhibitors such as SB203580.

Studies involving both *in vitro* and *in vivo* assays have supported the use of SB203580 in investigating the effects of p38 MAPK since only p38α and p38β are inhibited and the p38γ and p38δ isoforms remain unaltered. Threonine at position 106 within the ATP binding pocket of p38α and p38β MAPK isoforms, interacts with a fluorine atom in the SB203580 structure preventing ATP binding and thus their kinase activity. In contrast, the p38γ and p38δ MAPK isoforms contain a Methionine at this position, and this prevents SB203580 binding and thus inactivation (Eyers PA, 1998; Gum RJ, 1998). P38MAPK activation is involved in many aspects of cellular physiology such as in the control of cell cycle; cytoskeleton activation; normal immune and inflammatory responses; as well as in the transcriptional and translational control of pro-inflammatory cytokines (Cuenda A, 2007).

In vivo, p38 MAPKs are activated through environmental stresses and inflammatory cytokines, serum and growth factors (**Figure 7**). Together with the JNK family of protein kinases, p38 MAPKs are also known collectively as the Stress-Activated Protein Kinases (SAPKs). In knockout studies, mice lacking upstream activating components are not viable, and die in mid-gestation with defects in placenta and embryonic vasculature (Brancho D, 2003). Most of what we currently know today about the function of p38MAPK comes from experiments utilizing the specific pyridinyl imidazole inhibitors SB203580 and SB202190 (Cuenda A, 2007). SB203580 has been found to inhibit endothelial cell migration stimulated by vascular endothelial growth factor (VEGF) (Rousseau S, 1997). The roles of the four-p38 isoforms in chemotaxis have been evaluated using knockout cells derived from mice lacking the different isoforms. Only the p38α isoform is highly involved in these signals (Rousseau S, 2006).

Interestingly, p38α knockout mice are also embryonic lethal and lack embryonic vascularization. The importance of p38α in chemotaxis is related to the normal physiological functions like neutrophil migration and angiogenesis. Hypoxia activates p38α MAPK and is also increases VEGF expression (Cuenda A, 2007). The phosphorylation of HIF-1α is also necessary for HIF-1 activation. Mitrochrondrial ROS generated under hypoxia activates p38 MAPKs in mice cardiomyocytes and carcinomas. Scientific studies support a role for p38 MAPK in HIF-1α stability, phosphorylation and gene transcription in a manner distinct from anoxia (the complete lack of oxygen) or the hypoxia mimetic, desferroxamine (DFO). In p38 embryonic null fibroblasts, hypoxia-induced HIF-1α the nuclear translocation and protein stability is completely abolished. In contrast to hypoxia, anoxia or p38 embryonic null cells exposed to hypoxia mimetic,

DFO retains the ability to induce HIF-1α stability and nuclear localization for transactivation. (Minet E, 2001; Laderoute KR, 1999 ; Conrad PW, 1999; Kulisz A, 2002; Brooke ME, 2005). These results further support the view that hypoxia-signaling pathways that regulate HIF-1 are distinct from those involving other known HIF-1 stabilization factors.

In response to hypoxic stimuli p38 MAPK is directly activated in many cell systems (Conrad PW, 1999; Brooke ME, 2005). In fact, scientific studies confirm that the loss of hypoxia induced p38 MAPK through the use of myxothiazol, a mitochrondrial complex III inhibitor or glutathione peroxidase I, a scavenger of hydrogen peroxide can inhibit the hypoxia induced activation of HIF-1 (Brooke ME, 2005). Additional studies investigating the role of hydrogen peroxide on p38 MAPK show that physiological hypoxia leads to p38 phosphorylation through pathways involving the mitochrondrial electron transport chain III complex, suggesting that it is the intracellular concentration of H_20_2 or superoxide that is responsible for p38 hypoxic activation. In these studies, exogenous H_20_2, azide or ultraviolet radiation can increase ROS levels and induce p38 MAPK activation under normoxia, but the hypoxic response was not abolished in the presence of the myxothiazol or DIDS, an anion channel inhibitor that blocks the release of ROS from the mitcochrondria (Kulisz A, 2002; Khurana A, 2006). Taken together these studies further support a cell specific activation of HIF-1 through a hypoxia-induced p38 activation pathway distinct to other p38 activating stimuli.

Of great interest, the ubiquitin ligase Siah2 has been identified as a regulator of the stability of various protein substrates involved in stress and hypoxia induced responses. Of these substrates the prolyl hydroxylase-3 (PHD3) has been identified as a

key regulatory factor by Siah, capable of controlling the stability of HIF-1α more so under hypoxia than normoxia (Khurana A, 2006). PHD3 has homology to PHDs 1 and 2 but is induced and active under hypoxia only. The PHD3 gene product is a target of hypoxia-induced HIF mediated gene transcription that acts in negative feedback loop to modulate HIF-1 activity under hypoxia (Pescador N, 2005). Investigations into the activation and activity of Siah revealed that Siah is a substrate for hypoxia-induced p38 MAPK phosphorylation. This phosphorylation by p38 MAPK increases Siah2-mediated degradation of PHD3. In cells that lack the upstream activator of p38, MKK3/MKK6 Siah2 dependent degradation of PHD3 is severely impaired. In addition, phospho-mutant forms of Siah2, proteins where phosphorylation sites are mutated, also show a marked reduction in the ability to degrade PHD3, especially after hypoxia (Khurana A, 2006). Taken together these results suggest that in addition to phosphorylating HIF-1α to activate hypoxia induced HIF-1 mediated gene transcription, p38 MAPK activation is important in the regulation of specific protein substrates that function together to increase hypoxia induced HIF-1 nuclear translocation and DNA binding.

F. Activation and Role of VEGF receptors in Angiogenesis

Most of the effects of VEGF occur through the binding and activation of two distinct receptor tyrosine kinase receptors, called vascular endothelial growth factor receptor-1 (VEGFR1/FLT1) and vascular endothelial growth factor receptor-2 (VEGFR2/FLK1/KDR) (**Figure 3**). VEGFR-1 and VEGFR-2 are expressed on the cell surface of most endothelial cells but VEGFR-3 is largely restricted to lymphatic endothelial cells. VEGF-A is capable of binding both VEGFR-1 and VEGFR-2, while

placenta like growth factor (PLGF) and VEGF-B interact only with VEGFR-1 (**Figure 3**).

Even though VEGF-C and VEGF-D are capable of binding VEGFR-2 and VEGFR-3, VEGFR-2 is the major mediator of endothelial cell, proliferation, differentiation and survival, as well as microvascular permeability, vascular tone, and the production of vasoactive substances (Ferrara N, 2004). Upon ligand binding, phosphorylation of these receptor tyrosine kinases, allow the receptor to associate with and activate a wide range of intracellular signaling molecules, including phosphatidyl-inositol 3-kinase (PI3K), Shc, Grb2, and the phosphatases SHP-1 and SHP-2. Other downstream components include the activation of the MAPK cascade via Raf stimulation leading to gene expression and cell proliferation. Activation of PI3K after VEGFR activation also leads to PKB activation to increase cell survival. VEGF receptor signaling can also activate PLC-g leading to changes in cell proliferation, vaso-permeability, and angiogenesis (Brekken RA, 2001).

In contrast to VEGFR-2, VEGFR-1 does not produce effective mitogenic signal for endothelial cells; but during early embryonic development has inhibitory roles through the sequestration of VEGF to prevent its interaction with VEGFR-2. More importantly, VEGFR-1 has been shown to have important signaling roles involved in monocyte, hematopoietic stem cell and leukemic cell chemotaxis. VEGFR-1 is expressed not only in endothelial cells but also in cells of the monocyte and macrophage-lineages. In adult hood, VEGFR-1 seems to have a positive role through modulation of signals involving tyrosine kinase-activity (Shibuya, 2006). Studies involving VEGFR-1 show that it promotes tumor growth, metastasis and inflammation. In experiments using FLT1

null bone marrow cells, loss of FLT signaling significantly decreased both tumor growth and vessel formation within glioma xenografts. Vascular endothelial growth factor secretion by tumor cells increases the infiltration and accumulation of VEGFR-1 expressing bone marrow-derived myeloid cells within tumor tissues (Kerber M, 2008).

Transgenic mouse models and analysis of human tumor biopsies revealed that these bone marrow-derived myeloid cells, such as macrophages, neutrophils, eosinophils, mast cells and dendritic cells, all contribute to the formation and maintenance of blood vessels in tumors (Murdoch C, 2008; Shibuya, 2006; Shojaei F, 2008). Initially, these inflammatory cells are all attracted to the tumor microenvironment, at which point they begin mounting an immune response against the cancer cells. For example, the activation of T cells through the interaction of bone marrow-derived myeloid cells can promote tumor cell death (Lamagna C, 2006). Eventually, tumor cells down regulate self-expression of MHC-Class I molecules and escape immune surveillance, further disrupting the balance between cell death and growth. Tumor associated macrophages and infiltrating macrophages through distinct signaling mechanisms develop a pro-inflammatory-like phenotype and can both contribute independently to tumor growth by enhancing tumor cell proliferation. Tumor associated macrophages can also secrete growth factors that alter endothelial cell behavior promoting angiogenesis.

III. Leukocyte Recruitment to the Tumor Microenvironment

A. Mechanisms involved in Leukocyte recruitment

The immune system appears to have a dual function in angiogenesis. While on one hand they are able to recognize and reject tumor cells, they can also be recruited and become "enslaved" by tumor cells to increase tumor growth and survival (Noonan DM, 2008). In addition to highly proliferative tumor cells, the tumor microenvironment is a rich source of endothelial cells, fibroblasts, inflammatory cells and extracellular matrix molecules. The tumor microenvironment is often described as a highly pro-inflammatory environment. Here, cells of the innate immune system often suppress adaptive immunity and have a reduced ability to destroy tumor cells. Together with a subset of myeloid cells, they also facilitate tumor growth through the secretion of pro-angiogenic factors (Shojaei F, 2008; Nyberg P, 2008).

In addition to tumor cells, inflammatory cells are a significant source of vascular endothelial growth factor within the tumor microenvironment and have a multifaceted role in the development of angiogenesis. Currently, there are two major mechanisms known to contribute to pathological angiogenesis. The hypoxic tumor cells may initiate the angiogenic process, but many other cells support and maintain blood vessel formation. On one hand, it is hypothesized that vessel formation occurs primarily through the recruitment of stem cell-like endothelial progenitors recruited from the bone marrow. Once within the tumor microenvironment these cells differentiate and de-differentiate into mature endothelium or pro-inflammatory cells. On the other hand, investigators argue that the "differentiation into endothelium is a rare event and may never occur".

Other investigators support that it is the recruited inflammatory cells that secrete a host of angiogenic factors and it is this pro-inflammatory-like-response that promotes tumor growth *in vivo* (Shibuya M, 2006). Whatever the exact mechanism, there is no denying that these endothelial and inflammatory precursors both share overlapping cell surface markers, and may actually be similar cells whose fate is decided once at the tumor microenvironment (**Figure 8, 9**).

B. Physiological Response to Tumor Growth

To date, several lines of investigation have validated the hematopoietic systems' contribution to angiogenesis. In adult rodents, the bone marrow is the major site of hematopoeisis, followed by the spleen (Cotterell SEJ, 2000). As in the case of tumor growth, changes in the distribution of hematopoietic activity in the tissues do occur and as a result increase hematopoietic cell recruitment. The tumor microenvironment recruits bone marrow cells through the peripheral circulation (**Figure 8, 9**). In experimental models of murine infection, the spleen is also highly involved in hematopoeisis. Normally, the spleen filters out foreign organisms and old red blood cells from the bloodstream for destruction. Phagocytic cells then engulf and destroy bacteria, parasites and debris. During embryonic development and up to the end of fetal life, the spleen is the primary organ that manufactures red blood cells. After birth the bone marrow assumes this function. Whenever bone marrow breakdown occurs or becomes mobilized as in tumor growth, the spleen reverts to its fetal function and can act as a blood reservoir. The spleen also breaks down red blood cells in an effort to increase the number circulating of blood leukocytes (Cotterell SEJ, 2000).

Extensive work has already been done to identify infiltrating and recruited cells within the tumor microenvironment. The identification and role these cells play to either support or inhibit tumor growth is already well established. **Figure 9** depicts the cells found predominantly within the tumor microenvironment. These cells have been positively identified through the expression of cell surface markers as: mast cells, eosinophils, neutrophils, dendritic cells, m1/m2 polarized macrophages, hemangiocytes, Tie-2 expressing monocytes and a subset of myeloid derived suppressor cells (Murdoch C, 2008). Leukocytes and peripheral blood monocytes within the tumor microenvironment have been shown to enhance tumor progression by increasing cancer cell growth and spreading, angiogenesis and immuno-suppression (Sica A, 2008; Bosco MC, 2006). Hypoxic areas within tumor sites stimulate the recruitment of inflammatory cells into the tumor microenvironment through the migration and differentiation of monocyte derived peripheral blood cells (Bosco MC, 2006). These mononuclear phagocytes or primary monocytes often accumulate in large numbers at hypoxic areas where they terminally differentiate into inflammatory and tumor-associated macrophages or myeloid derived dendritic cells. Extensive work from several independent groups has demonstrated that hypoxia can mediate changes in mononuclear phagocyte gene expression and functional properties under different pathologic situations. Oxygen availability is a critical regulator of their functional behavior since hypoxia increases the expression of chemokine genes similar to those active on neutrophils. Current research strongly supports a role of mononuclear phagocytes at various differentiation stages as regulators of angiogenesis, pro-inflammatory cytokines, receptors and other inflammatory mediators mediating tissue neo-vascularization and cell activation (Bosco

MC, 2006). Angiogenesis occurs in several physiological and pathological conditions, such as embryo development and wound healing, diabetic retinopathy and tumors. Inflammatory monocytes-macrophages, T lymphocytes and neutrophils all actively participate in the angiogenic process through the secretion of cytokines that alter endothelial cell proliferation, migration and activation for blood vessel formation (Naldini A, 2005).

C. Myeloid Derived Suppressor Cells

Myeloid-derived suppressor cells closely associate with the tumor cells and are very active within the tumor microenvironment. These cells exhibit some level of immuno-suppression as they inhibit the tumor-specific lymphocyte responses and promote angiogenesis. These comprise of immature neutrophils, monocytes, macrophages, granulocytes and myeloid-derived dendritic cells. They exhibit a high level of plasticity and are capable of differentiating into macrophages, granulocytes and dendritic cells *in vitro*. In both humans and animal models with large tumors, myeloid-derived suppressor cell numbers significantly increases in the spleen and bone marrow. Experimental evidence supports their ability to also suppress the anti-tumor activity of NK cells and inhibit DC maturation. They have been identified as CD11b+ and Ly6G+ (also known as Gr1+), but also express F4/80, CXCR2 and CCR2 (chemokine receptors). Studies using Lewis Lung carcinoma tumors show that up to 5% of total cells within experimental tumors are these myeloid-derived suppressor cells. They may also contribute to tumor progression through the secretion of matrix proteases that further increases VEGF bioavailability (Noonan DM, 2008; Murdoch C, 2008).

D. Neutrophils

Classically, pathogen stimulation results in the rapid recruitment and sacrifice of neutrophils. Neutrophils are phagocytes capable of producing damaging oxidative radicals for tumor cell destruction. More recently, neutrophils have been recognized as an important contributor of pathological angiogenesis. Within the endometrium, vessel-associated neutrophils are the major source of VEGF, and their dysregulation can lead to excessive angiogenesis in endometriosis. In studies that involve neutrophil depletion or loss of function, angiogenesis, cancer growth and progression is significantly reduced (Noonan DM, 2008; Shibuya M, 2006). To date, several chemo-attractants have been identified in the trafficking of neutrophils. CXC-chemokines (example, monocyte-inflammatory proteins, MIP/CXCL8/IL-8/KC) secreted from human and mouse-derived tumor cells, stromal cells or inflammatory cells mediate chemotaxis of neutrophils, lymphocytes and monocytes. In one recent study, it was observed that CXCL8 production from cancer cells significantly enhanced CXCL12 secretion by fibroblasts. CXCL12 and CXCL8 were shown to enhance endothelial cell tube formation but not cancer cell proliferation and invasion (Matsuo Y, 2009).

Mature neutrophils and progenitors alike are commonly identified within the tumor microenvironment as Ly6G+/CD11b+ double positive cells (Shojaei F, 2008; Murdoch C, 2008). Once at the tumor site, neutrophils secrete MMP-9, one of many matrix metalloproteases present within the tumor microenvironment that result in the further release of potent chemotactic molecules. This gradient further sustains the recruitment of bone marrow progenitors to the tumor microenvironment. Together with neutrophils (early phase), Kobayashi and colleagues found that monocytes (late phase),

and macrophages but not dendritic cells have the ability to engulf irradiated leukemic cells from the peritoneal cavity. They also found that neutrophils and monocytes but not macrophages are effective at migrating from sites of inflammation and to secondary lymphoid tissues (parathymic lymph nodes), the blood and then spleen. These monocytes were either Ly6G +/- and some also express CD11c+ also found on myeloid derived dendritic cells (Terasawa M, 2008). These results suggest that in addition to immature dendritic cells, both neutrophils and monocytes are potent antigen presenting cells capable of presenting tumor antigens and stimulating naïve T-cells for tumor cell rejection.

E. Macrophages

Macrophages often make up to a significant proportion of the leukocytes that infiltrate the tumor microenvironment (Bingle L, 2002). Together with monocytes, monocyte derived macrophages also express the integrin CD11b+ (MAC-1) that bind to CD31/ICAM-1 on activated endothelium, mediating firm adhesion to the vascular endothelium for extravasation into the tissue (**Figure 10**) (Vainer B, 2000). Strong evidence supports the ability of tumor-associated macrophages to interact directly with tumor cells, producing an inflammatory circuit that promotes tumor growth and progression (Mantovani A, 1992). Macrophages can assume a wide range of phenotypes based on the chemokine-cytokine milieu within that environment.

One type, the M1 polarized macrophages, are regarded as potent effector cells capable of killing both microorganisms and tumor cells. These CD14+ activated macrophages also express the chemokine receptor, CCR7 whose ligands include CCL19

and CCL22 secreted from lymphoid organs. These chemokines are involved in the trafficking of cells to lymphoid tissue facilitating antigen presentation for a pro-inflammatory response. Also present within the tumor microenvironment are M2 polarized macrophages, previously identified as CD11b+/ (F4/80)+ or CD45+/CD11b+ double positive cells. M2 polarized macrophages are the most abundant of the phenotypes and can be induced by cytokines and glucocorticoids. These cells cannot kill pathogens and tumor cells. Instead, M2 polarized macrophages prime the inflammatory response. Tumor-associated monocyte-derived macrophages are more representative of M2 macrophages, as they exhibit little tumor cell cytotoxicity and promote tumor cell proliferation and further support the tissue remodeling process (Noonan DM, 2008; Shojaei F, 2008).

Hypoxia enhances an angiogenic, invasive and immunosuppressive phenotype in macrophages. Upon exposure to hypoxia, macrophages can produce a wide array of angiogenic molecules (VEGF, PIGF, FGF2, PDGF, HGF, Ang-1 and COX-2). They also secrete metalloproteases (MMP-1, -7, -9 and -12) that enhances invasion through the destruction of the extracellular matrix. Detailed molecular studies show tumor associated macrophages have defective NF-Kappaß responses and are unable to up-regulate inflammatory cytokines (IL-12). Strong evidence supports that these tumor-associated macrophages are derived from circulating monocytes and directly interact with tumor cells. In addition to secreting VEGF, macrophages also express VEGFR-1 and this represents one mechanism by which they are recruited to the tumor microenvironment through influences on cell migration. It has also been suggested that exposure of

monocyte-macrophages to VEGF secreted from tumor cells or hypoxic macrophages can influence the formation of this pro-tumor phenotype (Noonan DM, 2008).

F. Tie-2 Expressing Monocytes

Tie-2 expressing monocytes have been identified in human blood and tumors. Elimination of Tie-2 expressing monocytes in various tumor models inhibits tumor angiogenesis. The Tie2 receptor ligand, angiopoietin-2, is secreted from tumors and is a potent chemoattractant for tie-2 expressing monocytes. Together with angiopoietin-2, hypoxia can also up-regulate Tie2-receptor expression while down regulating its antitumor functions. Approximately, 1% to 2% of total leukocytes are Tie2+. A substantial fraction, about 20% of circulating monocytes express Tie2. In mice, the circulating Tie2+CD45+ hematopoietic cells are mostly CD11b+ and Ly6G/Gr-1 (low/negative). The surface marker profile of Tie-2 expressing monocytes is similar to that of monocytes, but distinct from the classical inflammatory monocytes and is thought to also comprise precursors of tissue macrophages (Lewis CE, 2007).

In experiments where Tie2+CD14+ cells were isolated from human peripheral blood and co-injected with human glioma cells, mice developed greater tumor vascularization when compared to CD14+Tie2- monocytes. Additional experiments eliminating Tie-2 expressing monocytes did affect the overall number of tumor-associated macrophages, suggesting that Tie-2 expressing monocytes have other fates within the tumor microenvironment (Venneri MA, 2007; Palma MD, 2005). Tie-2 expressing monocytes preferentially localize to the vicinity of tumor blood vessels in viable tumor areas and provide paracrine support to developing blood vessels in these

various models of pathological angiogenesis. They can also produce high levels of the pro-angiogenic factors such as basic fibroblast growth factor and matrix-remodeling proteins. They may also function as "pathfinders" for activated endothelial cells or form provisional endothelium-like structures for blood vessel formation (Lewis CE, 2007).

IV. Immunosuppressive Effects of Morphine

Today, morphine is widely accepted as a highly immunosuppressive drug (Weinert CR, 2008). The immunological effects of opioid analgesic drugs vary clinically both in human and animal studies. In humans, morphine decreases the effectiveness of several immuno-modulatory functions involving both arms of the immune system—innate and acquired immunity. Some of the observed effects include the interference of key intracellular pathways involved in immune regulation (Sacedote P, 2008). However there are more studies using animal models, which show that not all opioids induce the same immunosuppressive effects. Take for example, the potent opioid fentanyl: this drug exerts significant and relevant immuno-suppression in contrast to the partial agonist buprenorphine (Franchi S, 2007; Martucci C, 2004).

In the case of the opioid morphine, there are many studies supporting the immunosuppressive effects of morphine—see review (Weinert CR, 2008). Some of the immune functions suppressed by morphine treatment include but are not limited to the impairment of monocyte and neutrophil function, NK-cell-mediated cytotoxicity, lymphocyte proliferation, and the activation of programmed cell death in macrophages and lymphocytes. Some investigators report the ability to exert significant apoptotic

effects as a mechanism of cell death. These apoptotic effects have been shown to be associated with the down-regulation of protein kinase C activity, somatostatin effects and engagement of proapoptotic enzymes, and were successfully blocked by administration of the μ-receptor antagonist, naloxone. Although more studies are necessary, the existing studies strongly support the view that opioid receptors modulate the function and activity of a distinct subset of immune cells, altering their susceptibility to various infectious agents to transform the inflammatory response. In addition to the direct interaction with opioid receptors, morphine can also regulate the immune function indirectly as studies have shown that morphine is capable of varying nitric oxide release, exerting varying effects on cell adhesion and modulating stress hormone levels (McCarthy L, 2001; Sacerdote P, 1997; Schneemilch CE, 2004; Walters, 2003). In animal models, several independent laboratories have shown that sub-acute, chronic exposure to morphine, as well as drug withdrawal, sensitizes animals to the lethal effects of *E. coli* derived lipopolysaccharide (Eisenstein TK, 2006).

Considering the effects of morphine on the immune responses and the involvement of immune cells in the development of angiogenesis (see **Figure 11**), another important focus of these studies was to investigate the effects of morphine on the immune cell contribution to angiogenesis *in vivo*.

CHAPTER 2

LONG-TERM USE OF ANALGESIC MORPHINE INHIBITS TUMOR ANGIOGENESIS AND GROWTH BY SUPPRESSING HIF-1A/P38 MAPK ACTIVITY

Introduction

Morphine has been used since ancient times for pain relief and is still one of the most effective drugs available clinically for the management of severe to moderate cancer pain. Relief for approximately 90% of patients with cancer-related pain involves strong opioids such as morphine. Effective morphine doses and routes of administration vary between cancer patients, as the dose is titrated against either analgesia or opioid related side effects (Wiffen PJ, 2007; Cain DM, 2001; World Health Organization, 1983).

Surprisingly very little is known about the effects of long-term morphine use on tumor growth and progression; and the studies that do exist, show conflicting results. For example, in one study morphine treatment promoted tumor growth (Gupta K, 2002). In another study using the same tumor model, morphine inhibited tumor growth through a p53 dependent mechanism (Tegeder I, 2003). Of interest, both studies used the steroid dependent breast cancer cell line, MCF-7. This is particularly relevant since estrogen has been shown to internalize and reduce μ-opioid receptor function (Micevych PE, 2003). Thus, it is difficult to determine if the effect of morphine in these studies resulted from either a direct effect of morphine, or was a consequence of μ-opioid receptor down regulation. In addition the drug dosages (sub-analgesic) and routes of administration

(subcutaneous versus intra-peritoneal) varied between these studies and these factors may have contributed to the observed contradictory results.

As the solid tumor mass grows beyond 1-2 mm^3 it must establish a vascular supply. Angiogenesis is defined as the formation of new blood vessels from the endothelium of the pre-existing vasculature. Angiogenesis occurs mostly in response to the metabolic demands of the growing tumor under hypoxia (low oxygen tension) and nutrient deprivation. Vascular endothelial growth factor (VEGF) is one of the major pro-angiogenic growth factors known to induce vessel permeability, endothelial cell proliferation, migration and sprouting resulting in tumor growth, local tumor cell invasion and metastasis (Folkman J, 1996; Ryan HE, 1998). In addition, chronic morphine treatment has been shown to inhibit hypoxia-induced VEGF secretion from mouse cardiac and human umbilical vein endothelial cells (S Roy, 2003; Balasubramanian S, 2001).

VEGF expression is regulated by hypoxia inducible transcription factor, HIF-1α (Ferrara N, 1997; Forsythe JA, 1996). The active form of the HIF-1 complex is made up of one –α one –β subunit. While the β-subunit, is constitutively active and unaffected by the cell's oxygenation state; the α-subunit is unstable and undergoes rapid proteosomal degradation under normal oxygen tensions. Under hypoxia, hydroxylase enzymes, involved in the hydroxylation of HIF-1α for subsequent ubiquitination and proteosomal degradation, become less active allowing HIF-1 stabilization and nuclear translocation (Semenza GL, 1992; Epstein AC, 2001; Hirota K, 2005). The phosphorylation of HIF-1α is also necessary for HIF-1 activation. Mitrochrondrial ROS generated under hypoxia activates p38 MAPKs in mice cardiomyocytes and carcinomas. Scientific studies support

a role for p38 MAPK in HIF-1α stability, phosphorylation and gene transcription in a manner distinct from anoxia (the complete lack of oxygen) or the hypoxia mimetic, desferroxamine (Minet E, 2001; Laderoute KR, 1999 ; Conrad PW, 1999; Kulisz A, 2002; Brooke ME, 2005).

To date very few studies have investigated the effects of opioids on angiogenesis an essential process mediating tumor growth. Recently, naltrexone an opioid receptor antagonist has been suggested as an effective cancer therapeutic (Singleton PA, 2006); therefore it is important to know whether morphine given to cancer patients for pain relief can cause further detriment to these patients by increasing tumor growth through effects involving angiogenesis. *In* a chicken chorio-allantoic model of angiogenesis, β-endorphin peptides and morphine treatment have been shown to significantly inhibit the total number of blood vessels formed and on average produced shorter vessels when compared to placebo treated controls (Pasi A, 1991; Blebea J, 2000). In the present studies we show that long-term morphine treatment at physiologically relevant, and within analgesic doses affect tumor cell induced angiogenesis and tumor growth using the mouse Lewis Lung Carcinoma tumor model in mice. We further investigated the mechanism by which morphine inhibits hypoxia-driven transcriptional activation of VEGF in tumor cells *in vitro*.

Materials and Methods

Cell Culture, Hypoxia and Reagents

Lewis Lung carcinoma cells (LLCs) were obtained from ATCC and cultured in RPMI 1640+10% FBS+1% Penicillin Streptomycin. Unless otherwise mentioned all reagents were obtained from Sigma Aldrich, St. Louis USA. Sub-confluent, serum starved cells were treated with 1.0μM morphine sulfate under normoxia, defined here as normal room air in a 5% CO_2 / 37 °C incubator, or hypoxia. This cell line was derived from spontaneous tumors found within the lung of C57/BL6 mice and is an approved cell line for drug testing by the National Institute of Health.

To achieve hypoxia, culture dishes were placed in a modular chamber purchased from Billups Rotenberg Incorporated. The modular chamber was previously flushed with a mix of 0% O_2, 5%CO_2, 95 %N_2 at 10L per min for 15 minutes. This achieves $P0_2$ levels at 30mmHg. The following antibodies were used: Rat monoclonal antibody to mouse CD31-PE (BD Pharmingen) and HIF-1α antibodies (Novus Biologicals), P38 total and phospho antibodies (Thr 180/ Tyr 182, Cell Signaling Technology). The P38 MAPK inhibitor, SB203585 was purchased from Sigma. Morphine sulfate was obtained from National Institutes of Health.

Morphine treatment

Mice received morphine or placebo through pellet implantation method as previously described (Roy S, 2001). Briefly, 75mg morphine pellets, placebo and or 30mg Naltrexone pellets (NIH/NIDA) were inserted in a small pocket created by a small incision on the animal's dorsal side; and resealed using surgical wound clips (Stoelting, Wooddale, IL). Previous experimentation showed that these pellets are able to deliver

morphine at steady state levels (10mg/kg) up until day 9-11. Supplemental doses of morphine were then administered from days 7-14, at 20mg/kg/day intra-peritoneal; and this was further escalated to 30mg/kg/day from on day 15-21.

Enzyme Linked Immunosorbent Assay (ELISA)

The concentration of mouse or human VEGF-A protein expression was determined with a Duo-set ELISA kit per manufacturer's instructions using diluted culture supernatants (R&D Systems, Minneapolis, MN).

RT-PCR

Total cellular RNA was isolated using the Qiagen's RNeasy Minikit per manufacturer's instructions (Valencia, CA); and DNASE I treated (Invitrogen USA). Reverse transcription and real time PCR was performed as described in (Balasubramanian S, 2001) on an ABI Prism 7500 instrument using a Sybr Green PCR Master Mix (Applied Biosystems, Foster City, CA) for mouse VEGF and GAPDH/r18s. All assays were performed in triplicates and normalized to GAPDH mRNA in the same cDNA set. Data is expressed as fold change over control (untreated cells) using the ddCt method as described in (Dussault AA, 2006). MOR expression was determined using the primers described in (Balasubramanian S, 2001).

In vivo Matrigel Plug Angiogenesis Assay

Matrigel plug assay was performed as described with a few modifications (Yokoyama Y, 2004). Pelleted animals were injected subcutaneously with 1.0×10^6 LLC

cells admixed in a ratio of 3:1 matrigel: HBSS respectively (Sigma, St. Louis, MO). After 7 days animals were sacrificed; matrigel plugs were surgically removed; and photographed (20x, BIPL, University of Minnesota). Plugs were fixed in10% formalin overnight and histological analysis (hematoxylin and eosin staining was performed at the University of Minnesota, Fairview Clinical Pathology and Lab Services. In subsequent experiments, matrigel plugs were snap-frozen in liquid nitrogen and cryostat sections were used for morphometric analysis for blood vessel formation was determined using fluorescent tagged monoclonal antibodies against CD31 found on mature endothelial cells.

Morphometric Analysis for blood vessel density

Cryostat cut, 8µm thick frozen sections of matrigel plugs were fixed in ice-cold acetone and non-specific binding was blocked with 1 % bovine serum albumin in PBS. For CD31-staining (dilution 1:50), sections of matrigel plug or tumors (n=10) per treatment group (placebo vs. morphine vs. morphine + naltrexone) were used to determine blood vessel density as previously described (Wild R, 2000). Briefly, single photon captured, CD31-PE digital images were binarized and skeletonized using the Reindeer Plug In Functions for Adobe Photoshop.

In Vivo mouse Tumor Growth Assay

Athymic mice, 7–9 weeks of age (Jackson Labs, Bar Harbor, ME) were housed in SPF facility and experiments were carried out according to approved protocols by the IACUC at the University of Minnesota. Approximately, 2.0 x 10^6 LLC cells admixed in

matrigel/HBSS were injected subcutaneously into the animals' right flank. Mice received morphine and placebo through pellet implantation method. Tumor size was measured using calipers. The tumor volume was calculated using the formula [(L) X (0.5W) X0.52]; L=longest length and W=widest width. On day 21 tumors were removed (n=10 per group), and photographed using a digital camera (BIPL, University of Minnesota). Tumor wet weights were recorded, and a part of the tumor was then fixed in 10% neutral buffered formalin for 24 hrs and processed for histology. The rest of the tumor samples were snap frozen in liquid nitrogen. Five-micron thick cryostat sections were used for CD31 morphometric analysis for vessel density and HIF-1α expression.

HIF-1alpha staining

The primary antibody for HIF-1α protein used in this study was polyclonal (1:50) and obtained from Novus Biologicals (USA). After incubation with primary antibody overnight at 4^0C, the sections were incubated with FITC fluorescent-tagged secondary antibodies (1:500) in blocking buffer at room temerature (RT) for 1 hour. Sections were then co-stained for CD31, using CD31-PE antibodies at RT/1hr in 1% bovine serum albumin. Slides were washed and airdried sections were then mounted with DAPI/antifade for analysis using an Olympus BX60 Upright Fluorescent Microscope (Biomedical Imaging and Processing Lab, University of Minnesota).

Protein Extraction and Western Blot Analysis

Protein extracts were prepared on ice for HIF-1α and p38 MAPK activation in western blot analysis. Proteins were collected in a denaturing lysis buffer that contained

protease inhibitors (Sigma). Bradford protein quantification (BIORAD, Hercules, CA) was used to determine protein concentration and 10-40 μg aliquots was separated by SDS-PAGE gel electrophoresis and analyzed by immunoblotting with an anti-HIF-1 antibody (1:1000) or phospho-p38 MAPK (1:500). To control for loading, equal protein samples were run on separate membranes and an anti-Pol II antibody (1:200; Santa Cruz Biotechnology, Inc.) or p38 total was used. For total cell lysates, equal amounts of lysates were determined using the Bradford Assay; and were analyzed by SDS-PAGE and immunoblotted with the appropriate antibodies. The immunoreactive bands were visualized using chemiluminescence (Amersham Pharmacia Biotechnology). BIOrad software was used for densitometric analysis (Biomedical Imaging and Processing Lab, University of Minnesota).

Electromobility Shift Assay (EMSA)

Nuclear extracts were prepared from LLC cells pretreated with 1.0μM morphine sulfate and exposed to normoxia or hypoxia for comparison to untreated controls using the Nu-CLEAR EXTRACTION KIT (Sigma catalog no. N-XTRACT). Nuclear extract (10μg) was labeled with ^{32}P-labeled double-stranded oligonucleotide probes (labeled with ATP using a polynucleotide kinase (50,000cpm/ng) for the Hypoxia Response Element-specific HIF1a-binding sequence (5′-TCA GT**A CGT** GAC CAC ACT CAC CTC -3′) and (3'-AGACA**T GCA** CTG GTG TGA GTG GAG-5') as described by manufacturer (Promega, Madison, WI). DNA protein complexes were resolved by polyacrylamide gel electrophoresis. The gels were dried overnight and HIF-1 binding to the probe was confirmed after autoradiography with an intensifying screen.

MTT Cell Viability Assay

Lewis Lung carcinoma cells were plated in 96 well plates in 1% Fetal bovine serum containing growth media. Cells were pretreated with increasing concentrations of morphine for 72 hrs. After 72 hrs incubation MTT was added at 20mg/ml per well and allowed to incubate for another 4hrs in a 37% incubator. After which, cell were solubilized with 100% DMSO. Plates were read in a plate reader at 450nm absorbance. Untreated controls were compared to morphine treatment by determining the percent change in cell viability as follows: % Change in cell viability= (sample- control)/(mean control)*100%.

Tunnel Staining and Apoptosis

To determine the presence of apoptotic cells Terminal deoxynucleotidyl transferase mediated dUTP nick end label staining was performed on tumor cells cultured on 8 well chamber slides and on 5-8 micron thick frozen, cryostat cut sections of 21 day tumor tissues. Tissue sections were warmed using a slide warmer at 65^0C/30 minutes. Sections were then deparaffinized in xylenes (2X at 5 minutes). Sections were then rehydrated in ETOH (95%, 85, 70%, H2O) for 5 minutes each. Slides were next treated with 10ug/ml Proteinase at 37'C for 15 minutes in 10mM Tris (pH 7.5 at 37^0C). Slides were then washed in TBS (3X at room temperature for 5 minutes); followed by distilled water (2x/RT for 5 minutes). Sections were then equilibrated in TdT buffer 10 minutes at 37^0C then labeled using TdT buffer + Enzyme-FITC labeled for 1 hr/37^0C humidified chamber. Slides were washed in 1x and visualized in the presence of nuclear stain, DAPI (4', 6-diamidino-2-phenylindole). Captured images were analyzed and merged using

Adobe Photoshop.

HIF-1alpha Duo-set Kit

To determine the levels of HIF1alpha, nuclear and cytoplasmic proteins were isolated from experimental cells as recommended by the manufacturer. Protein inhibitors were added to fresh lysis buffer, prepared to extract the cytoplasmic or nuclear protein fractions separately. Aliquots were used to determine protein concentration using the Bradford Assay. Biotin labeled ds oligonucleotides, were added to proteins and incubated for 30 minutes at room temperature, together with the controls, that did not contain any nuclear extracts. To determine specificity of binding through competition, 3x the amount of unlabeled ds oligonucleotides were incubated in the presence of Biotin labeled ds oligonucleotides. To 5% BSA blocked ELISA plates 10ug of nuclear or 40 ug of cytoplasmic proteins with the appropriate buffers were added and allowed to incubate at room temperature for 2hrs. Plates were aspirated and washed in 1xPBS. The recommended concentration (1:200 dilution) of Streptavidin-HRP was added to each well and incubated at room temperature for 20 minutes in the dark. Plates were washed, after which developing solutions were added and optical density determined for ach well using a microplate reader at 450nm. Data is represented as the relative HIF1alpha levels after subtraction of O.D from values of Biotin labeled and unlabeled ds oligonucleotides.

Statistics

All numerical data are expressed as a mean ± SE. Differences of means between different treatment groups were compared using a one-tail Student's T-test; a value of $P < 0.05$ was considered statistically significant.

Results

Morphine inhibits hypoxia-induced VEGF secretion in Lewis Lung Carcinoma cells

In previous studies, we have demonstrated that morphine, in mouse cardiac myocytes and human umbilical vein endothelial cells that express the mu-opioid receptors (MOR), can inhibit hypoxia-induced VEGF secretion (Balasubramanian S, 2001; Roy S W. J., 2001). Tumor cells within the hypoxic core of the tumor mass are stimulated to secrete proangiogenic factors such as VEGF known to initiate angiogenesis and thus improve tumor growth and tumor cell survival (Hicklin DJ, 2005). To further investigate whether morphine treatment will have similar effects on tumor cells, we also assessed in mouse Lewis Lung carcinoma cells (LLC) MOR expression. As shown in **Figure 12A** (lane 1), RT-PCR data indicated LLC have a basal level of MOR expression, and this is increased upon morphine sulfate treatment (**Figure 12A**, lane 2).

To test the effect of morphine on hypoxia-induced VEGF secretion, we treated LLC with morphine sulfate (1.0uM) and subjected the cells to hypoxia using a modular chamber for 48 hrs as described in methods. VEGF levels in culture supernatants were determined by ELISA and compared to normoxic cells, cells cultured in a 37^0C incubator with normal room air, 21% 0_2. Shown in **Figure 12B**, hypoxic treatment of LLC cells resulted in a 5-fold increase in VEGF secretion when compared to normoxic cells. In contrast, morphine treatment significantly reduced hypoxia-induced VEGF secretion from LLC (30%, **Figure 12B**). VEGF is regulated at both the protein and message levels, therefore we further examined if the effect of morphine on VEGF was also at the transcriptional level. As determined by real time RT-PCR, hypoxia induced a

transcriptional activation of VEGF in LLC 7-fold greater than normoxia (**Figure 12C**). Similar to the effect on protein secretion, morphine also suppressed the hypoxic activation of VEGF gene transcription *in vitro* ($p<0.05$). Taken together these results suggest in addition to cardiac and endothelial cells, LLC also express the MOR. In addition, morphine also inhibits its hypoxia-induced VEGF secretion *in vitro* at the translational and transcriptional level and this can potentially reduce hypoxia induced tumor-cell angiogenesis.

Morphine inhibits tumor cell induced angiogenesis in vivo

Tumor cells experiencing hypoxia are stimulated to secrete VEGF. VEGF is one of the major contributors of angiogenesis (Folkman J, 1996; Forsythe JA, 1996) and since morphine pretreatment suppressed hypoxia-induced VEGF secretion from tumor cells *in vitro* we next tested the effect of chronic morphine treatment on tumor-induced angiogenesis *in vivo* (**Figure 13**). Briefly, Lewis lung carcinoma cells were admixed in matrigel and injected subcutaneously into the flanks of athymic mice. At the contra-lateral site mice were implanted with either a placebo or morphine pellet. After 7days, LLC containing matrigel plugs were removed and photographed (**Figure 14**). Matrigel plugs taken from placebo treated mice were rosy red in appearance indicative of successful LLC-induced angiogenesis *in vivo* (**Figure 14A**). In contrast, plugs taken from morphine treated mice were very pale with a few blood vessels mostly at the periphery (**Figure 14D**). This data suggests that morphine can inhibit hypoxia-induced angiogenesis by LLC cells.

To further analyze the effect of morphine on hypoxia induced tumor-cell angiogenesis in vivo, matrigel plugs were paraffin-embedded, sectioned and hematoxylin and eosin stained for tissue architecture. As indicated by the arrows in **Figure 14B**, hematoxylin and eosin stained sections of plugs taken from placebo mice reveal well-developed vessels among tumor cells. In contrast, as shown in **Figure 14E** vessels within plugs from morphine treated mice were not as developed and readily identifiable. Considering the immunosuppressive effects of morphine and the role of immune cells in angiogenesis, we next analyzed the tissue for leukocyte infiltration. As shown in **Figure 14C**, matrigel from placebo treated mice show a greater infiltration of host inflammatory cells from the vessels at the periphery of the matrigel when compared to sections from morphine treated mice (**Figure 14F**).

In subsequent experiments, matrigel plugs were snap frozen and sectioned to confirm the effect of morphine on tumor cell induced angiogenesis. Here, we assessed blood vessel density by staining for CD31 (also known as platelet endothelial cell adhesion molecule -1 (PECAM-1), **Figure 14G-H**) present on mature endothelial cells of intact blood vessels and quantified using morphometric analysis (**Figure 14I-J**). Briefly, CD31-PE stained sections were analyzed using fluorescent microscopy, and digital fluorescent images were binarized and skeletonized to determine relative blood vessel density; relative number of branch points or branching; and average blood vessel length within treatment groups (Wild R, 2000). Morphometric analysis confirmed, when compared to placebo, long tern morphine treatment significantly reduced blood vessel density (**Figure 14K**; $p<0.02$); blood vessel branching (**Figure 14L**; $p<0.01$); and even the overall blood vessel length (**Figure 14M**; $p<0.04$). Taken together, the data suggests

morphine through the inhibition of hypoxia induced-VEGF can inhibit hypoxia-induced angiogenesis by tumor cells *in vivo* as well as alter the pattern of inflammatory cell recruitment required for sustained angiogenesis.

Morphine inhibits tumor angiogenesis *in vivo* through the opioid receptors

To assess the involvement of the opioid receptors in morphine's inhibition of hypoxia-induced tumor cell angiogenesis, we next tested the effect of naltrexone, an opioid receptor antagonist, in the presence of morphine on hypoxia-induced tumor cell angiogenesis *in vivo*. These experiments were conducted similar to the above experiments, with the addition of a third group of mice. In this third group, mice received both morphine and naltrexone pellets through implantation as described in methods. Morphological examination of matrigel plugs from placebo (**Figure 15A**) and morphine+naltrexone (**Figure 15C**) treated animals were highly vascularized, in contrast to matrigel plugs taken from morphine treated animals (**Figure 15B**). The matrigel plugs were processed for hematoxylin and eosin staining. Similar to previous experiments, blood vessel containing red blood cells were easily distinguishable within tumor cells in plugs taken from placebo (**Figure 15D**) and morphine+naltrexone (**Figure 15F**) mice but not after morphine treatment (**Figure 15E**).

To confirm the effect of naltrexone in the presence of morphine treatment on angiogenesis, we next examined vessel density within matrigel plugs using morphometric analysis as previously described (Wild R, 2000). As shown in **Figure 15**, when compared to placebo treatment (**Figure 15G, J**) blood vessel density (**Figure 15M**; $p<0.003$); branching (**Figure 15N**; $p<0.005$); and even total vessel length (**Figure 15O**; $p<0.002$)

within the matrigel plugs was significantly reduced after morphine treatment (**Figure 15H, K**). Co-treatment with naltrexone (**Figure 15I, L**) reversed this morphine-mediated inhibition on tumor-induced angiogenesis and was more similar to placebo treatment. Taken together our data suggest morphine inhibits hypoxia-induced tumor-cell angiogenesis *in vivo* and since co-treatment with naltrexone reversed this inhibition, the effect of morphine is likely mediated through the classical opioid receptors.

Morphine reduces Tumor Growth in mice by suppressing angiogenesis

Since morphine inhibited hypoxia induced tumor-cell angiogenesis in vivo, we next sought to determine whether chronic morphine treatment would also inhibit tumor growth. To test this hypothesis, athymic mice were first implanted with placebo or morphine pellet. Lewis lung carcinoma cells were then injected subcutaneously, into the animals' right flank. Since cancer patients receive morphine as needed, patients often develop tolerance and as a result require escalating doses for pain management. We modeled our experiments to reflect this type of drug administration (**Figure 16**). In this model of tumor growth, mice received morphine through pellet implantation from day 1 through day 9. At day 10-11 pellets become encapsulated and this reduces morphine steady state levels, so mice were supplemented with morphine intra-peritoneal on days 9-13 at 20mg/kg per day. On day 14, morphine doses were further escalated to 30mg/kg intra-peritoneal until day 21. This method of morphine administration is more representative of that in cancer patients receiving morphine for severe to moderate cancer pain management clinically.

Our results show when compared to placebo, morphine treatment significantly reduced tumor growth over the 21-day period tumor volumes was measured (**Figure 17A**); $p < 0.007$). Tumor wet weights at the time of necropsy further validated morphine's effect on tumor growth. Gross morphology of representative tumors obtained from placebo (**Figure 17C**) and morphine (**Figure 17D**) treated animals is shown. Compared to tumor wet-weights from the placebo group, morphine treated animals had significantly lower wet-weights ($p<0.01$) and on average weighed 52% less (**Figure 17E**). The changes in tumor volume and wet weights confirm that morphine treatment similar to the pattern of drug administration for cancer patients can suppress tumor growth in mice.

Comparison of hematoxylin and eosin stained tumor sections from placebo mice showed a larger tumor cell mass with more blood vessels, indicated by intense CD31-PE staining (**Figure 17E, F, I**). In contrast, hematoxylin and eosin stained tumor sections from morphine treated mice reveal a relatively smaller amount of tumor cells and reduced CD31 positive blood vessels. (**Figure 17G, H, K**). To determine if morphine's inhibition on tumor growth was indeed due to a decrease in angiogenesis (morphometric analysis using CD31), blood vessel density of residual tumors was analyzed and counterstained with DAPI for tissue architecture (**Figure 17F, H**). As shown in **Figure 17I-J**, CD31 staining of placebo sections identified an intricate network of blood vessels that was underdeveloped in sections taken from morphine treated mice, Figure 16K-L. Our results suggests that tumors from morphine treated animals had a significantly lower blood vessel density ($p < 0.006$); **Figure 18M**); blood vessel branching ($p<0.003$; **Figure 18N**); as well as average blood vessel length ($p < 0.004$; **Figure 18O**) when compared to placebo treatment.

Tumor cells exposed to hypoxia and reduced nutrients often undergo apoptosis (7-8). To further determine if chronic morphine treatment affected tumor cell survival, tumor sections was processed for TUNEL labeling as an indication of apoptosis. Morphine treated tumor sections (**Figure 18Q**) showed a higher level of apoptosis within hypoxic regions as compared to placebo (**Figure 18P**). Quantification of apoptotic tumor cells using Metamorph confirmed that morphine treatment resulted in significantly greater apoptotic tumor cells when compared to placebo (**Figure 18R**, $p<0.04$)

Pro-angiogenic factors necessary for angiogenesis, such as VEGF are regulated by hypoxia inducible transcription factors (HIF). Since HIF-1α can increase tumor cell survival under hypoxia (Folkman, 1971; Ryan HE, 1998), we next examined whether chronic morphine treatment altered HIF-1α expression, the oxygen regulatory component of the functional HIF-1 transcription factor, within the tumor tissue. Interestingly, tumor sections from placebo treated animals (**Figure 17S**) showed qualitatively more areas positive for HIF-1α expression (green) when compared to the morphine treated group (**Figure 17T**). The expression of HIF1 was also more closely associated with the tumor cells, rather than the CD31+ endothelial cells (**Figure 18A**). Taken together, these results suggest that morphine altered the tumor microenvironment by inhibiting HIF-1α accumulation, reducing hypoxia induced tumor cell angiogenesis and thus tumor growth.

Effects on morphine treatment on cell viability *in vitro*

To elucidate the mechanism by which morphine inhibited tumor growth, we further investigated the effect of morphine on Lewis lung carcinoma cells viability *in vitro*. To do this, a wide range of morphine concentrations (2nM-2mM) was used to

assess Lewis lung carcinoma cells viability after *in vitro* long-term culture using the MTT assay. The treatment of Lewis lung carcinoma cells with morphine for 72 hours showed no significant effects on cell viability when compared to saline treatment (**Figure 18B**). To rule out the possibility that morphine directly induced Lewis Lung carcinoma apoptosis *in vivo* to reduced tumor growth, we assessed the effect of morphine on Lewis Lung carcinoma cells apoptosis *in vitro* using Tunnel Labeling. To do this, Lewis Lung carcinoma cells were treated with morphine and placed under normoxia and hypoxia-inducing conditions as described in methods. Compared to saline treatment, under normoxia, morphine did not induce apoptosis any further (**Figure 18C**). In contrast, under hypoxic conditions, morphine increased tumor cell apoptosis but the concentrations (>500uM-1.0mM) required to produced this apoptosis in vitro was greater than that which could be achieved i*n vivo* for pain management (1140ng/ml or ~2.0uM). These results suggest that the effect of morphine on tumor growth is not a direct effect of morphine on tumor cell apoptosis but through indirect effects on angiogenesis by suppressing tumor cell expression of hypoxia-induced VEGF.

Effects of morphine treatment on HIF-1α *in vitro*

Figure 18A, showed that HIF1alpha expression was more closely associated with the tumor cells than CD31 positive endothelial cells, so next we further examined the effect of morphine on HIF-1α stability in Lewis lung carcinoma cells *in vitro*. The trans-activation by HIF-1 is necessary for VEGF transcription (Forsythe JA, 1996), so we next tested the hypothesis that reduced HIF-1α observed *in vivo*, may have resulted from decreased HIF-1α nuclear localization to reduce VEGF transcription and synthesis. To do

this, equal amounts of nuclear extracts from saline and morphine treated LLC cultures were subjected to an Electromobility shift assay to assess the ability of LLC nuclear HIF-1α binding to its hypoxia response element, a unique DNA binding site (HRE) found within its target genes. As shown in **Figure 19A**, nuclear extracts from LLC cells exposed to hypoxia for 24 hours produced greater HRE binding when compared to nuclear extracts from normoxic morphine untreated cells (**Figure 19A**; lane 2 and 1 respectively). In contrast, morphine treatment of hypoxic Lewis lung carcinoma cells resulted in a clear reduction in the amount of HIF-1 capable of binding to its HRE (**Figure 19A**, compare lane 2 and 3). These results suggest that the decrease in DNA binding in the presence of morphine leads to a reduction in target gene transcription and therefore, expected to decrease HIF-1α regulated VEGF gene transcription.

To further investigate the effects of morphine on HIF-1α regulation and to understand why morphine reduced HIF-1-DNA binding we next assessed nuclear HIF1α expression levels using Western Blot. Nuclear extracts from saline-treated normoxic Lewis lung carcinoma cells were compared to saline treated and morphine treated hypoxic cells. Our results show when compared to normoxia, hypoxia increased HIF1α nuclear expression almost 3-fold and morphine treatment reduced the hypoxia induced HIF1α nuclear expression by 50% (**Figure 19B**). To further confirm the effect of morphine on HIF1α nuclear expression, we measured HIF1α expression using a HIF1α duo-set kit as described in methods. Here we included the hypoxia mimetic, cobalt chloride ($CoCl_2$) as a positive control. Similar to $CoCl_2$, hypoxia increased HIF1α nuclear expression, but was reduced to control levels with morphine pretreatment (**Figure 19C**).

To further understand the effect of morphine on hypoxia induced HIF1α nuclear expression, we next analyzed total cellular expression of HIF1α using Western Blot analysis. Interestingly, normoxic Lewis lung carcinoma cells express detectable levels of HIF-1α protein (**Figure 19D**); and 6hrs of hypoxia treatment resulted in both the accumulation of HIF-1α and the appearance of a second, slower migrating band (**Figure 19D**; lane 2). In contrast, analysis of total lysates from morphine-treated hypoxic Lewis lung carcinoma cells showed an increased accumulation of the lower band and reduced appearance of the second, slower migrating band prominent after hypoxic treatment (**Figure 19**, lane 3). We further verified the appearance of this second slower migrating band identified in hypoxic Lewis lung carcinoma total proteins by separating the nuclear and cytoplasmic protein fractions. As shown in **Figure 19E** lanes 1 and 2, western blot analysis revealed that the higher migrating band appeared predominantly within the nucleus and the lower band in the cytoplasmic fractions (see arrow). These results suggest that *in vitro* morphine treatment prevents the post-translational modification of HIF-1α required for its nuclear translocation.

Mechanism of morphine mediated regulation of HIF-1

The accumulation of HIF-1α is partially regulated through prolyl hydroxylases enzymatic activity. HIF-1α undergoes several post-translational modifications that alter its activity; hydroxylated HIF-1α is degraded quite rapidly in the cytoplasm; and phosphorylated HIF-1α promotes its nuclear translocation and dimerization with its nuclear partner HIF-1ß (Epstein AC, 2001; Semenza GL, 1992). Iron and ascorbic acid are essential co-factors necessary for prolyl hydroxylase activation. Under hypoxic

conditions, oxygen another essential substrate for prolyl hydroxylase activation becomes rate limiting (Seko Y, 1997). Similarly Desferroxamine, a hypoxia mimetic, modulates PHD's through Fe^{2+} chelation. To determine if morphine modulation of HIF-1α accumulation involved PHD enzymes we tested the effect of morphine on Desferroxamine induced HIF-1 stabilization by assessing HIF-1α binding to its HREs. Similar to hypoxia, 100 μM Desferroxamine increased the amount of HIF-1α bound to the HRE (**Figure 19**A, compare lane 1 and 4). Unlike morphine treated hypoxic cells (**Figure 19A**, lane 3), morphine co-treatment did not alter the HIF1-HRE binding in Desferroxamine co-treated normoxic cells (**Figure 19A**, lane 5). These results suggest morphine's effect on hypoxia-induced changes in HIF-1α is likely to be independent of the prolyl hydroxylase enzymatic activity.

Previous studies indicate hypoxia rapidly induces MAPK activity in many cells via the mitochondrial ROS system (reactive oxygen species) and this represents an alternative pathway for hypoxia induced HIF-1α accumulation (Conrad PW, 1999; Kulisz A, 2002; Brooke ME, 2005; Laderoute KR, 1999 ; Seko Y, 1997). In particular**,** p38 MAPK has been shown to be essential for the post-translational modification of HIF-1α. P38 MAPK activation has been shown to be essential in HIF-1α phosphorylation and nuclear translocation (Brooke ME, 2005; Seko Y, 1997). To assess if morphine's effects on HIF-1α, involved p38 MAPK signaling, we first tested the effects of morphine on hypoxia induced p38 MAPK activation. As shown in **figure 20A**, treatment of Lewis lung carcinoma cells for 4hrs under hypoxic conditions was sufficient to up-regulate p38 MAPK phosphorylation 3-fold over control levels (compare lanes 2 and 1 respectively). In contrast, morphine pretreatment of LLC cells (**Figure 20A**-lane 3) prevented this

hypoxia induced increase in p38 MAPK phosphorylation. Similarly, LLC pretreated with SB253085, an inhibitor of p38 MAPK phosphorylation, abolished hypoxia-induced phosphorylation of p38 MAPK and reduced the ratio of phosphorylated p38: total p38 proteins below control levels (**Figure 20A**, lane 4). These results show that morphine treatment resulted in a concomitant decrease in hypoxia-induced p38 MAPK activation.

To further confirm the effect of morphine on p38 MAPK activity we next investigated the effect of inhibiting p38 MAPK on hypoxia-induced HIF-1α expression. As shown in **Figure 20B**, hypoxic treatment of LLC resulted in an increase HIF-1α nuclear accumulation (**Figure 20B**; compare lane 2 and 1) and as expected morphine pretreatment reduced the hypoxia induced HIF-1α nuclear accumulation (**Figure 20B**; compare lane 2 and 3). Of greater interest, SB253085 pretreatment inhibited hypoxia induced HIF-1α posttranslational modification similar to morphine treatment (**Figure 20B**, lane 4 and 3 respectively). SB253085 treatment in the presence of morphine further reduced LLC expression of HIF1α below basal levels. These results suggest that the phosphorylation activity of p38 is essential for HIF1α cytoplasmic activation and nuclear translocation. Taken together morphine treatment may be modulating HIF-1α phosphorylation for translocation to the nucleus through pathways that involve the inhibition of p38 MAPK activation.

Finally we wanted to determine if inhibition of p38 affected VEGF mRNA transcription in Lewis Lung carcinoma cells. Similar to the effects seen on HIF-1α, 24hrs of hypoxia treatment resulted in a 4-fold increase in VEGF mRNA expression as determined by real-time PCR. In contrast, morphine and SB253085 treatment, individually under hypoxia, resulted in a significant reduction in VEGF gene

transcription when compared to hypoxia alone ($p < 0.02$; **Figure 20C**). Additionally, morphine and SB253085 co-treatment of hypoxic Lewis Lung carcinoma cells resulted in a further decrease in VEGF transcription when compared to morphine pretreated hypoxic cells ($p<0.05$; **Figure 20C**) alone. Taken together, our data suggests that morphine treatment suppresses hypoxia-induced p38 MAPK activity and this alters HIF-1α phosphorylation and nuclear accumulation to inhibit VEGF transcription and thus protein secretion essential for angiogenesis.

Morphine suppresses VEGF transcription, and secretion through inhibition of HIF-1 in ovarian cancer cells

In the next series of experiments, we sought to determine if the effect of morphine on VEGF A was unique to just the Lewis lung cancer cells, so we investigated the effect of morphine on the human ovarian cancer cell line MA148. Here we first assessed the effect of morphine on VEGF-A transcription using real time PCR. Under normal conditions, morphine did not increase or affect basal level of VEGF gene transcription in MA148 human ovarian cancer cells. As shown in **Figure 21A**, Real time PCR data show that exposure of MA148 to 6hrs hypoxia, was sufficient to increase VEGF-A transcription 40-fold, and morphine treatment significantly inhibited this hypoxia-induced increase in VEGF transcription ($p<0.04$). To further investigate and confirm the effect of morphine on the hypoxia-induced responses, we next tested the effect or morphine on another HIF-1 responsive gene, Glut1. Similar to the regulation seen with VEGF-A, morphine under normal conditions exerted no significant effects on MA148 Glut1 basal gene expression (**Figure 21B**). As expected, hypoxic treatment resulted in a

significant increase in Glut-1 gene expression, approximately 20 fold over control levels (**Figure 21B**). Similar to the effect on VEGF-A, morphine suppressed this hypoxia-induced increased in Glut-1 by 50% ($p<0.02$, **Figure 21B**).

In these studies we also tested the effect of inhibiting p38 MAPK activity on VEGF-A and Glut-1 gene expression through pharmacological manipulation with SB253085, a compound that inhibits p38 MAPK kinase activity. Our results show that inhibition of p38 MAPK activity in MA148 also reduced both VEGF-A and Glut-1 hypoxia-induced gene transcription by 75% (**Figure 21A-B**). Morphine in the presence of SB253085 further reduced VEGF-A and Glut-1 gene transcription, but this was not significantly less than SB253085 treatment alone. These results suggests that p38 MAPK activity is involved in the hypoxia signaling pathways that control hypoxia-induced VEGFA transcription in MA148 human ovarian cancer cells and morphine is acting in similar pathways to alter VEGF expression.

VEGF-A is also regulated through its secretion, so we next examined the effect of morphine on VEGF-A secretion from MA148 human ovarian cancer cells. Cell culture supernatants were tested using a human VEGF-A ELISA Duo-Set kit (**Figure 21C**). Our results indicated 48-hours hypoxic treatment resulted in an increase in MA148 secretion of VEGF-A proteins to levels 6 times (~3000pg/ml) greater than control cells, incubated in normal room air (~500pg/ml VEGF-A; $p<0.017$). To further assess the role of HIF-1 transcription factor control of VEGF-A and the effects of morphine on VEGF expression, we measured the levels of HIF-1α from MA148 cells cultured under normal room air and compared it to cells incubated under hypoxia using the HIF-1α Duo-set kit. **Figure 21D**

shows a comparison of the relative expression of HIF-1α nuclear and cytoplasmic expression under normal and hypoxic conditions.

As shown in **Figure 21D** the hypoxic treatment of MA148 cells increases the stability of HIF-1 since hypoxia increased both the cytoplasmic accumulation of HIF-1α and its nuclear translocation. Figure 20D also show that morphine pretreatment prevented this increase in nuclear HIF-1α translocation, which was due to the decrease in HIF-1α cytoplamsic accumulation, to levels even below control cells. Morphine treatment results in the degradation of HIF-1α preventing its nuclear translocation and thus VEGF gene transcription. Interestingly, inhibition of p38 MAPK activity with SB253085 prevented the hypoxia-induced accumulation of HIF-1α similar to the effect observed with morphine. Morphine in the presence of SB253085 did not reduce HIF-1α any further. Nevertheless, our results suggest that morphine inhibits the hypoxia-induced nuclear activation of HIF-1 through the inhibition of cytoplasmic accumulation and pathways that involve hypoxia-induced p38MAPK activity.

Discussion

In these studies, we demonstrate that morphine can inhibit hypoxia induced vascular endothelial growth factor secretion in mouse Lewis lung carcinoma cells through the suppression of hypoxia induced p38MAPK activation and HIF-1α to suppress angiogenesis, and thus tumor growth. To understand the effects of morphine on hypoxia-induced angiogenic response of LLC, we tested the effects of morphine on two of the known pathways that modulate HIF-1 activation: 1) the prolyl hydroxylase (PHD) and 2) the hypoxia-induced p38 MAPK pathway. In these studies we used the hypoxia mimetic, Desferroxamine (DFO), to examine morphine' effect on the inhibition of HIF-1α. DFO mimics a hypoxic state by reducing the available iron to the prolyl hydroxlase enzymes and thus increase the stability of HIF-1α protein, nuclear translocation and DNA binding. LLC cells exposed to high amounts of DFO resulted in an increased nuclear protein binding to the HRE over untreated cells but this was not affected any further by morphine pretreatment. It is from these results that we draw the conclusion that morphine acts in an alternate pathway to reduce HIF-1 stability in LLCs. Additionally we show that SB253085, a p38 MAPK inhibitor, attenuated LLC hypoxia induced HIF-1α nuclear localization and VEGF gene transcription in a manner similar to morphine. In addition, morphine and the p38 MAPK inhibitor act synergistically on HIF1α and VEGF gene transcription: suggesting that morphine's inhibition on VEGF secretion involves p38 MAPK and not PHD enzymatic activity. This result was surprising to us as there is several reports that indicate DFO like hypoxia can induce reactive oxygen species (ROS) production. However this increase may be the result of a dose effect. High dose DFO induced ROS may also become quickly neutralized as the cells are treated under normal

oxygen tensions, which favor a functional mitochondrial respiratory chain. Other investigations indicate that the hypoxia signaling pathways that involve p38 is distinct from the DFO. The p38 hypoxic induction is dependent on the production of (ROS) generated by the mitochondrial complex III and are required for hypoxic activation of HIF-1 (Chandel NS, 2000). *In vitro* studies indicate a direct interaction of p38 with HIF-1α since p38 null embryonic fibroblasts loses their ability to activate HIF-1α under hypoxia. In contrast, p38 null cells exposed to either anoxia or DFO retains the ability to activate HIF-1α (Brooke ME, 2005). In neurons, morphine has been shown to decrease normoxic p38MAPK activation to induce cellular apoptosis (Hu S, 2005), however little information is available on the effects of morphine on hypoxia induced p38MAPK activation and its impact on cell survival. The mechanism by which morphine alters p38MAPK activity may involve its ability to inhibit mitochondrial ROS generation. Morphine treatment alone under normoxia has no effect on ROS formation but can inhibit Doxorubicin induced mitochondrial ROS production in SH-SY5Y neuroblastoma tumor cells (Xin L, 2007), a pathway known to mediate the hypoxia induced p38MAPK activation and HIF-1alpha phosphorylation (Conrad PW, 1999; Kulisz A, 2002; Brooke ME, 2005; Seko Y, 1997). To date very little studies exist on the effect of morphine on ROS production under normal conditions and there are no studies under hypoxic conditions. Morphine has been shown to increase tumor cell apoptosis in a p53 dependent manner (Tegeder I, 2003). *In vivo* morphine treatment resulted in more apoptotic tumor cells than placebo. The morphine pellets used achieve steady state levels within 1-2 hrs after implantation mimicking a chronic state of morphine administration that continues until day 9-11. Even though RT-PCR shows LLC cells express the μ-opioid receptor, and

therefore morphine could have mediated direct effects on tumor cells; additional experiments *in vitro* using TUNEL labeling of LLC treated with increasing concentrations of morphine showed no significant increase in apoptosis over untreated cells. Concentrations above 1.0mM were required to significantly increase LLC apoptosis under hypoxic conditions *in vitro*. We therefore conclude that morphine's inhibition on tumor growth is primarily through its effects on angiogenesis and the increased tumor cell apoptosis observed *in vivo* was a consequence of reduced angiogenesis. Naltrexone is an opioid receptor antagonist, at the mu-, delta-, and kappa binding sites. In these studies naltrexone reversed the inhibition of morphine on tumor angiogenesis. This suggests that the opioid receptors are involved in morphine's inhibition of angiogenesis. Additional studies in performed in mu-opioid receptor knockout (MOR-KO) mice indicate that morphine fails to suppress angiogenesis *in vivo***,** further confirming the importance of the MOR in this process. In contrast to previous studies investigating the effect of morphine on tumor growth (Gupta K, 2002), our method of morphine administration through pellet implantation, delivers systemic morphine peaking at blood plasma levels within 300-400 ng/ml; depicting a state of chronic morphine exposure as seen with cancer patients using morphine for severe to moderate pain management. Additionally, patients on chronic morphine for cancer pain management are generally given higher doses, than individuals who are not able to tolerate morphine. The dose used in this study is well within the clinical dose of morphine used for pain management, which ranges between 11-1440 ng/ml (Aherne GW, 1979). Furthermore, single, sub-analgesic doses used in previous studies (Gupta K, 2002) may have led to a state of drug tolerance that could have indirectly altered the normal baseline levels. Alternatively, the effects observed in those

experiments may have been the result of a tolerant system cycling between periods of withdrawal. In these studies to avoid tolerance and withdrawal, our experimental animals received supplemental doses of morphine. Tumor cell expression of VEGF is instrumental in attracting endothelial cells into the tumor microenvironment and orchestrating vessel formation. Once endothelial cells migrate into the tumor microenvironment the recruitment of endothelial cell progenitors from the bone marrow has shown to be an important step for vascularization. Although the phenotype has not been well defined or the mechanism clear, they can directly incorporate themselves into the blood vessels or de-differentiate into either M2 polarized macrophage that supports the pro-tumor phenotype (Noonan DM, 2008; Nyberg P, 2008; Shojaei F, 2008). In more recent reports, long-term morphine treatment, in a Model of Wound-Healing, inhibited the recruitment of endothelial progenitors suppressing angiogenesis and delaying wound closure. Also in this model, morphine impaired angiogenesis in animals and reduced capillary tube formation in cultured endothelial cells treated with morphine (Lam CF, 2008). These results further support the inhibitory morphine of morphine on angiogenesis and tumor growth. Morphine administration in our studies is similar and more representative of the chronic high dose morphine used during clinical applications for cancer pain management. Taken together, our results demonstrate that morphine is a potential inhibitor of tumor growth, through the suppression of tumor angiogenesis and by inhibiting the activity of hypoxia-induced p38 MAPK, HIF-1α and VEGF (**Figure 22**). These findings support the use of morphine in cancer pain management with little to no detrimental side effects.

Figure 12A

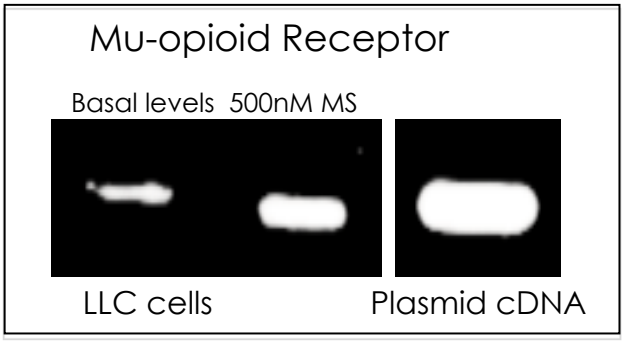

Figure 12A: Mu-opioid receptor expression in Lewis Lung carcinoma cells.

Lewis Lung carcinoma cells were harvested after saline and morphine treatment overnight *in vitro*. Total RNA was isolated and mu-opioid receptor expression was determined by Reverse Transcriptase Polymerase chain reaction. A cDNA plasmid construct encoding the mu-opioid receptor generated from mice brain was used as the positive control for detection and presence of the mu-opioid receptor.

Figure 12B

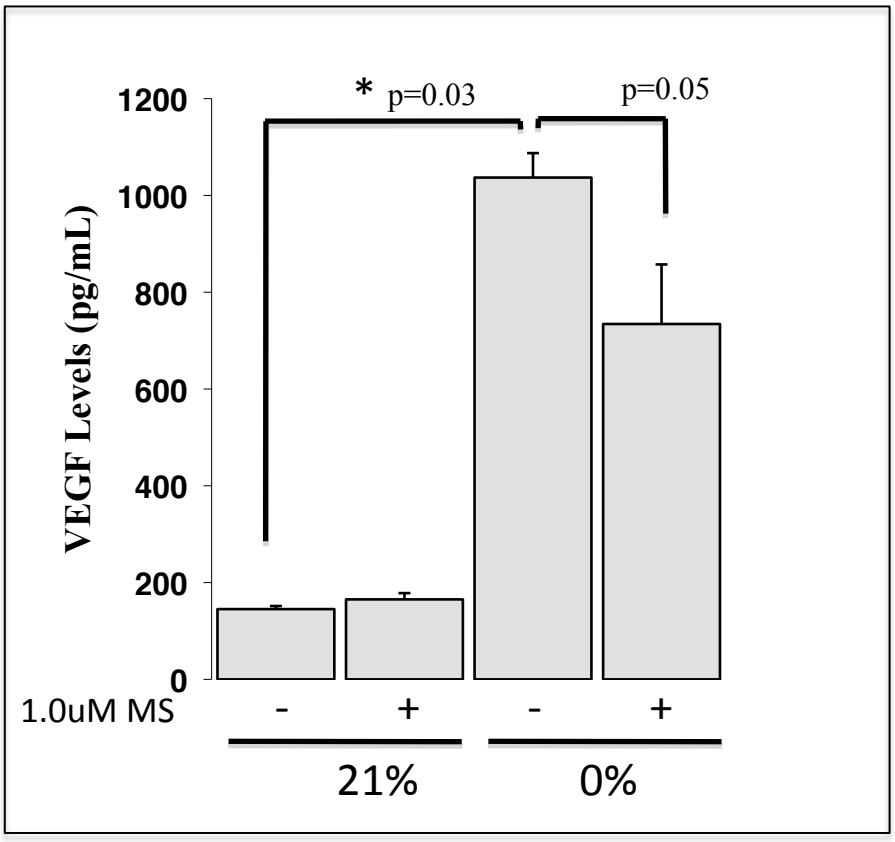
* p=0.03
p=0.05
1200
1000
800
600
400
200
0
VEGF Levels (pg/mL)
1.0uM MS
-
+
-
+
21%
0%

Figure 12B: Morphine pretreatment suppresses hypoxia induced VEGF expression from Lewis Lung carcinoma cells *in vitro*.

Supernatant were harvested after 72 hrs of culturing Lewis Lung carcinoma cells with either saline or morphine treatment *in vitro.* Mouse VEGF A protein secretion as was determined by Enzyme Linked Immuno-sorbent Assay using the mouse VEGF-A Duo-set Kit. VEGF concentration was determined from the generation of standard curves and data represented as the mean concentration (n=3). Data is shown from one representative experiment from 3 individual experiments. For comparison between groups, significance was determined using a Student's T-test.

Figure 12C

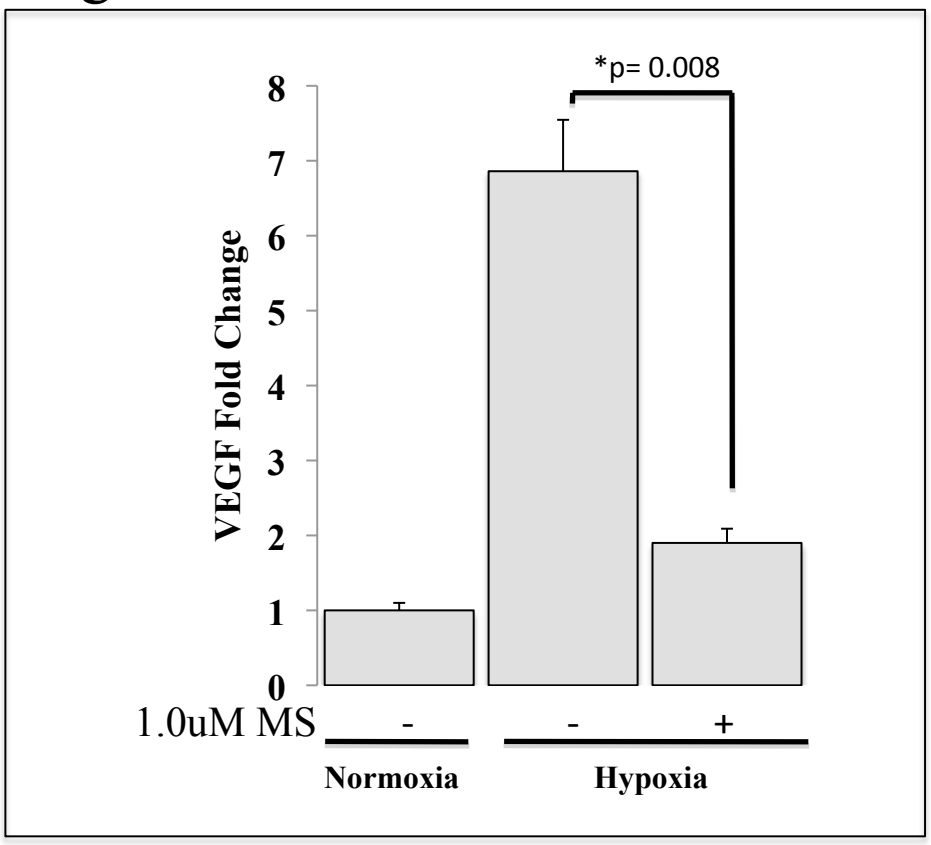

Figure 12C: Morphine pretreatment inhibits hypoxia induced VEGF mRNA expression from Lewis Lung carcinoma cells *in vitro*. Lewis Lung carcinoma cells were harvested after with either saline or morphine treatment, under normal and hypoxic conditions *in vitro*. Total RNA was extracted and mouse VEGFA mRNA was determined using real-time RT-PCR. Data is expressed as fold change in mRNA expression as determined after normalization with 18s ribosomal RNA and comparison to untreated controls. Data is shown from one representative experiment from 3 individual experiments. Significance was determined using a paired student's T-test.

Figure 13

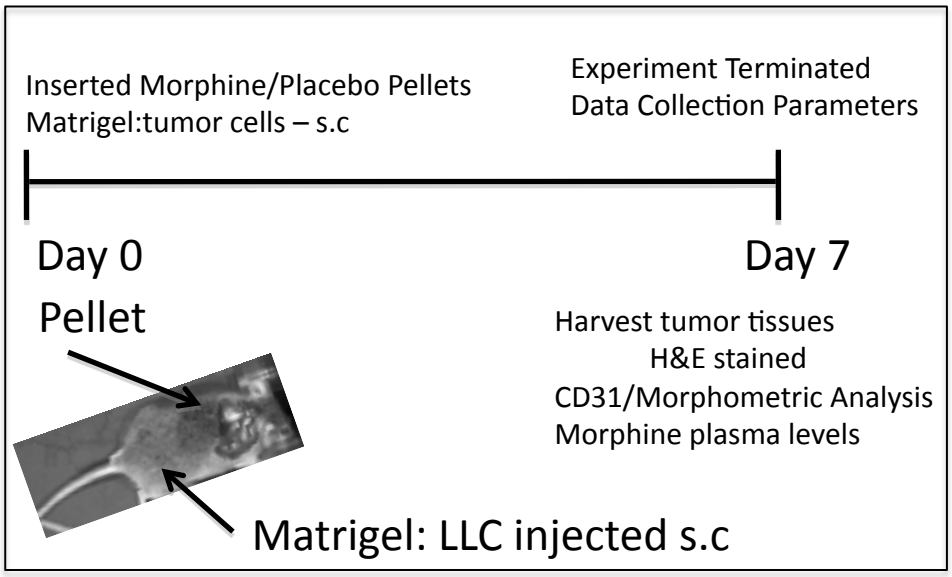

Figure 13: Model used to investigate the effect of morphine on tumor cell induced angiogenesis *in vivo*.

Approximately $1x10^6$ cells Lewis lung carcinoma cells were admixed in matrigel and injected subcutaneously into the flanks of athymic mice. At the contra-lateral site mice were implanted with either a placebo or 75mg morphine pellet. After 7days, LLC containing matrigel plugs were surgically removed, and photographed. In some experiments plugs were paraffin-embedded and processed for hematoxylin and eosin staining. In subsequent experiments plugs were snap frozen, and cryostat cut sections used for fluorescent immuno-histochemistry using CD31 for blood vessel density.

Figure 14A-F

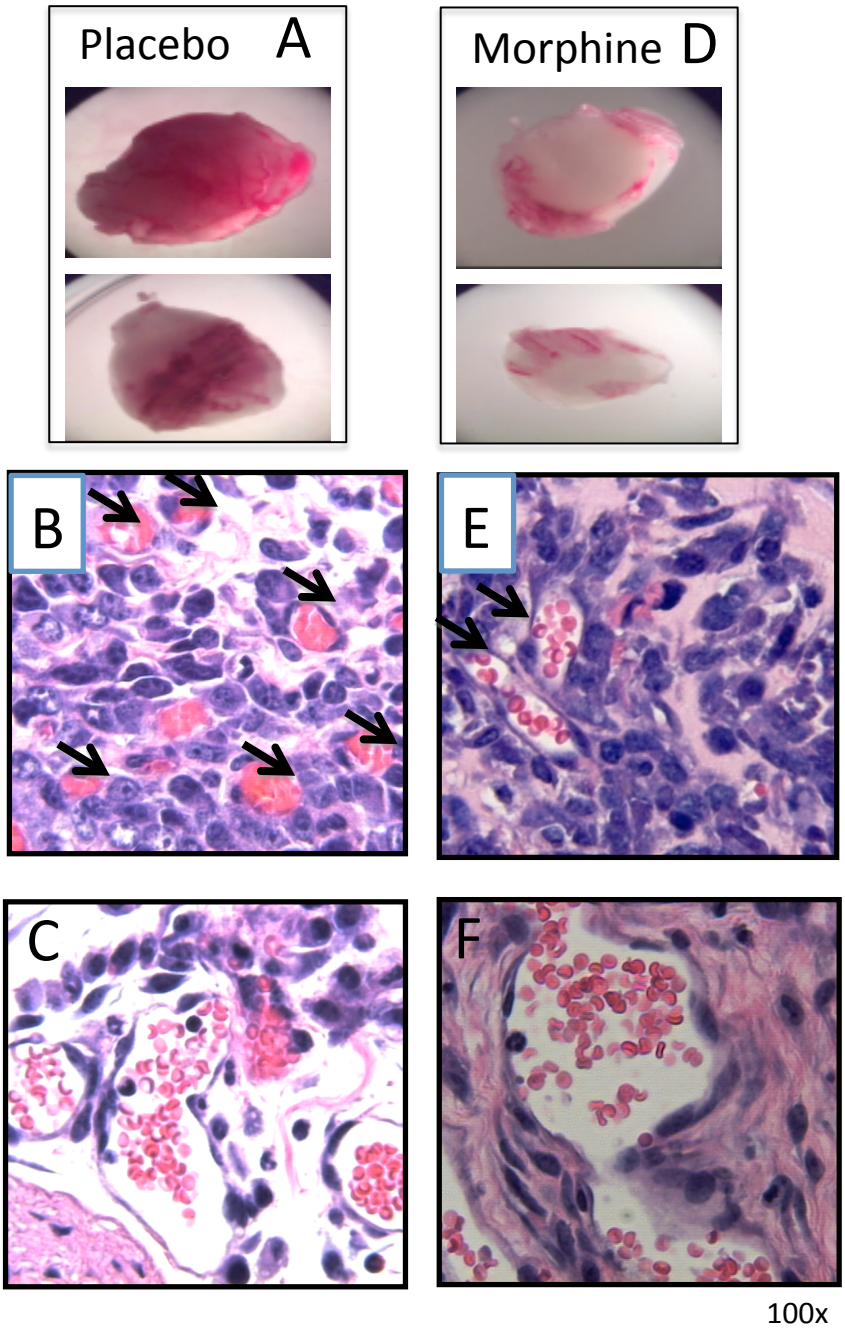

Figure 14A-F: Morphine inhibits tumor cell induced angiogenesis *in vivo*.

Images show representative whole matrigel plugs taken from placebo (A) and morphine treated (D) mice. Hematoxylin and eosin stained sections of matrigel plugs shows more blood vessels per field examined from placebo (B, arrows) compared to morphine treatment (E). Tissue histology also shows greater infiltrating leukocytes from vessels at the periphery of the matrigel plugs (C-placebo, F-morphine).

Figure 14G-J

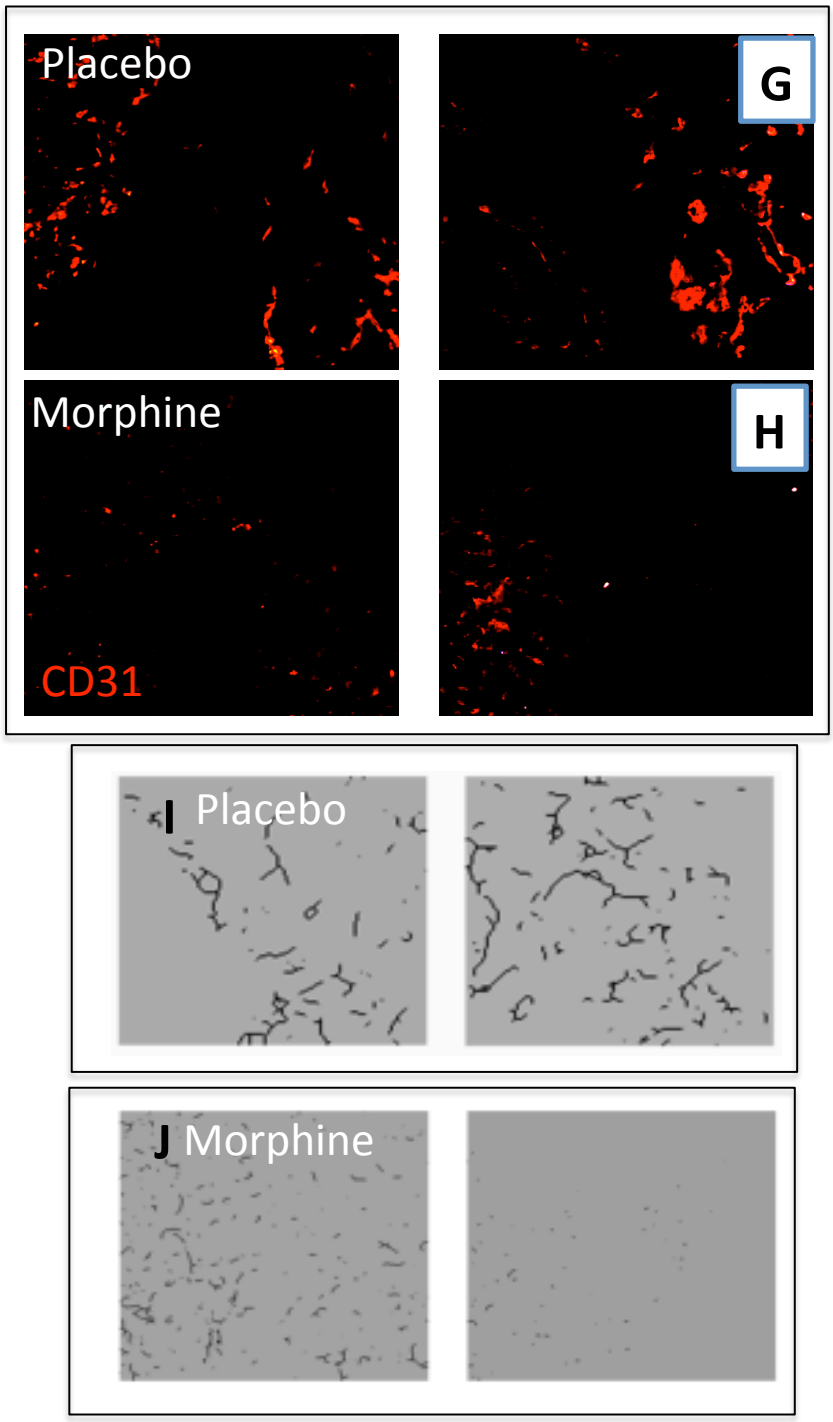

Figure 14K-M

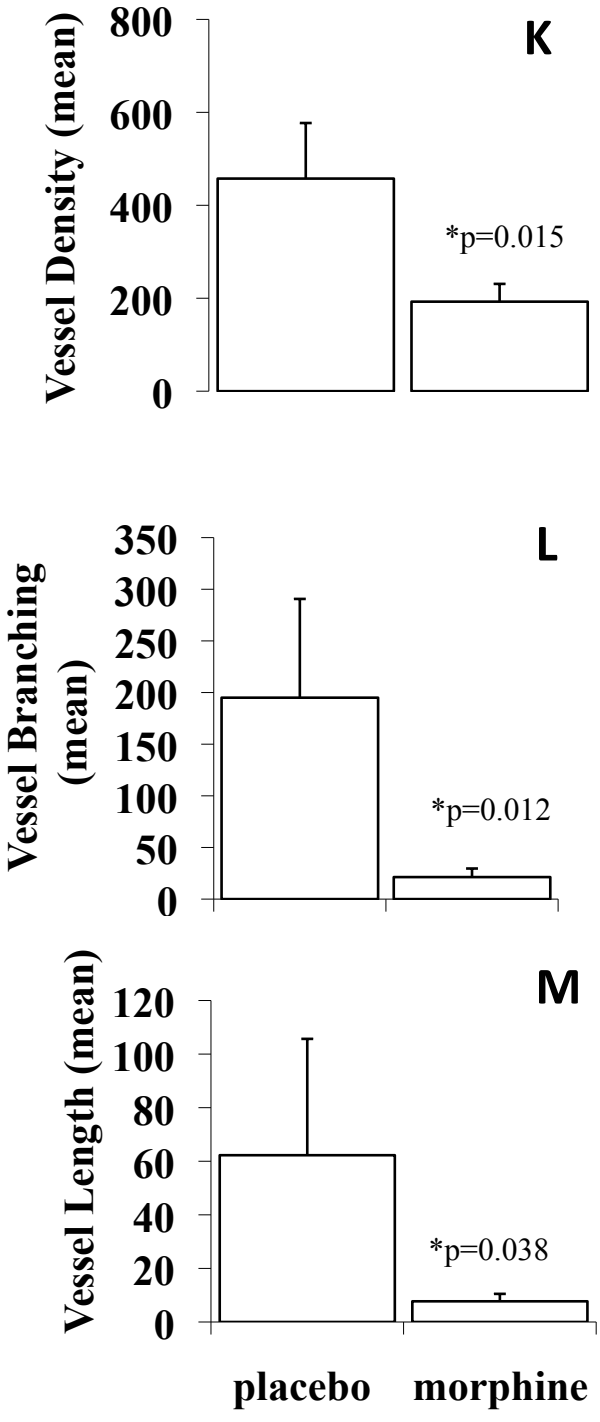
K
Vessel Density (mean)
800
600
400
200
0
*p=0.015
L
Vessel Branching (mean)
350
300
250
200
150
100
50
0
*p=0.012
M
Vessel Length (mean)
120
100
80
60
40
20
0
*p=0.038
placebo
morphine

Figure 14G-M: Morphometric analysis for blood vessel density

Morphometric analysis for blood vessel was determined using at least 10 images, collected from 3-4 different sections of the matrigel plug (n =5 per group). Sections were stained with CD31-PE (red, G-H) and digital fluorescent images were captured. Images were binarized and skeletonized (I-J) and then measured using Reindeer Plug in Functions for Adobe Photoshop for quantification of relative blood vessel density (K); branching (L); and length (M) within treatment groups.

Figure 15A-F

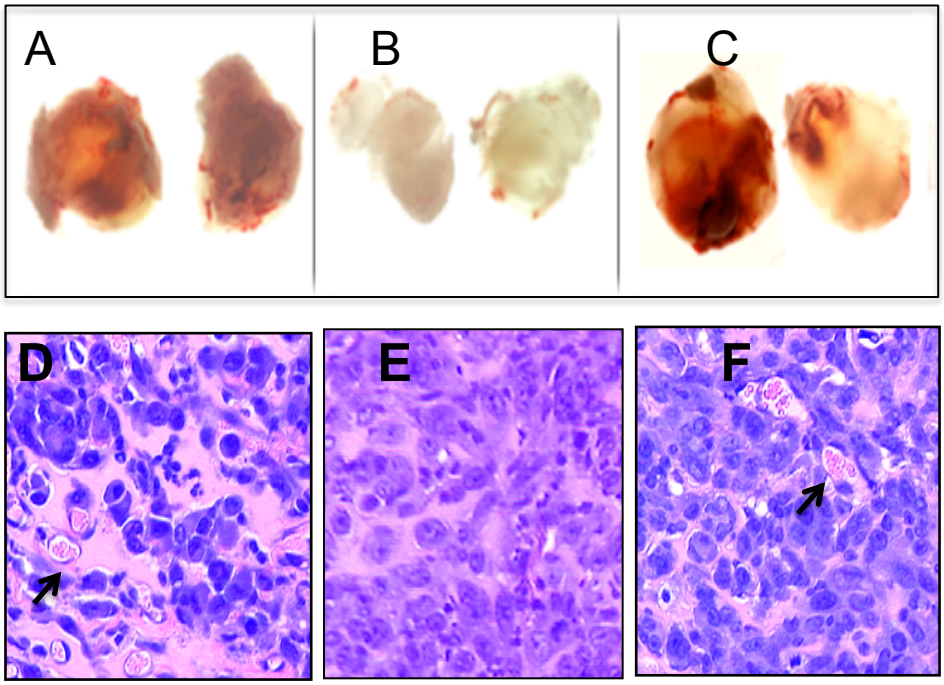

Figure 15: Naltrexone reverses morphine's inhibition on tumor cell induced angiogenesis.

Experiments were conducted as described, with the addition of a third group cotreated with morphine and naltrexone through pellet implantation. Shown are whole matrigel plugs taken from placebo (A) morphine (B) and morphine+naltrexone (C) mice. Also shown are H&E stained sections of matrigel plugs (D-F) showing blood vessel (arrows).

Figure 15G-L

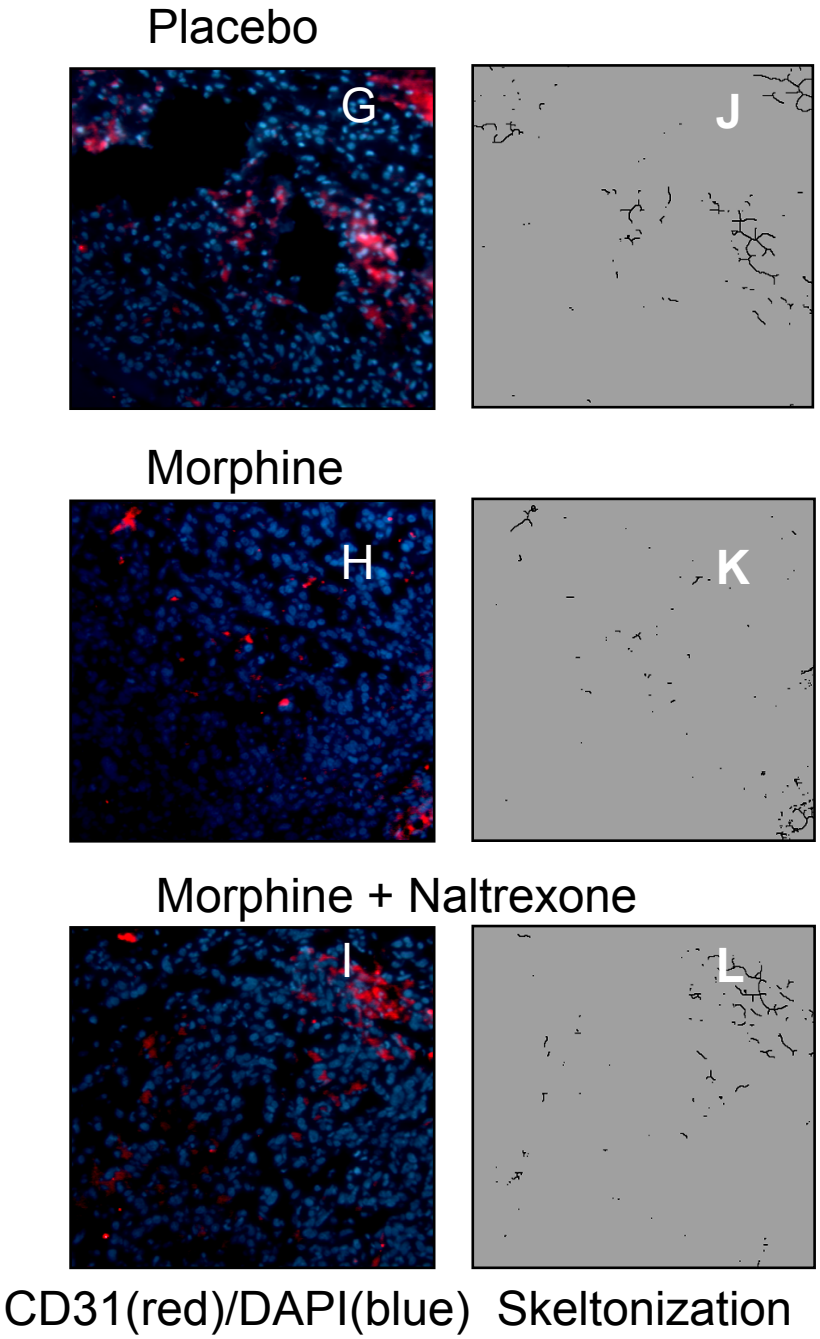
Placebo
G
J
Morphine
H
K
Morphine + Naltrexone
I
L
CD31(red)/DAPI(blue)
Skeltonization

Figure 15M-O

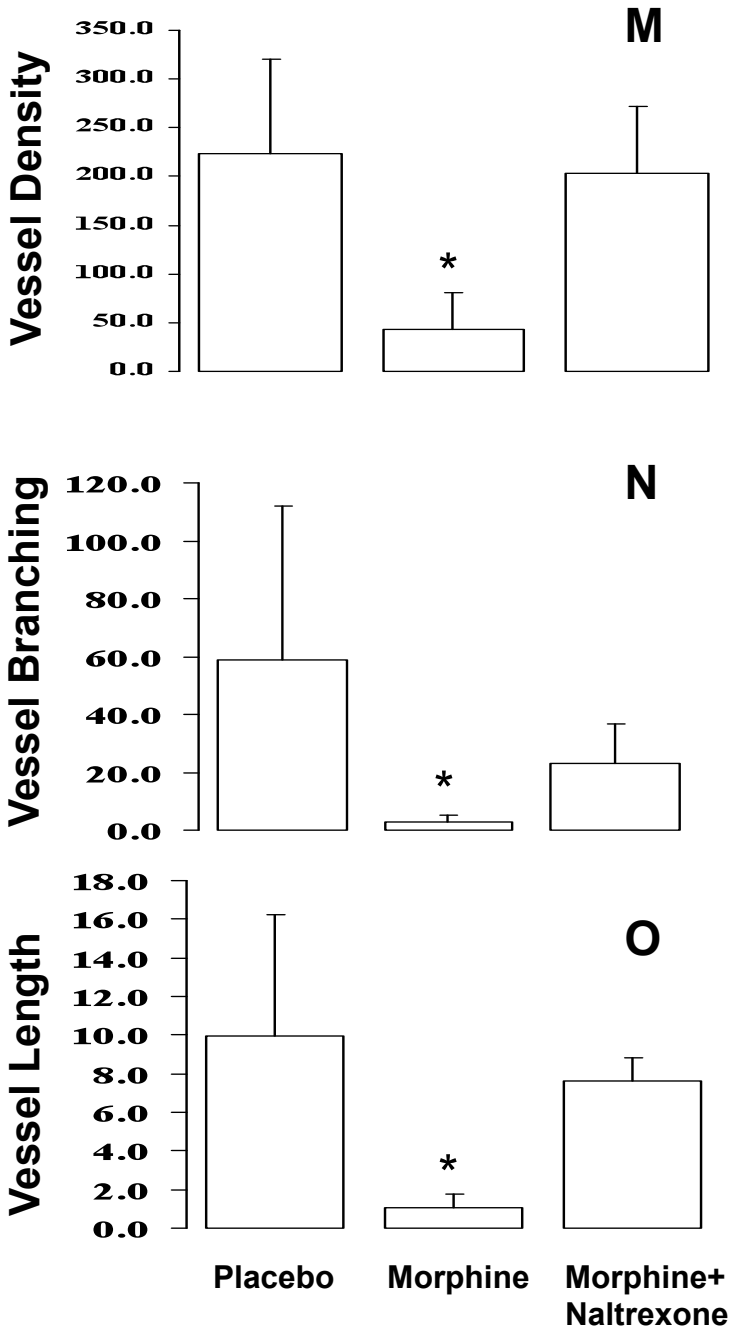
M
Vessel Density
350.0
300.0
250.0
200.0
150.0
100.0
50.0
0.0
*
N
Vessel Branching
120.0
100.0
80.0
60.0
40.0
20.0
0.0
*
O
Vessel Length
18.0
16.0
14.0
12.0
10.0
8.0
6.0
4.0
2.0
0.0
*
Placebo
Morphine
Morphine+ Naltrexone

Figure 15G-O: : Naltrexone reversed blood vessel formation in the presence of morphine as confirmed by morphometric analysis

Frozen sections were processed and stained with CD31-PE monoclonal antibodies. Images were captured in the presence of DAPI (blue, nuclear stain) using a fluorescent microscope. Graph shows the relative blood vessel density (M); vessel branching (N) and length within treatment groups, and (*) depicts that significant to placebo treatment.

Figure 16

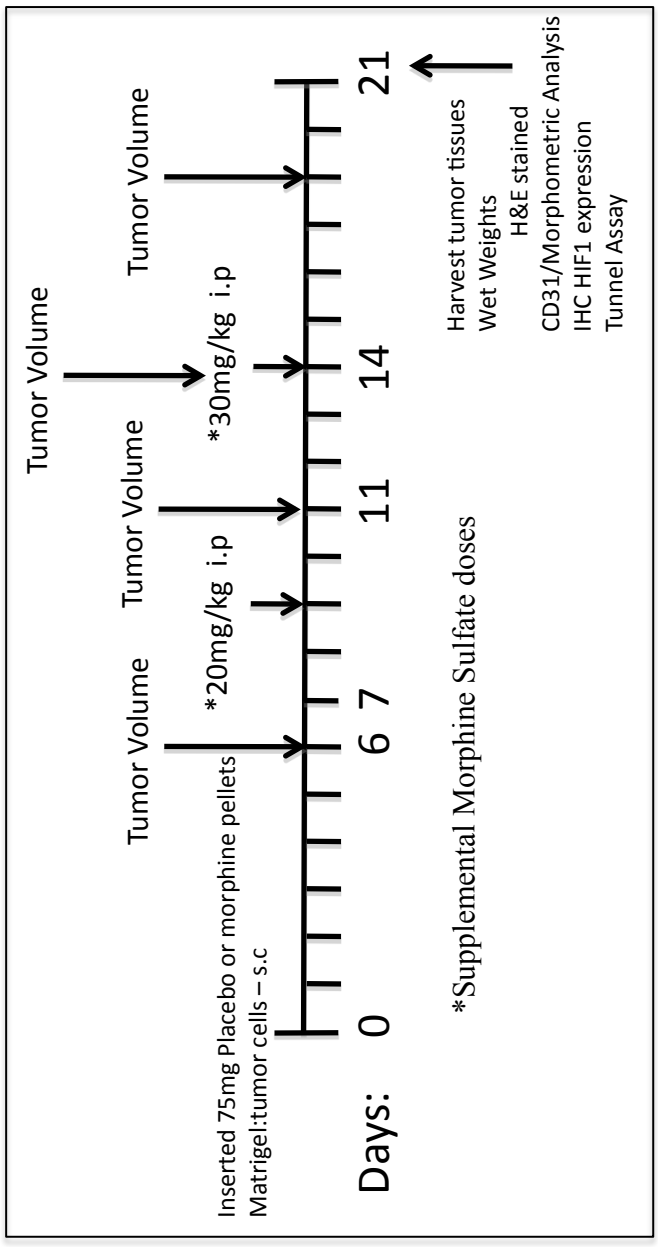
Tumor Volume
Tumor Volume
Tumor Volume
Tumor Volume
*20mg/kg i.p
*30mg/kg i.p
Inserted 75mg Placebo or morphine pellets
Matrigel:tumor cells – s.c
Days: 0 6 7 11 14 21
*Supplemental Morphine Sulfate doses
Harvest tumor tissues
Wet Weights
H&E stained
CD31/Morphometric Analysis
IHC HIF1 expression
Tunnel Assay

Figure 16: Diagram depicts model used to investigate the effect of morphine on tumor growth *in vivo*. mouse Tumor Growth Assay.

Athymic mice, 7–9 weeks of age obtained from Jackson Labs, Bar Harbor, ME were housed in a SPF facility and experiments were carried out according to approved protocols by the IACUC at the University of Minnesota. Approximately 2.0 x 10^6 Lewis Lung cancer cells were admixed in a 3 matrigel: 1 HBSS mix and then injected subcutaneously into the animals' right flank. Mice received morphine and placebo through pellet implantation method, and supplemental doses were given through out the experiment, minimizing tolerance and withdrawal. The tumor volume was calculated using the formula [(L) X (0.5W) X0.52]. On day 21 tumors were removed (n=10 per group), and photographed using a digital camera (BIPL, University of Minnesota). Tumor wet weights were recorded, and a part of the tumor was fixed in 10% neutral buffered formalin and processed for histology. The rest of the tumor samples were snap frozen in liquid nitrogen. Five-micron thick cryostat sections were used for CD31 morphometric analysis for vessel density; HIF-1α expression and Tunnel Staining for Apoptosis.

Figure 17A

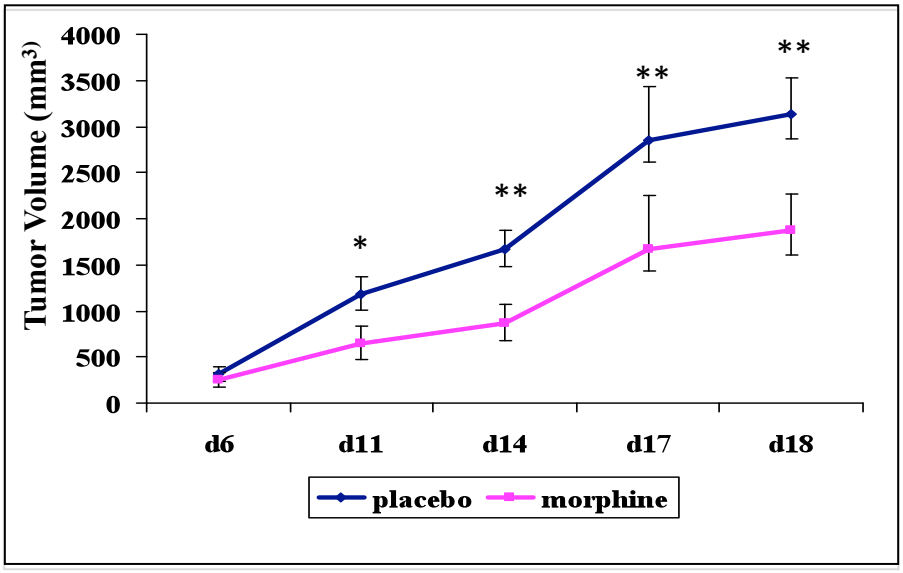
Tumor Volume (mm3)
4000
3500
3000
2500
2000
1500
1000
500
0
*
**
**
**
d6
d11
d14
d17
d18
placebo
morphine

Figure 17B

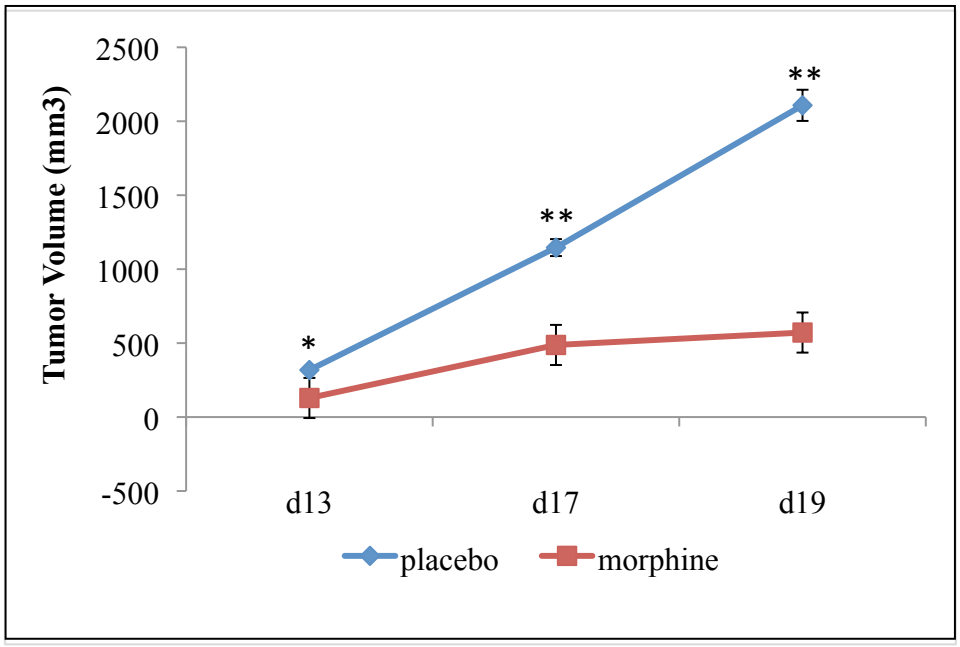
Tumor Volume (mm3)
2500
2000
1500
1000
500
0
-500
d13
d17
d19
*
**
**
placebo
morphine

Figure 17A-B: Morphine treatments reduces tumor growth using the mouse Lewis Lung carcinoma tumor model. Graph shows tumor volume measurement over the 21 day period. Tumor volume is shown over time from placebo (blue) and morphine (pink) treated mice. Data is shown from 2 individual experiments (n=10). The tumor volume was calculated using the formula [(L) X (0.5W) X0.52]. Significance was determined using a paired student's T-test between groups. Significance was set at $p<0.05$ and *($p<0.02$);**($p<0.005$).

Figure 17C-E

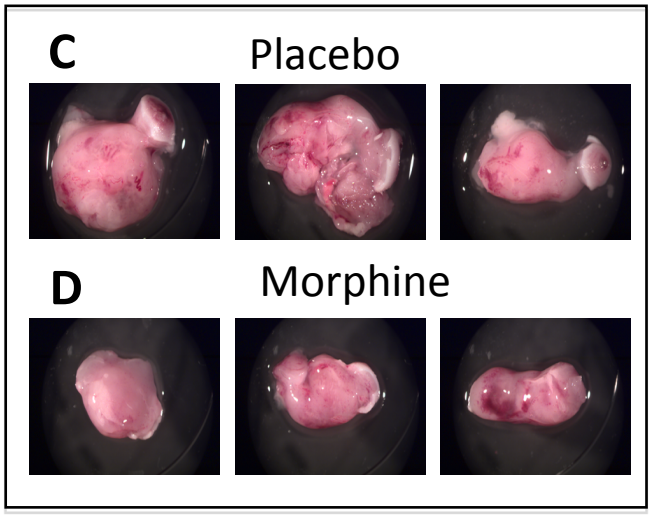
C
Placebo
D
Morphine

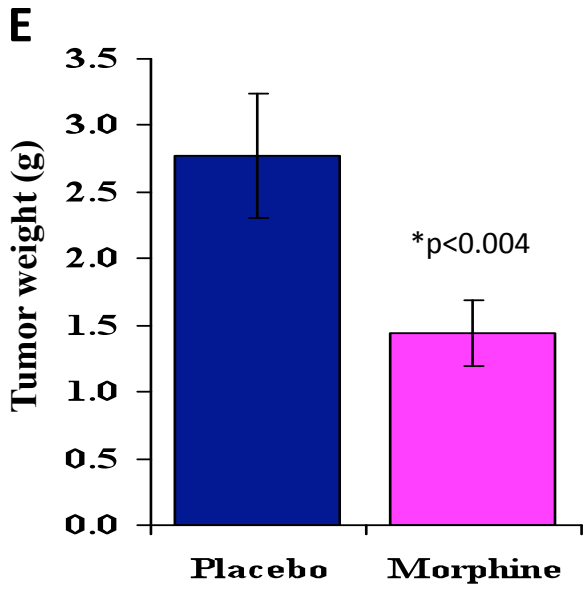
E
Tumor weight (g)
3.5
3.0
2.5
2.0
1.5
1.0
0.5
0.0
*p<0.004
Placebo
Morphine

Figure 17C-E: Morphine significantly reduced Lewis Lung carcinoma tumor growth.

Gross morphology of Lewis Lung carcinoma derived tumors after surgical removal on day 21 from tumor bearing mice treated with either placebo (C) or 75 mg morphine pellet (D) (n=10). Graph shows tumor wet-weights measured in grams (g) at the time of necropsy on day 21 (E; $p<0.05$).

Figure 17F-H (Tumor tissues)

Placebo

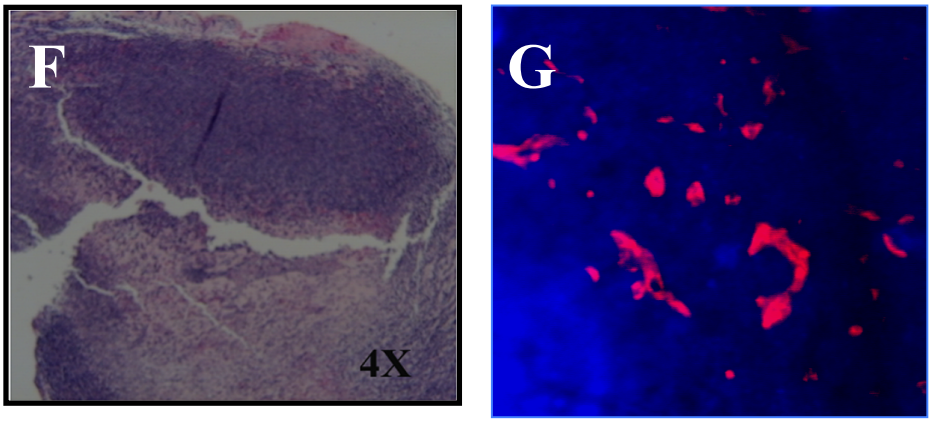

Morphine

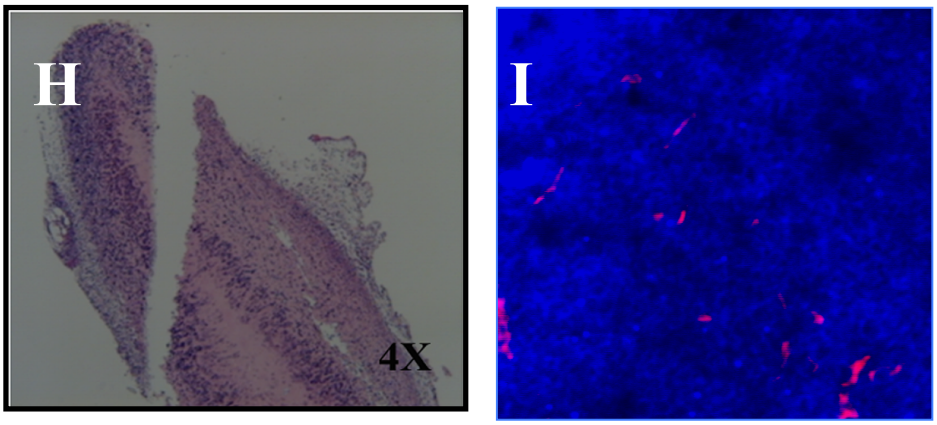

Hematoxylin Eosin Stained

CD31 (red) DAPI (blue)

Figure 17I-L

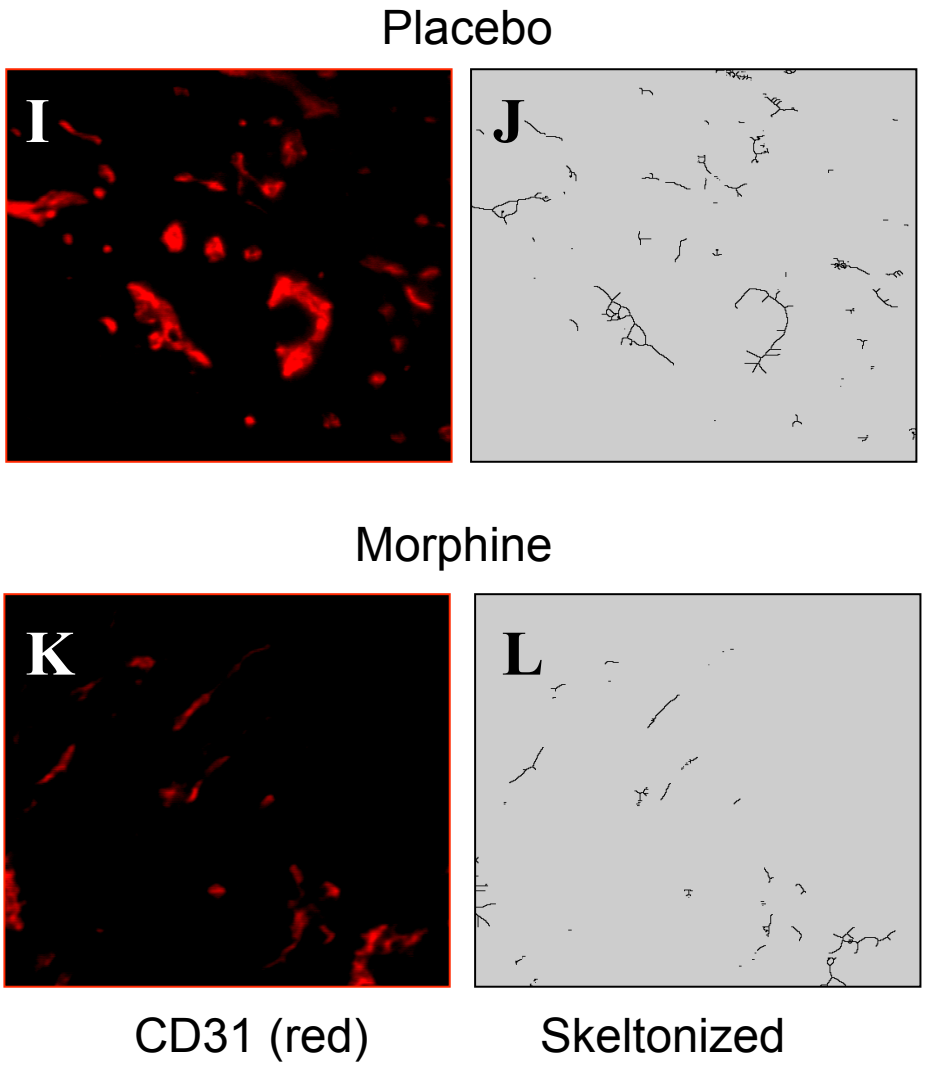

Figure 17M-O

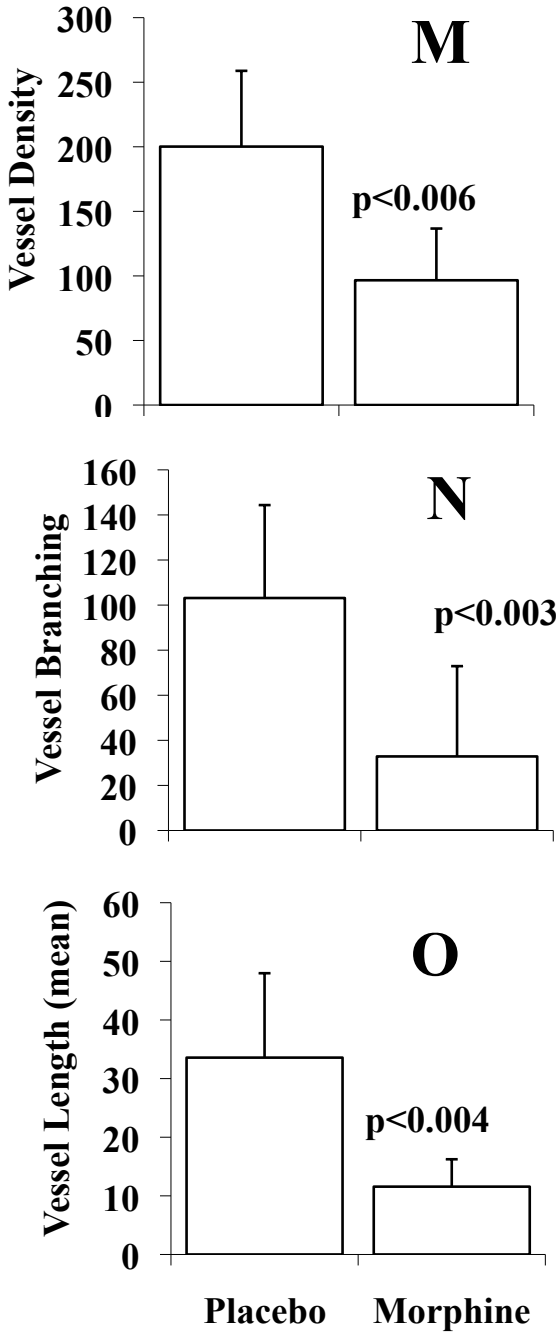
M
Vessel Density
300
250
200
150
100
50
0
p<0.006
N
Vessel Branching
160
140
120
100
80
60
40
20
0
p<0.003
O
Vessel Length (mean)
60
50
40
30
20
10
0
p<0.004
Placebo
Morphine

Figure 17F-O: Morphine treatment inhibited angiogenesis to reduce tumor growth.

Hematoxylin and eosin stained tumor sections showed increased tumor cellularity indicated by the more intense purple hematoxylin staining for cell nuclei in placebo (E) as compared to morphine (G) treatment. Images show CD31-PE (red) counterstained with the nuclear stain, DAPI (blue) after being merged; placebo (F) and morphine (H). Fluorescent microscope images of CD31-PE stained sections and corresponding skeltonized images from placebo (I, J) and morphine used in the morphometric analysis (red- I, K); showing corresponding skeletonized images (J, L) for mean vessel density (M), branching (N) and length (O). Significance was determined using a paired student's T-test between groups. Significance was set at $p<0.05$.

Figure 17P-Q

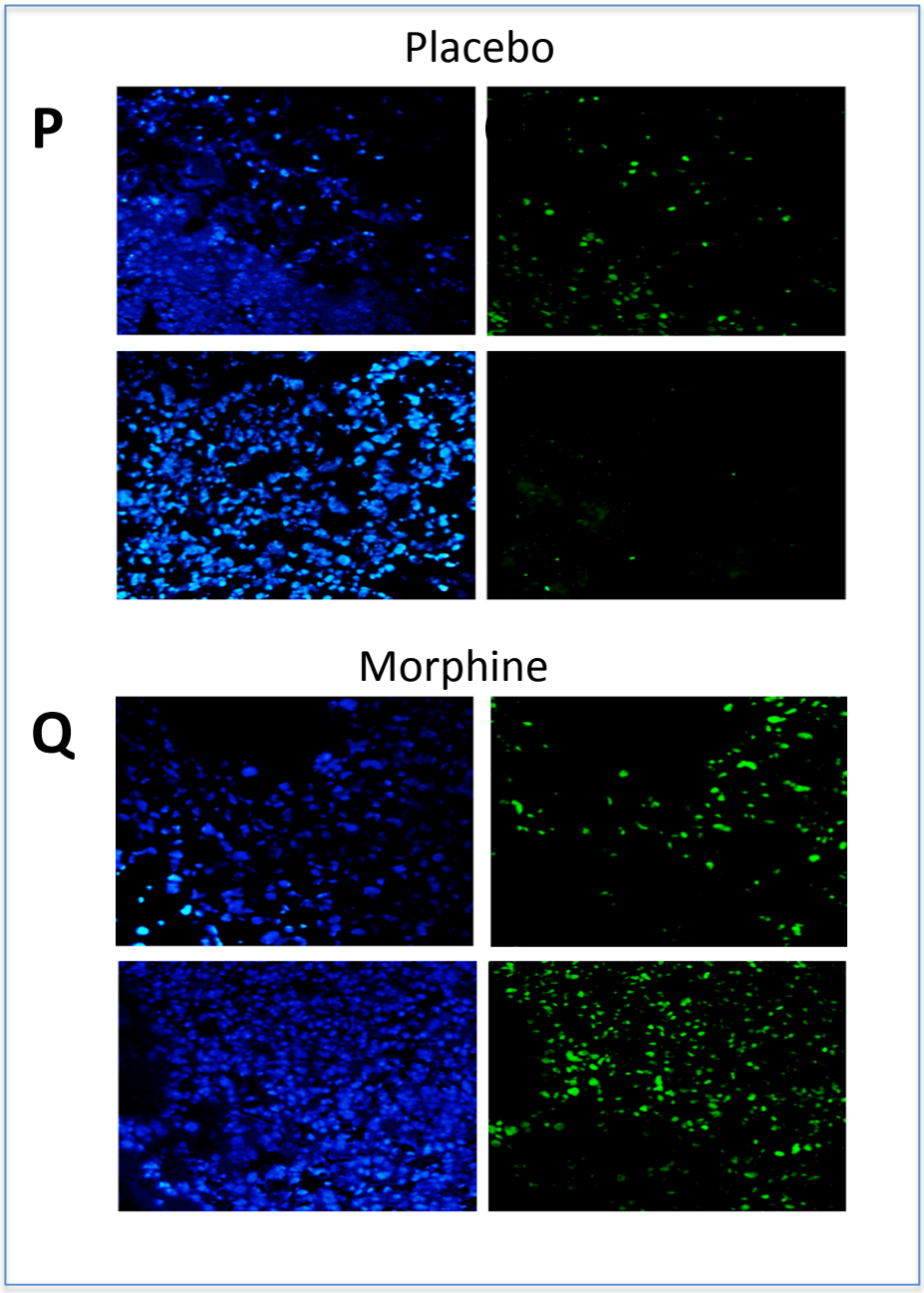

Figure 17R

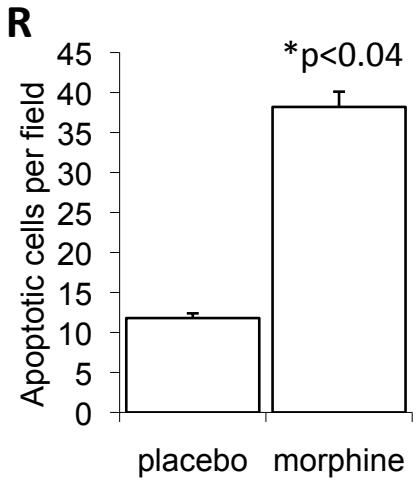

Figure 17P-R: Morphine treatment resulted in a concomitant increase in apoptotic cells within the tumor microenvironment.

Tumor sections are shown after Tunnel Labeling from placebo (P) and morphine (Q). Graph shows the quantification (R) for apoptotic tumor cells (green), counter stained with DAPI (nuclei, blue). Images were processed in Metamorph to determine the number of apoptotic cells per field (n=10).

Figure 17S-T

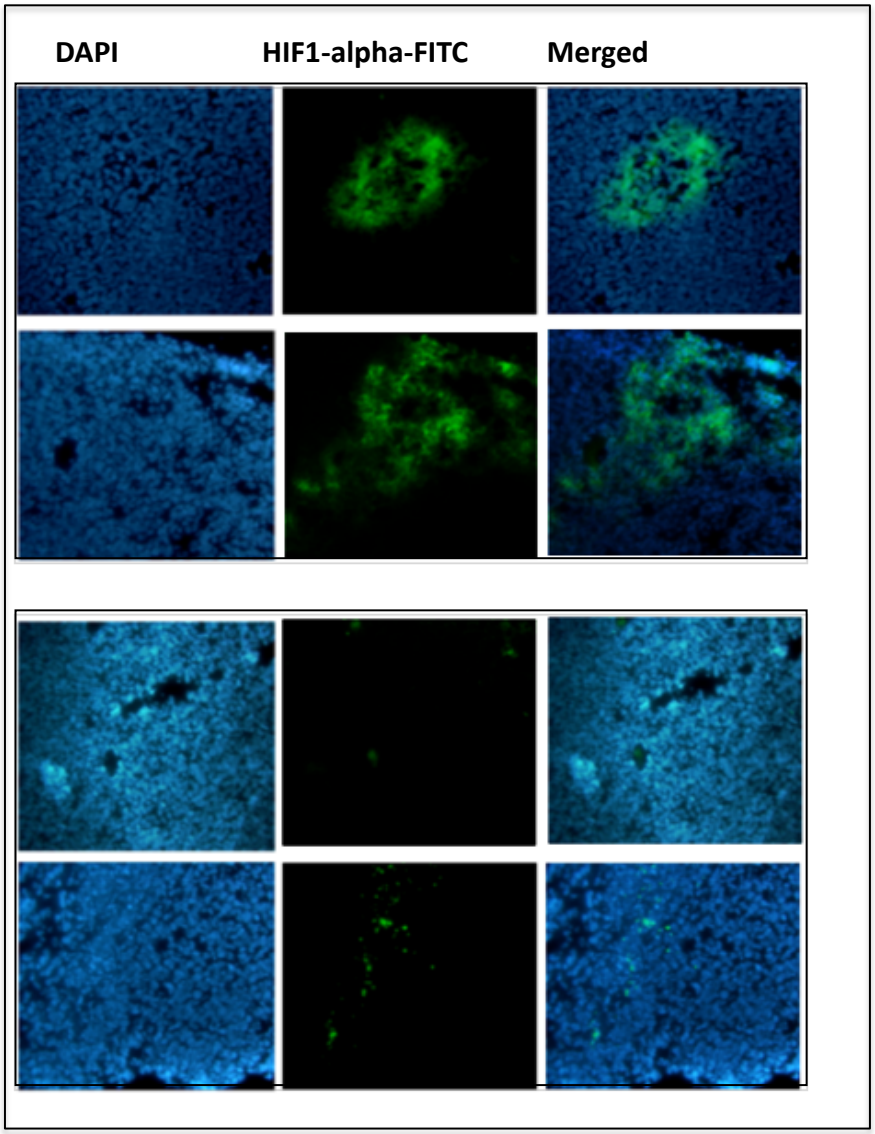

Figure17S-T: Morphine treatment resulted in a concomitant decrease in HIF1-alpha expression within the tumor microenvironment.

Paraffin-embedded sections from placebo (S) and morphine (T) were processed as described and then stained with primary polyclonal HIF1α antibodies and secondary FITC conjugated antibodies. Stained images were visualized in the presence of DAPI, nuclear stain (blue) (n=5 mice per group).

Figure 18A

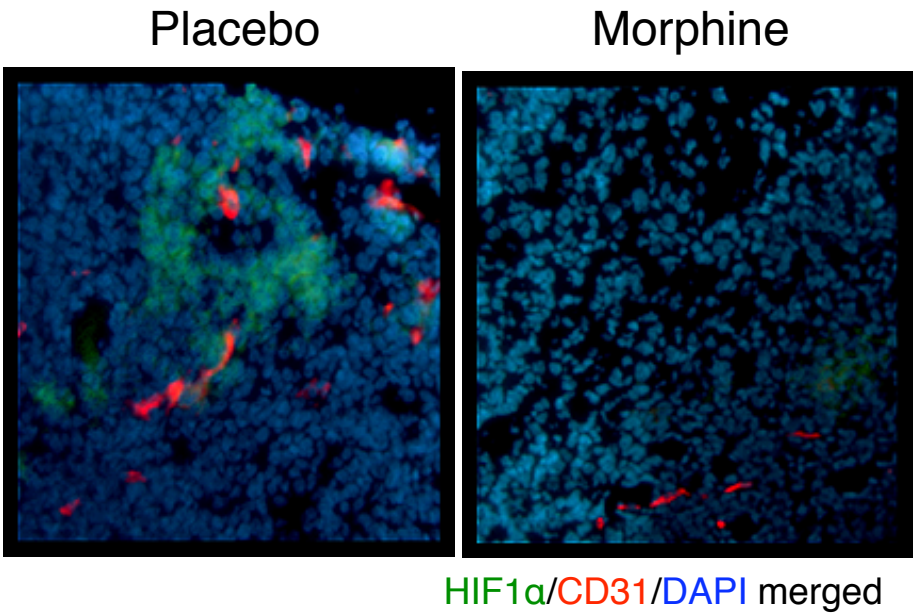

Figure 18A: HIF-1alpha expression within Lewis Lung carcinoma tumor microenvironment

Tumor sections taken from placebo and morphine were first stained for HIF-1α (green) as described. Sections were then stained for CD31 (red) and images captured in the presence of the nuclear stain DAPI (blue). Adobe Photoshop was used to screen and merge corresponding HIF-1α , CD31 and DAPI images. Merged images showed that HIF-1α was associated more with the tumor cells than the CD31+ endothelial cells.

Figure 18B

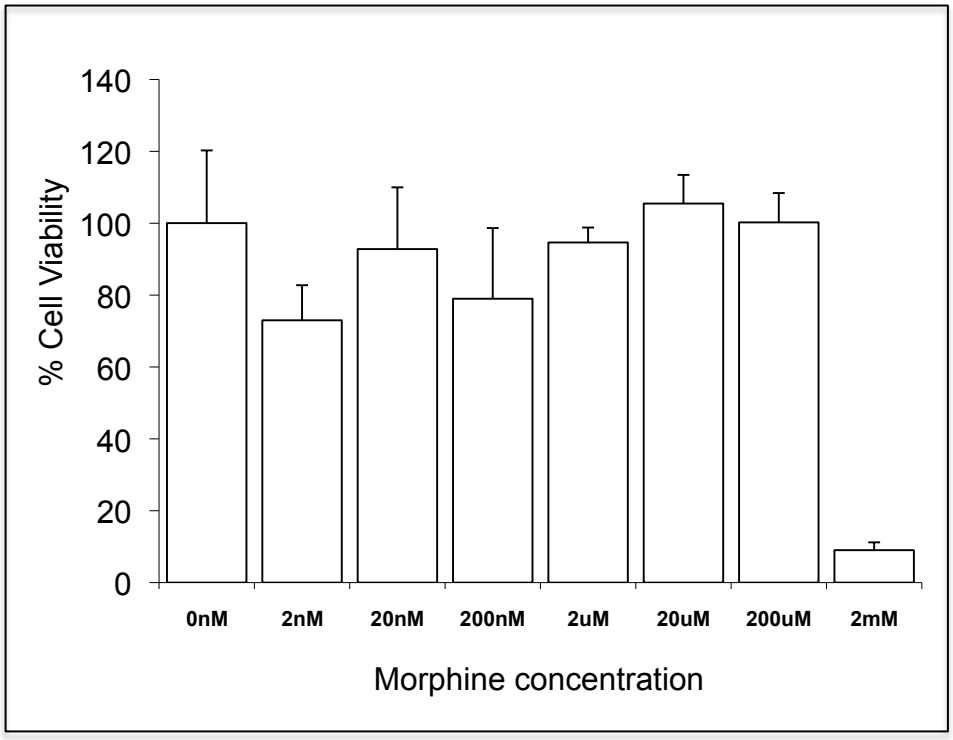

Figure 18B: Effect of long term morphine on Lewis Lung carcinoma cell viability *in vitro*.

LLC cells were plated in 96 well plates at low density and viability assessed in 1% serum+growth media containing morphine at 2nM-2.0mM final concentration. Cells were incubated in a 37^0C incubator for 72hrs without changing the growth media, after which the MTT assay was used to determine cell viability. The change in cell viability is represented as a % of control (morphine-untreated LLC cells).

Figure 18C

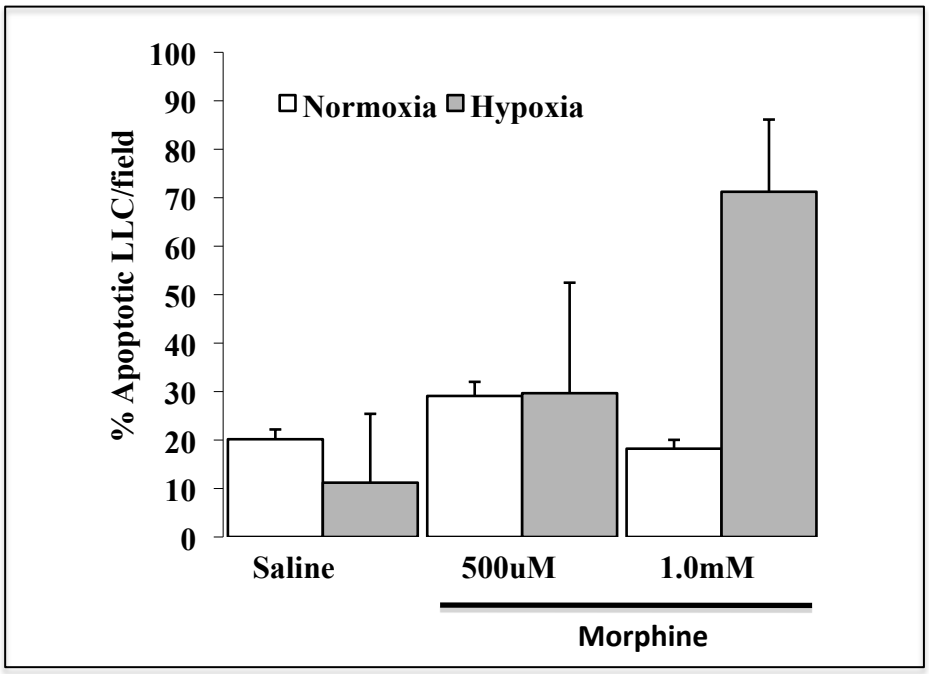

Figure 18C: Effect of morphine on tumor cell apoptosis *in vitro*.

Lewis Lung Carcinoma cells were plated on 8-well chamber slides. Cells were treated with increasing morphine concentrations under low serum. After 48hrs, growth media was removed, cells were fixed and labeled with Tunnel stain. Graph shows the quantification of apoptotic cells, as the % of cells apoptotic out of total cells present in that field. At lower concentrations under normoxia, morphine did not induce any significant apoptosis compared to controls. However, at higher morphine concentrations apoptosis was more prominent under hypoxia ($p<0.05$).

Figure 19A

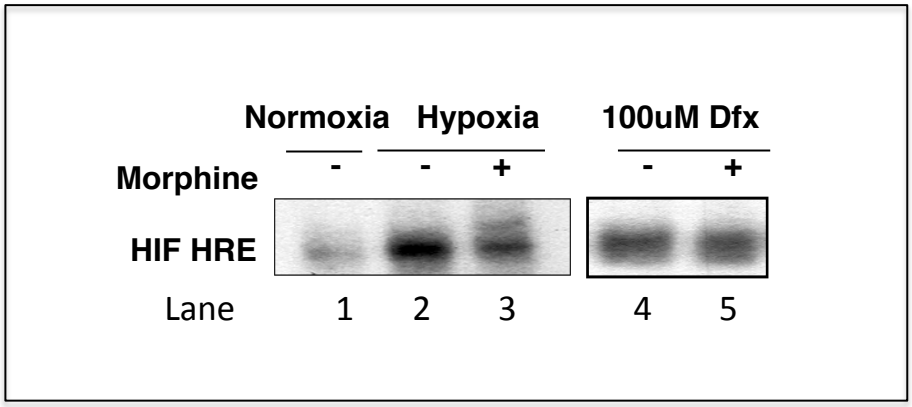

Figure 19A: Morphine inhibits hypoxia-induced but not DFO-induced activation of HIF-1.

Control cells kept under normoxia, hypoxic morphine untreated and treated cells, and cells treated with the hypoxia mimetic, DFO under normoxia in the absence and presence of morphine were harvested and nuclear proteins isolated. Equal amounts of nuclear extracts (10ug) were incubated with the Hypoxia Response Element-specific HIF1a-binding sequence (5′-TCA GT**A CGT** GAC CAC ACT CAC CTC -3′) and (3'-AGACA**T GCA** CTG GTG TGA GTG GAG-5') as described. The DNA protein complexes were resolved by poly-acrylamide gel electrophoresis in an Electromobility Shift Assay.

Figure 19B

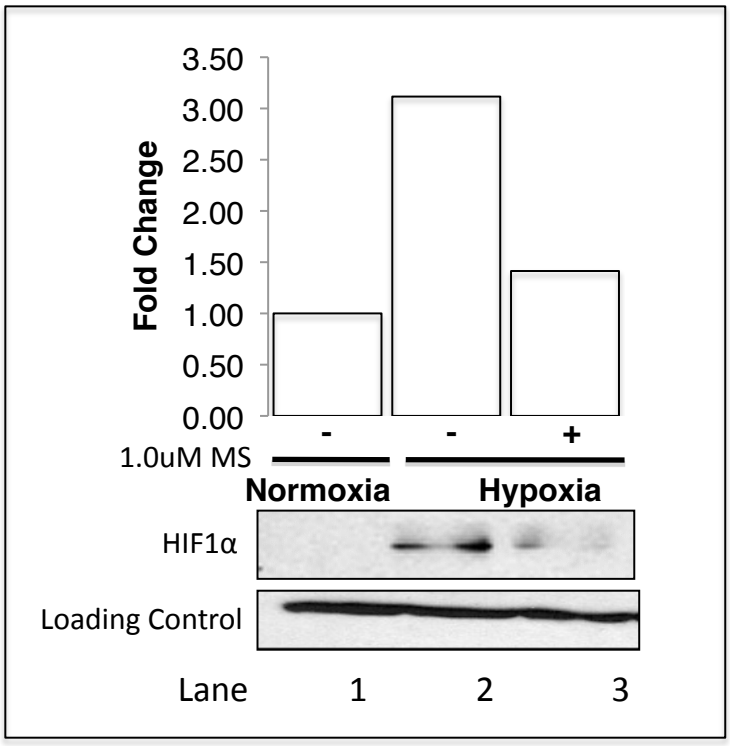
3.50
3.00
2.50
2.00
1.50
1.00
0.50
0.00
Fold Change
-
-
+
1.0uM MS
Normoxia
Hypoxia
HIF1α
Loading Control
Lane
1
2
3

Figure 19B: Morphine inhibits nuclear translocation of HIF-1α. using Western Blot Analysis.

Lewis Lung carcinoma control cells, hypoxic morphine untreated and pretreated cells were treated as described in methods. Cells were harvested and equal amounts of nuclear proteins were subjected to a Western Blot Assay to determine HIF-1α protein expression using monoclonal antibodies directed to the ODD domain of the HIF-1α proteins. Antibody probed blots were visualized using ECL detection reagent. Graph represents fold change determined from the densitometric ratio of HIF1alpha to POLII and compared to control, normoxic cells.

Figure 19C

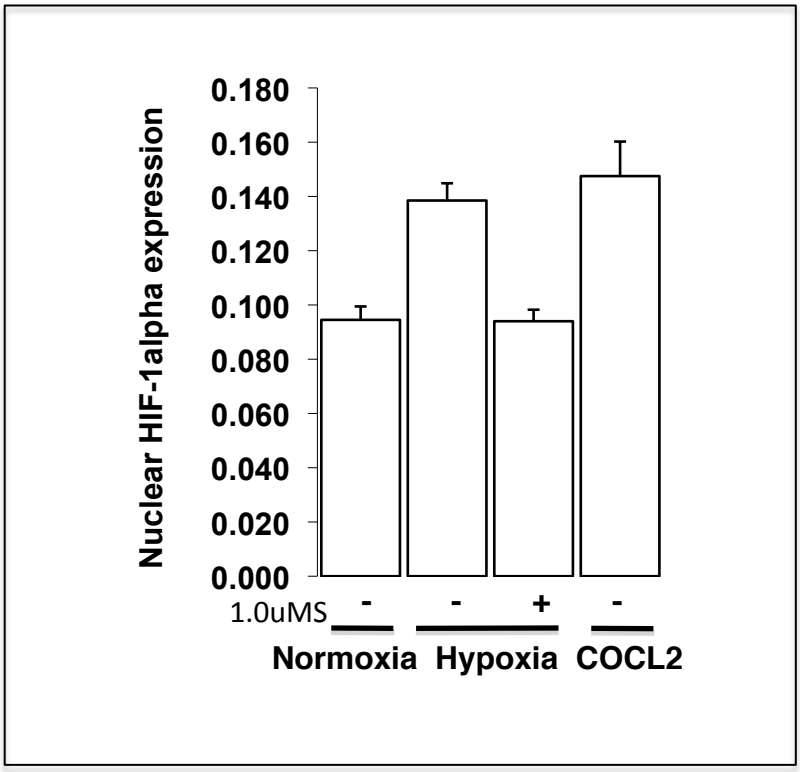
Nuclear HIF-1alpha expression
0.180
0.160
0.140
0.120
0.100
0.080
0.060
0.040
0.020
0.000
1.0uMS
-
-
+
-
Normoxia
Hypoxia
COCL2

Figure 19C: Morphine treatment inhibits nuclear translocation of HIF-1α.

The HIF1alpha Duo-Set Kit was used to further validate the effect of morphine on the nuclear expression of HIF-1α. Here, nuclear proteins were isolated from experimental cells and biotin labeled using ds oligonucleotides for HIF-1α. Specificity of binding through competition, was determined by added 3x the amount of unlabeled ds oligonucleotides. Labeled proteins was added to pre-coated plates as directed by manufacturer and optical density determined using a microplate reader at 450nm. Data is represented as the relative HIF1alpha levels after subtraction of optical density from values of biotin labeled and unlabeled ds oligonucleotides. Cobalt chloride was used here as a positive control, a known activator of HIF-1.

Figure 19D-E

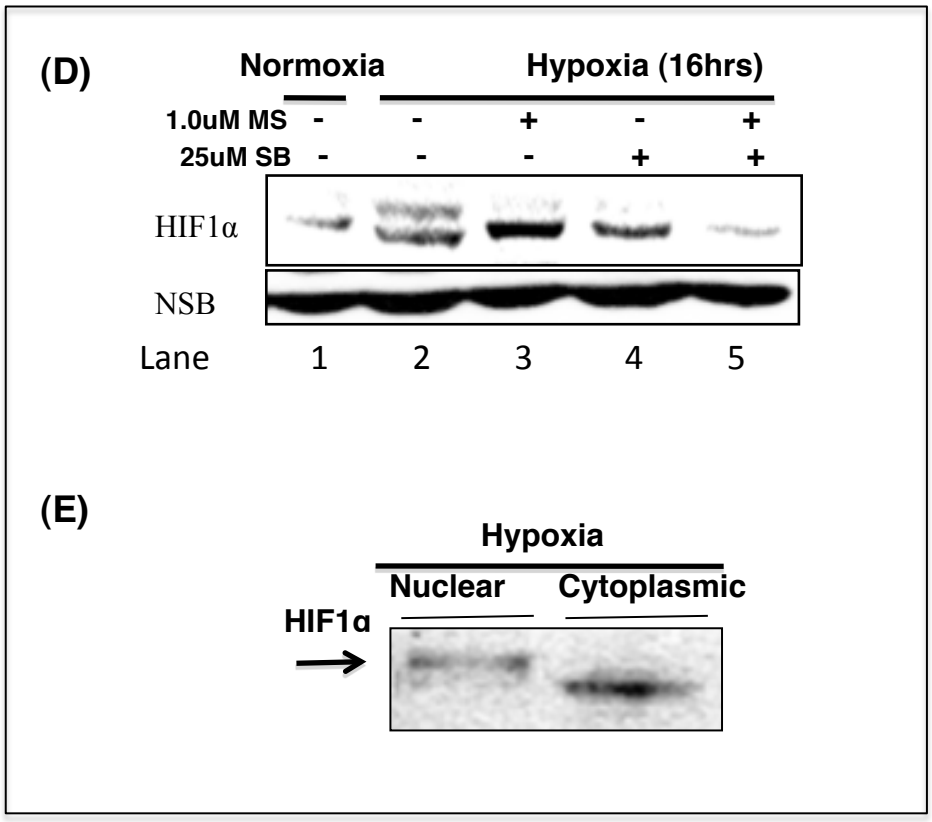
(D)
Normoxia
Hypoxia (16hrs)
1.0uM MS - - + - +
25uM SB - - - + +
HIF1α
NSB
Lane 1 2 3 4 5
(E)
Hypoxia
Nuclear
Cytoplasmic
HIF1α

Figure 19D-E: Morphine inhibits the hypoxia induced activation of HIF-1 similar to p38 MAPK inhibitor, SB203585 .

Lewis Lung carcinoma cells were cultured and harvested as described in methods to determine the total cellular expression of HIF1α using Western blot Analysis (D). Nuclear and cytoplasmic proteins were further separated after hypoxia treatment and then were used to determine the localization of the higher migrating band also using Western blot Analysis (E), immuno-blotting with the appropriate HIF-1α antibodies.

Figure 20A

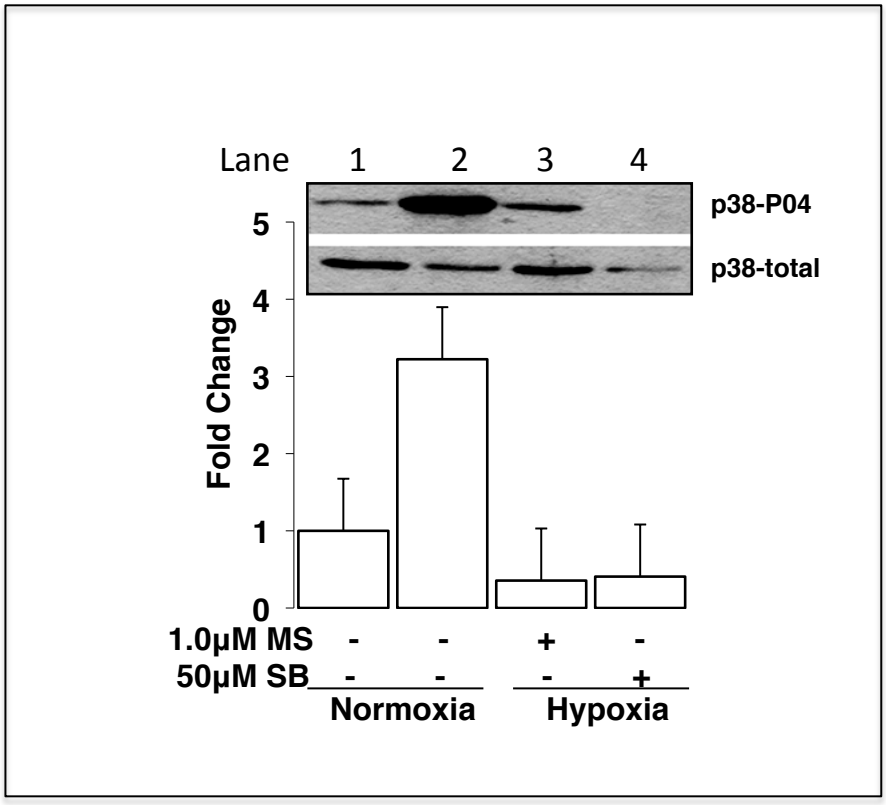
Lane 1 2 3 4
p38-P04
p38-total
Fold Change
0
1
2
3
4
5
1.0μM MS - - + -
50μM SB - - - +
Normoxia
Hypoxia

Figure 20A: Morphine inhibits hypoxia-induced activation of P38MAPK in vitro.

Lewis Lung carcinoma cells were cultured under normoxia and hypoxia in the presence and absence of morphine and the p38 MAPK inhibitor SB203585. Equal amounts of proteins was determined using the Bradford Assay was subsequently analyzed using Western Blot Analysis. Blots were incubated with total and phosho-P38 antibodies. Densitometric units were determined using BIORAD software. Graph shows the relative expression of activated p38; p38-phospho that was first normalized to total-p38, and then compared to control cells.

Figure 20B

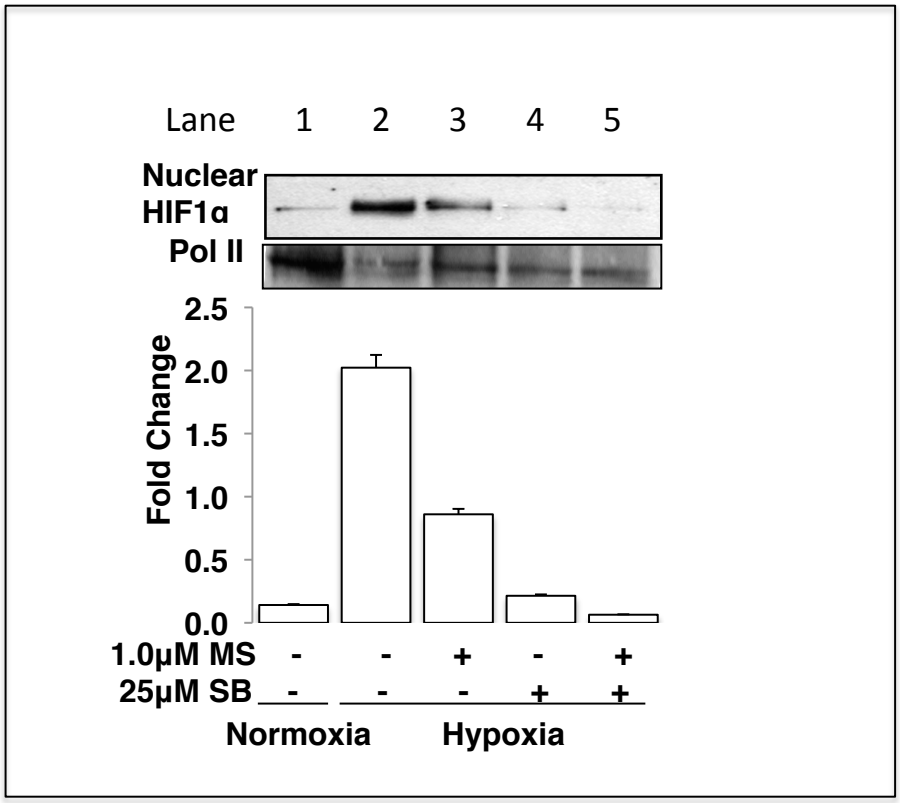

Figure 20B: Morphine and inhibition of P38MAPK synergistically decreases HIF-1alpha nuclear localization *in vitro*.

Cells were cultured as described and protein extracts were subjected to Western Blot Analysis using antibodies for HIF1α and POLII. Densitometric units were determined using BIORAD software and ratio of nuclear HIF1α to POLII was calculated. Graph shows the fold change compared to controls.

Figure 20C

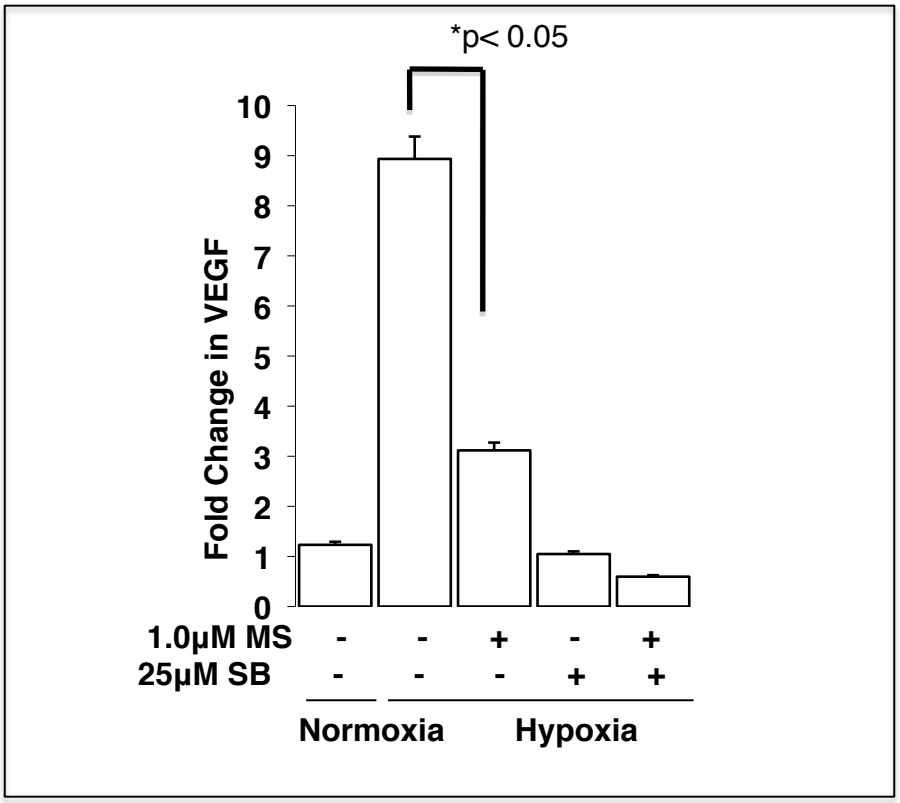

Figure 20C: Inhibition of hypoxia induced p38 MAPK activation leads to decreased hypoxia-induced VEGF expression *in vitro*.

Lewis Lung carcinoma cells were cultured as described and total RNA was isolated. Mouse VEGFA mRNA was determined using real-time RT-PCR. Data is expressed as fold change in mRNA expression as determined after normalization with GAPDH and comparison to untreated controls.

Figure 21A

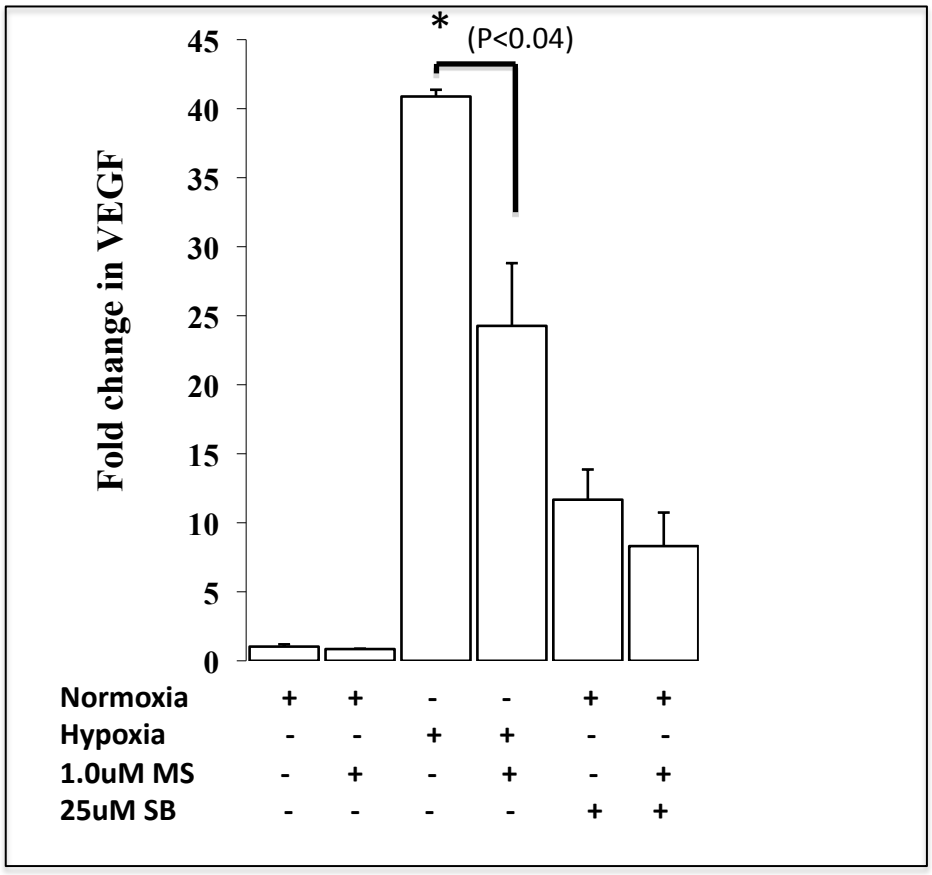

Figure 21A: Morphine suppresses hypoxia induced VEGFA gene expression from human Ovarian carcinoma cells *in vitro*.

MA-148 ovarian cancer cells, were treated similar to LLC cells as described and total RNA was isolated. Human VEGF A primers were used to determine the relative VEGF A gene expression using real-time RT-PCR. Data is expressed as fold change over control cells after normalization with housekeeping gene GAPDH.

Figure 21B

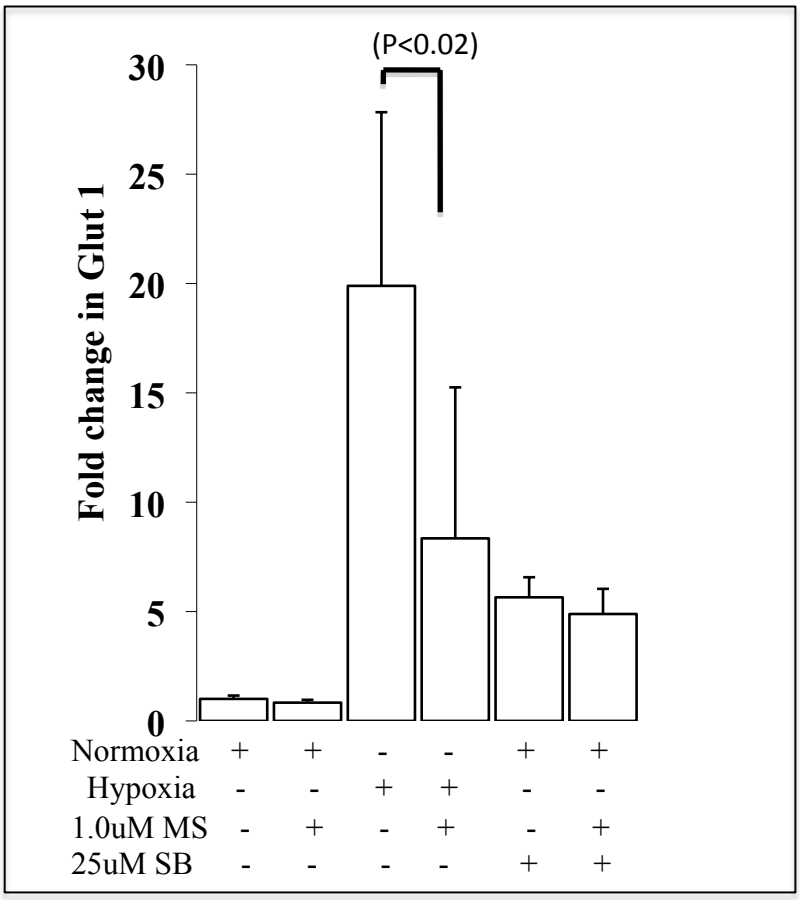

Figure 21B: Morphine inhibits hypoxia induced Glut1 gene expression from human Ovarian carcinoma cells *in vitro*.

MA-148 ovarian cancer cells, were treated similar to LLC cells as described and total RNA was isolated. Human Glut1 primers were used to determine the relative Glut-1 gene expression using real-time RT-PCR. Data is expressed as fold change over control cells after normalizing with GAPDH.

Figure 21C

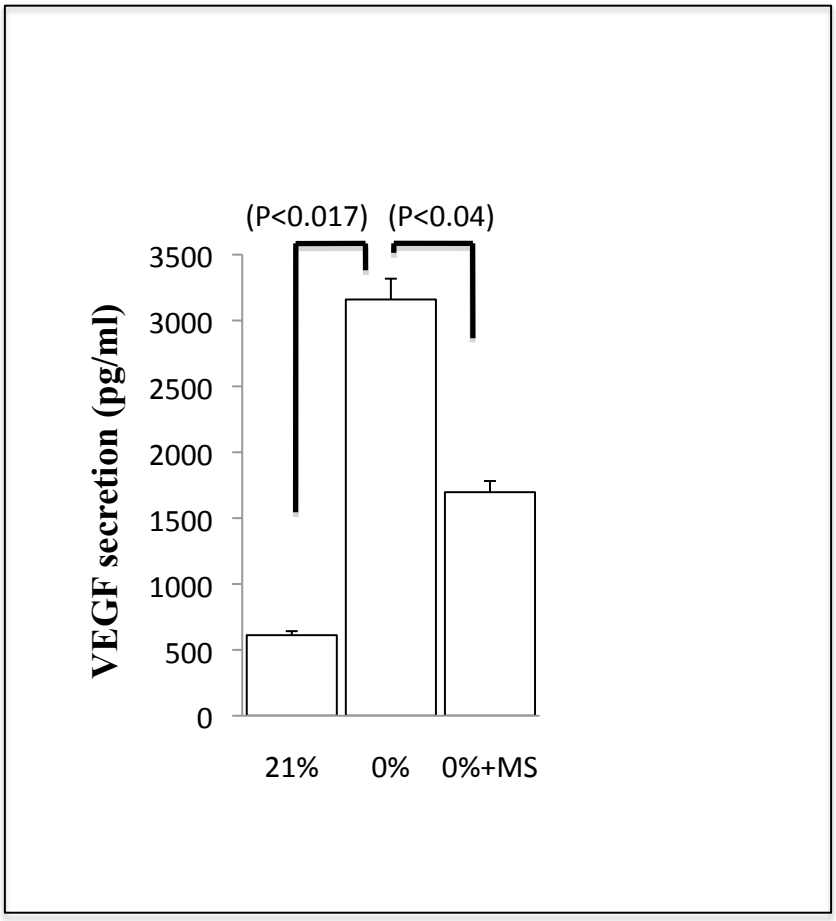

Figure 21C: Morphine inhibits VEGFA protein expression from human ovarian carcinoma cells *in vitro*.

MA-148 ovarian cancer cells were subjected to hypoxia in the presence and absence of morphine for 48 hrs and cell free supernatants were used in an ELISA to determine VEGF A protein secretion in pg/ml.

Figure 21D

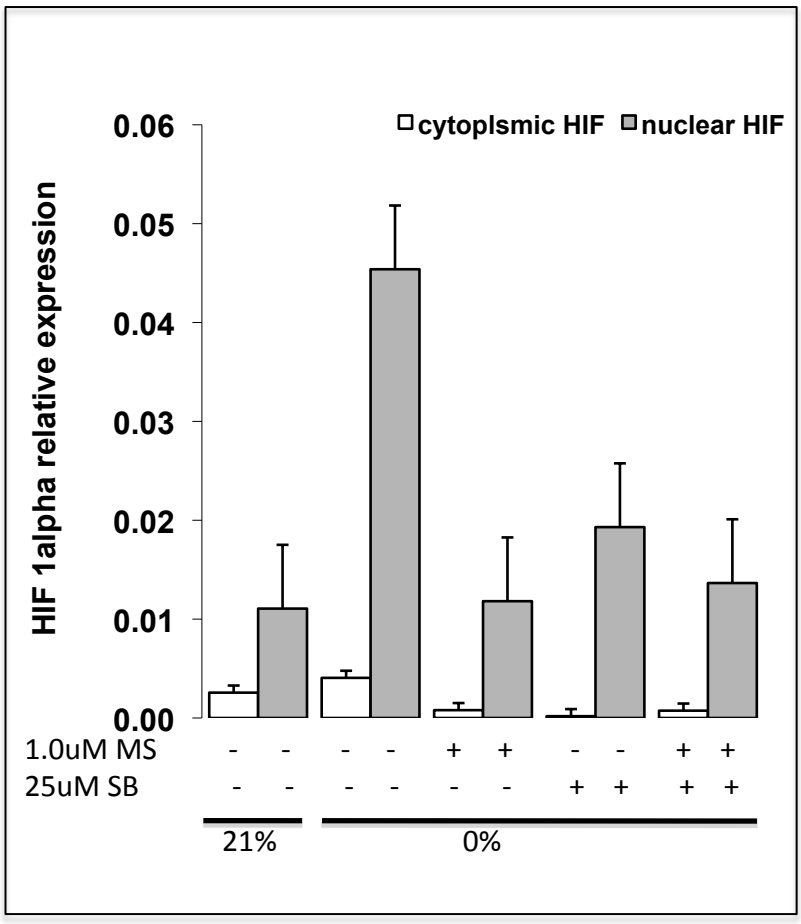
cytoplsmic HIF
nuclear HIF
HIF 1alpha relative expression
0.06
0.05
0.04
0.03
0.02
0.01
0.00
1.0uM MS
25uM SB
- - - - + + - - + +
- - - - - - + + + +
21%
0%

Figure 21D: Morphine inhibits hypoxia induced HIF-1α cytoplasmic accumulation and nuclear localization in human Ovarian carcinoma cells *in vitro*.

The HIF1alpha Duo-Set Kit was used to further validate the effect of morphine on the nuclear expression of HIF-1^{α} in MA-148 ovarian cancer cells. Here, nuclear proteins and cytoplasmic protein were isolated from experimental cells and HIF1alpha expression determined as described. Data is represented as the relative HIF1alpha levels after subtraction of optical density from values of biotin labeled and unlabeled ds oligonucleotides.

Figure 22

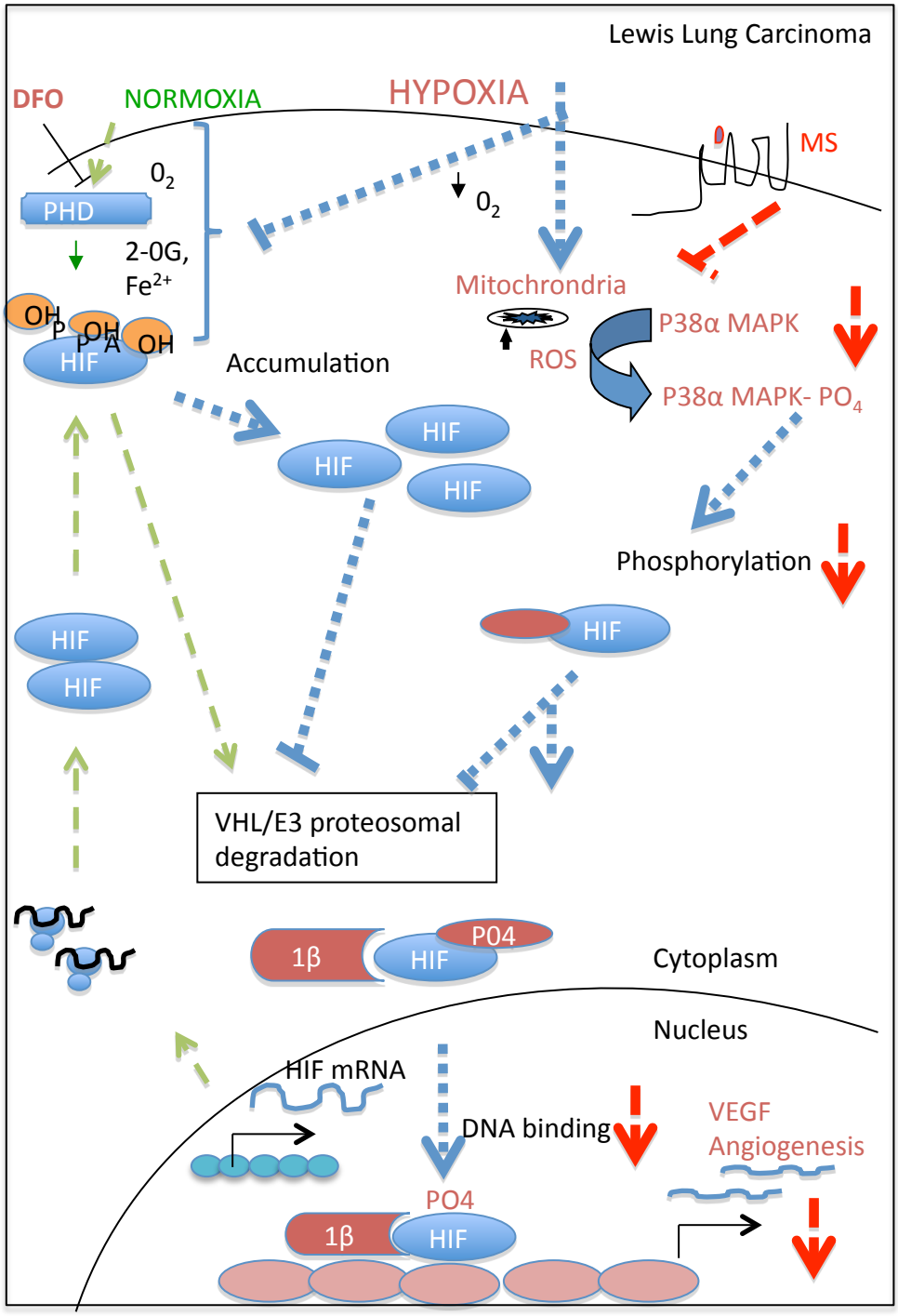
Lewis Lung Carcinoma
DFO
NORMOXIA
HYPOXIA
MS
0_2
PHD
2-0G,
Fe^{2+}
OH
P
OH
P
A
OH
HIF
Accumulation
0_2
Mitochrondria
ROS
P38α MAPK
P38α MAPK- PO_4
HIF
HIF
HIF
Phosphorylation
HIF
HIF
HIF
VHL/E3 proteosomal
degradation
1β
HIF
P04
Cytoplasm
Nucleus
HIF mRNA
DNA binding
VEGF
Angiogenesis
PO4
1β
HIF

Figure 22: A signaling model for the effect of morphine on hypoxia induced HIF-1α. Based on our current findings we propose that morphine alters the hypoxic activation of the p38 MAPK signaling pathway that activates HIF-1. Under hypoxia p38 MAPK activation leads to an increased HIF-1α nuclear accumulation. Morphine treatment reduced this hypoxia induced MAPK p38 to decrease HIF-1α levels and thus VEGF transcription necessary for tumor induced angiogenesis.

CHAPTER 3

CHRONIC MORPHINE INHIBITS MONOCYTE MIGRATION AND RECRUITMENT TO INHIBIT TUMOR INDUCED ANGIOGENESIS

Introduction

The tumor microenvironment is a rich source of endothelial cells, fibroblasts, inflammatory cells and extracellular matrix molecules. There are also cells from the immune system present in the tumor microenvironment since immune cells appear to have a dual function in tumor growth. Leukocytes are recruited to the tumor microenvironment and influence tumor cells, promoting tumor growth and tumor cell survival (Noonan DM, 2008). Scientific studies from transgenic mouse models and analysis of human tumor biopsies suggest that bone marrow-derived myeloid cells, such as macrophages, neutrophils, eosinophils, mast cells and dendritic cells, all contribute to the formation and maintenance of blood vessels in tumors (Murdoch C, 2008; Shibuya, 2006; Shojaei F, 2008).

The tumor microenvironment is often described as a highly pro-inflammatory environment. Here cells of the innate immunity suppress the adaptive immunity and have a reduced ability to destroy tumor cells. These pro-inflammatory cells are a significant source of vascular endothelial growth factor within the tumor microenvironment and have a multifaceted role in the development of angiogenesis (Shojaei F, 2008; Nyberg P, 2008). The hypoxic tumor cells may initiate the angiogenic process, but many other cells support and maintain blood vessel formation. Recruited stem cell-like endothelial progenitors and monocytes from the bone marrow differentiate and de-differentiate into mature endothelium or pro-inflammatory cells (Shibuya M, 2006).

Extensive work has already been done to identify infiltrating and recruited cells within the tumor microenvironment. The identification of and roles these cells play to either support or inhibit tumor growth is already well established. These cells have been positively identified through the expression of cell surface markers as: neutrophils, M2 polarized macrophages, Tie-2 expressing monocytes, and a subset of CD11b+/CD14+ myeloid derived suppressor cells (Murdoch C, 2008). Hypoxic areas within tumor sites stimulate the recruitment of inflammatory cells into the tumor microenvironment through the migration and differentiation of monocyte derived peripheral blood cells (Bosco MC, 2006). Current research strongly supports a role of mononuclear phagocytes at various differentiation stages as regulators of angiogenesis, pro-inflammatory cytokines, receptors and other inflammatory mediators, mediating tissue neo-vascularization and cell activation (Bosco MC, 2008).

Morphine is widely accepted as a highly immunosuppressive drug (Weinert CR, 2008). In humans morphine decreases the effectiveness of several immune responses involving both arms of the immune system, innate and acquired immunity (Sacerdote P, 2008). Morphine treatment leads to the impairment of monocyte and neutrophil function, as well as NK-cell-mediated cytotoxicity. Opioid receptors have been shown to modulate the activity of a distinct subset of immune cells, altering their susceptibility to various infectious agents and inhibiting the inflammatory response. Morphine can also regulate the immune function indirectly as studies show that morphine is capable of varying nitric oxide release, cell adhesion and even modulating stress hormone levels (McCarthy L, 2001; Sacerdote P, 1997; Schneemilch CE, 2004; Walters, 2003).

Considering the effects of morphine on immune responses and the involvement of immune cells in the development of angiogenesis, the following studies were designed to investigate the effects of morphine on bone marrow-derived progenitor cell migration and recruitment towards a tumor microenvironment. These studies also further characterized the leukocyte phenotypes attracted towards a lung cancer tumor-derived tumor microenvironment in the presence and absence of morphine treatment.

Materials and Methods

Morphine Treatment

Mice received morphine or placebo through the pellet implantation method as described previously (Roy S, 2001). Briefly, 75mg morphine pellets or placebo pellets (NIH/NIDA) were inserted in a small pocket created by a small incision on the animal's dorsal side, which was resealed using surgical wound clips (Stoelting, Wooddale, IL).

Matrigel Plug Tumor Conditioned Media Angiogenesis Assay

Mice received placebo or morphine by pellet implantation (anterior dorsal) method followed by subcutaneous injections of 500uL matrigel admixed 1:3 with tumor cell media on the posterior right flank. The tumor cell media was derived from long-term cultures of Lewis Lung Carcinoma in a 37^0C incubator in normal air.

Matrigel was purchased from Sigma, St. Louis, MO). After 7 days, the animals were sacrificed and the matrigel plugs were surgically removed. Plugs were fixed in10% formalin overnight and histological analysis was performed at the University of Minnesota, Fairview Clinical Pathology and Lab Services. Plugs were paraffin embedded and hematoxylin and eosin stained. In subsequent experiments, matrigel plugs were snap-frozen in liquid nitrogen and cryostat sections were used for morphometric analysis using CD31 immuno-fluorescent staining for blood vessel density.

Morphometric Analysis for Blood Vessel Density

Snap-frozen matrigel plugs were cryostat sectioned into 8-10μm sections. Matrigel plug sections were fixed in ice-cold acetone and non-specific binding was

blocked with 1% BSA in PBS. For CD31-staining (dilution 1:50), sections of matrigel plugs (n=5) per treatment group were used to determine blood vessel density as described previously (Wild R, 2000). Briefly, captured digital images were binarized and skeletonized using the Reindeer Plug In Functions for Adobe Photoshop. A toolkit was used to measure the average blood vessel density, branching and length.

COAT-A-COUNT Serum Morphine In-vitro Diagnostic Test Kit

On the day of termination of the experiments, blood was collected from experimental mice and serum was separated and stored at -80'C. The concentration of morphine in experimental mice serum was determined by Radio-Immuno-Absorbent Assay using equal volumes of serum samples (n=2) as directed by manufacturer (Diagnostic Products Corporation, Los Angeles CA). The serum concentration of morphine was expressed in ng/ml and the number of experimental animals tested was (n=5).

Bone Marrow Recruitment and Adoptive Transfer Model

C567BL6 male mice 7-8 weeks old were first treated with placebo or morphine through pellet implantation as described previously (Roy S, 2001). Bone marrow from sex and age-matched mice were isolated from the long bones of transgenic luciferase positive mice. The luciferase positive bone marrow was prepared into single cell suspension in hanks' buffered salt solution. Red blood cell lysis buffer (Sigma, St. Louis, MO) was used in red blood cell lysis. Trypan blue exclusion was used to count the number of live cells and 20 x 10^6 cells/500ul were injected into the peritoneal cavity of drug treated mice. An incision was used to make a small pocket at the contralateral side

of the pellets and mice were also implanted wih a $1mm^2$ PVA sponge that was presoked with tumor derived supernatant. The Lewis Lung carcinoma cells were cultured under normal room air for three days and this media was collected without cells and stored at -80^0C in aliquots. Experiemental mice were administered 100ul of a 15mg/ml Luciferin stock solution intra-peritoneally 15 miuntes prior to whole body imaging using the Xenogen Imaging System (Biomedical Processing and Inaging Lab, University of Minnesota). Mice bone-marrow recipients were imaged at 24 hours post-innoculation of luciferase positive donor bone marrow progenitors to monitor the migration of lucifrease positive bone marrow progenitors out of the peritoneal cavity and toward the chemokine gradient that was set up using the PVA sponge presoaked with tumor cell-conditioned media. After 1 and 4 days post innoculation, PVA sponges were removed and recruited cells, isolated and further characterized using Fluoresecent activated cell sorting.

Fluorescent Activated Cell Sorting and Analysis

To characterize the cells recruited into the Polyvinylalchol sponges, sponges were placed in a microfuge tube and spun for 10 minutes at 4^0C at 1500rpm. Sponges were then removed and placed in a fresh tube and 500ul of PBS was added. Using the tip of a 1000-P micropipettor, the sponge was squeezed to one side of the tube and the expelled fluid was immediately pipeted out and transferred to the previous tube. This was repeated with a fresh volume of 500ul of PBS. Cells were then spun down into a pellet and the supernatant stored at -80^0C. Cell pellets were washed in 1x PBS and then resuspended in 100*u*l 1xPBS, and fixed through the addition of 4% paraformaldehyde overnight at 4^0C. Cells were then washed and non-specifically blocked using 1% bovine serum albumin in

1X PBS. A fraction of the cells was then used to stain for cell surface markers present on cells of the bone marrow. Cells were diluted in 1% bovine serum albumin in 1X PBS and 1:200-1:1000 antibody dilutions were used for overnight staining at 4^0C. Stained cells were washed and immediately analyzed using the Guava Easy Cyte FACS system (Guava Technologies, USA). Stained cells were compared to non-stained cells. Guava Express plus was used to determine cell surface expression of markers. Machine settings were done using the non-stained cells to determine the background associated with cell auto-fluorescence.

Confocal Microscopy

Aliquots of stained cells prepared for FACS analysis were used to make cytospins for each antibody used. Cells were then visualized using a Confocal Microcope (40X) after being counter stained with the nuclear dye DAPI. Bright light and fluorescent images were captured and later merged using Adobe Photoshop.

Statistics

All numerical data are expressed as a mean ± SE. Differences of means between different treatment groups were compared using a one-tail Student's T-test; a value of $P < 0.05$ was considered statistically significant.

Results

Morphine Inhibits Recruitment of Leukocytes towards a Tumor Microenvironment

Morphine is well known to suppress numerous functions of the immune system and is therefore regarded as a highly immunosuppressive agent (Weinert CR, 2008). Pro-inflammatory monocytes contribute significantly to the formation and maintenance of angiogenesis (Noonan DM, 2008; Murdoch C, 2008). To test the effect of morphine on leukocyte recruitment towards the tumor microenvironment, mice were first treated with either placebo or morphine pellets through pellet implantation. Next, mice were injected subcutaneously with a 3:1 ratio of matrigel admixed with supernatant derived from long term cultures of Lewis lung carcinoma cells (CM). These tumor cells have a high basal level of chemokines. In this model, the matrigel plug created a chemotactic gradient stimulating the cell migration response towards a "tumor microenvironment". This experimental design was used to determine if the effect of morphine on tumor growth was solely through the effects on tumor cells or involved other host derived stromal cells.

Matrigel plugs containing tumor cell conditioned media was removed after 7 days and processed for hematoxylin and eosin staining. As shown in **Figure 23**, the undersurface of skin, atop of the matrigel developed strong, connected blood vessels in placebo mice (**Figure 23A**). In contrast to placebo, morphine mice displayed weaker, less connected vessels (**Figure 23D**). In **Figure 23B**, placebo treated mice showed more intense hematoxylin staining and thus cell infiltration within areas outside the host vessels, located at the periphery of the matrigel plugs. In contrast, as shown in **Figure 22E** morphine treatment resulted in a reduction in the hematoxylin staining and this was more reduced as we looked further away from the major blood vessels into the core of the

matrigel plugs. Examination of the sections towards the inner core of the matrigel plugs showed a reduced cell recruitment pattern and migration/infiltration into the plug containing tumor cell-derived conditioned media. As shown in **Figure 23C**, cells from placebo treated animals were capable of migrating into the core of the matrigel plug and accumulated as evidenced by the intense hematoxylin and eosin staining; in contrast, fewer cells migrated into matrigel plugs from morphine treated mice **(Figure 23F).** Lewis Lung carcinoma cells can secrete high basal levels of chemokines, sufficient to recruit host leukocytes to the tumor microenvironment. As we expected, this staining was reduced in sections analyzed from morphine treated mice. Comparison of placebo and morphine treated sections show leukocytes' infiltration out of the blood circulation and into the surrounding muscle tissue of experimental mice. These results suggest, in addition to effects on hypoxic tumor cells, that morphine treatment can inhibit host cell recruitment and migration towards the tumor microenvironment *in vivo*.

Clinical studies report that the dose required for analgesic effects of morphine vary between cancer patients. Patients that receive morphine orally at a dose of 40-4800 mg often result in serum levels around 1.0 -2106 ng/ml. Morphine administration through parenteral route of administration often occur within 10-9062 mg, and this result in serum levels ranging from 7- 21,730 ng/ml (Tiseo PJ, 1995). To ensure that this method of morphine administration achieved blood levels within analgesic range, mice blood serum samples were collected at the time of matrigel plug removal and tested for morphine using the Morphine Coat-A-Count Serum kit. The morphine serum levels from morphine treated wild type and MORKO mice show that this method of pellet implantation produced morphine blood levels between 200-400ng/ml. This concentration falls within

physiological levels, and is seen among cancer patients receiving morphine for pain management. Taken together, the data generated from these experiments suggest that morphine at doses used clinically for pain management is capable of inhibiting leukocyte infiltration towards a tumor microenvironment.

Morphine Inhibits the Migration of Myeloid Derived Bone Marrow Cells to the Tumor Microenvironment

The initial source of inflammatory cells in the tumor microenvironment is from the circulating peripheral blood pool. In contrast, the sustained migration of cells necessary for maintaining angiogenesis is primarily derived from bone marrow. Tumor and stromal cell expression of VEGF recruit bone marrow-derived progenitors that contribute to tumor growth by incorporating themselves into the developing blood vessels (Lee TH, 2006). To determine if morphine inhibited bone marrow migration to suppress angiogenesis, we performed the following experiment. Polyvinyl-alcohol sponges (PVA) presoaked with conditioned tumor cell media from a long-term culture of normoxic cells were implanted subcutaneously at the anterior-dorsal right side of experimental mice. Experimental animals also received placebo or morphine through pellet implantation at the anterior-dorsal left side. In these experiments, bone marrow-suspensions from naïve luciferase positive mice, approximately $40x10^6$ cells per 500*u*L per mice were injected into C57BL/6 recipient wild type mice. After 24 hours post intra-peritoneal injection of Luciferase+ bone marrow cells, animals were administered 100ul of a 15mg/ml Luciferin at the sponge site and xenogen images were captured after 10 minutes post Luciferin administration. As shown in **Figure 24A**, xenogen-captured images of two representative

mice, show high expression of luciferase-positive bone marrow cells at the sponge sites (see arrows) reflecting a greater migration of luciferase+ bone marrow cells and thus increased cell recruitment when compared to morphine (**Figure 24B**). In these experiments the migration of bone marrow cells from the site of injection, from the peritoneal cavity to the PVA-tumor conditioned media sponge site in morphine treated mice were blunted as evidenced from the reduction in luciferase signaling (**Figure 24A-B**). Taken together, these results suggested that the reduction in leukocyte recruitment to the tumor microenvironment is as a result of defects in migration.

Morphine inhibited the recruitment of myeloid derived bone marrow cells to the tumor microenvironment

To further confirm the effect of morphine on leukocyte recruitment to the tumor microenvironment and its effects on migration to the PVA sponges-containing tumor cell media were removed after 1 and 4 days after post intra-peritoneal injection of donor bone marrow cells. Experimental mice were sacrificed and the PVA sponges removed and the total number of infiltrating bone marrow cells were determined using Guava Technologies FACS system and Guava Express Plus program. PVA sponges were placed microfuge tubes, and cells were centrifuge out of the PVA sponges. As shown in **Figure 25A**, the total number of cells isolated from placebo treated animals was determined to be within the range 3.0-10.4 x10^7cells/ml. In contrast, morphine treatment through pellet implantation resulted in a significant decrease in cell recruitment ($p<0.00001$) into the PVA sponges containing conditioned tumor cell media. Guava express plus software determined the relative number of cells recruited into the PVA sponges derived from

morphine treated animals were within 1.2-2.8x10^7 cells/ml. These results further confirmed the inhibitory effect of morphine on cell migration to the tumor microenvironment. These results further support the view that morphine inhibits leukocyte recruitment to further inhibit angiogenesis and thus tumor growth *in vivo*.

Quantification of CD45+ Bone marrow derived progenitors in the PVA sponges

In this model we expected that the recruitment of cells, other than bone marrow cells, as many other cells types are required in the repair and regeneration processes. To further verify the presence of the bone marrow derived myeloid cells within the PVA sponges, we next quantified the relative number of CD45+ expressing cells between placebo and morphine treatment. The mean % values of CD45+ cells per 5000 cells examined after staining and FACS ranged from 28-47% of total cells infiltrated into the PVS sponges. As shown in **Figure 25B**, the relative number of CD45+ cells from PVA sponges taken after placebo treatment was approximately 2.3 x 10^7 cell/ml +/- 6 x 10^6. Morphine treatment of mice resulted in a significant reduction in the total number of bone marrow myeloid derived CD45+ cells ($p<0.0005$), of mean value 1.1 x 10^7 cell/ml +/- 3.0 x 10^6. Taken together, these results support the view that morphine inhibits the migration and recruitment of CD45+ bone marrow derived myeloid cells towards a chemotactic gradients and this can potentially reduced angiogenesis within the tumor microenvironment.

Characterization of cells recruited to PVA sponges containing conditioned tumor media

There is strong evidence linking bone marrow derived myeloid cells to enhanced tumor angiogenesis and growth (Noonan DM, 2008; Shibuya, 2006). In the rest of these studies, we further investigated the role of inflammatory cells in tumor angiogenesis. We further characterized the leukocytes recruited in response to tumor cell derived chemokines from the PVA sponges after 1 and 4 days post-implantation. The relative number of CD11b+ cells was determined through Fluorescent Activated cell sorting and staining with fluorescently conjugated antibodies (**Figure 26A**). CD11b+, a trans-membrane protein involved in the binding to CD31on quiescent endothelial cells mediating cell adhesion (Vainer B, 2000). CD11b+ expression is primarily found on a subset of blood derived hemangiocytes, tie2+ monocytes, M2 macrophages, and neutrophils (Shojaei F, 2008).

Blood derived hemangiocytes, tie2+ monocytes, M2 macrophages, and neutrophils contribute to angiogenesis and work together to increase tumor growth. Results from the fluorescent activated cell sorting analysis using CD11b-FITC conjugated antibodies show that CD11b+ cells made up approximately 0.7-5.66% of the total cells infiltrated into the PVA sponges containing conditioned tumor cell media. The relative number of CD11b+cells infiltrated into the sponges increased from day 1 to day 4 under placebo treatment, see **Figure 26A**. Similar to the pattern seen with placebo treatment, the number of infiltrating cells into the PVA sponges also increased from day 1 to day 4 in the presence of morphine. However, morphine treatment significantly

decreased the number of infiltrating cells expressing CD11b, when compared to placebo treatment on day 1 ($p<0.004$) and day 4 ($p<0.01$).

To further characterize the PVA sponge cells we next stained PVA cells with antibodies against CD14, the Toll-like receptor's co-receptor, a protein that bind the *E. coli* cell wall component lipopolysaccaride. CD14 is found predominantly on a subset of monocyte progenitors, tie2 expressing monocytes, M2 macrophages, and neutrophils (low). The results from the fluorescent activated cell sorting analysis, using CD14-FITC conjugated antibodies show that CD14+ cells made up approximately 1.02-33.56% of the total cells infiltrated into the PVA sponges containing conditioned tumor cell media. The relative number of CD14+cells infiltrated into the sponges on day 1 was similar to that for day 4 under placebo and morphine treatment, see **Figure 26B**. Similar to the patterns were observed with seen with morphine treatment. In addition, morphine treatment significantly decreased the number of infiltrating cells expressing CD14 monocytes when compared to placebo treatment on day 1 ($p<0.003$) and day 4 ($p<0.00001$). Taken together, these results suggest that morphine can reduce myeloid cell derived monocyte infiltration into the tumor microenvironment to suppress VEGF-induced angiogenesis required for tumor growth.

Morphine inhibits M2 monocyte-macrophage polarization/differentiation at the tumor microenvironment

Hypoxic areas within tumor sites stimulate the migration and differentiation of monocyte derived peripheral blood cells (Bosco MC, 2006). These mononuclear phagocytes or primary monocytes often accumulate in large numbers at hypoxic areas

where they terminally differentiate into inflammatory and tumor-associated macrophages. These cells further recruit monocytes and endothelial cell progenitors from the bone marrow (Bosco MC, 2006). To this effect, we next determined the relative number of M2 polarized macrophages through double staining for F480/CD14+ cells using a fraction of the total PVA sponge cell population. As shown in **Figure 27**, on day 4, the number of M2 macrophages, possibly differentiated from the monocytes, was doubled the amount on day 1. In addition, morphine treatment resulted in a significant reduction in the amount of double positive F4/80+; CD14+ M2 macrophages within the PVA sponge on day 1($p<0.002$) and day 4 ($p<0.005$).

Morphine treatment inhibited neutrophil recruitment to the tumor microenvironment.

To characterize the recruited leukocytes, another fraction of the total population of cells was analyzed for markers of neutrophils, namely Ly6G, and CXCR2. Ly6G are present on large number of neutrophils progenitors. PVA sponge cells were stained with anti-Ly6G-FITC conjugated antibodies and fluorescent activated cell sorting analysis showed that the number of cells expressing the Ly6G cell surface markers were greater in placebo than morphine treatment on day 1 by 29.4%. The relative number of Ly6G+ cells recruited towards the tumor microenvironment decreased by day 4 (**Figure 28A**). Also on day 4, the relative number of cells recruited to the PVA sponges was significantly less than morphine treatment ($p<0.00004$).

To further validate the effect of morphine on neutrophils, relative number of cells expressing the chemokine receptor CXCR2 found mostly on mature neutrophils with

segmented nuclei was determined using CXCR2-PerCP conjugated antibodies and FACS. As shown in **Figure 28B**, the recruitment of CXCR2+ cells increased from day 1 to day 4. Compared to placebo, morphine treatment resulted in a 35.5% decrease in CXCR2+ cells on day 1 but was insignificant. On day 4, however morphine treatment had a significantly lower number of CXCR2+ cells ($p<0.0009$) present within the PVA sponges.

To verify the FACS data for positive identification of neutrophils progenitors and mature cells, cytospin preparations of fluorescently labeled cells were examined under confocal microscopy. As shown in **Figure 28C**, cells had a granular extracellular surface reminiscent of neutrophils containing granules. Ly6G positive cells were visualized with the nuclear DAPI stain, and a merged image is shown in **Figure 28E**. These images show cells with segmented nuclei with strong cell surface expression of Ly6G proteins (**Figure 28E**). Also shown in **Figure 28F**, are merged images of cells expressing CXCR2, double labeled with Ly6G after DAPI visualization. In this particular frame, cells are double and single labeled for both markers, confirming the presence of both mature and immature neutrophils. Taken together these cells confirmed the presence of neutrophils and their reduced recruitment in the presence of morphine to the tumor microenvironment to potentially reduce angiogenesis *in vivo*.

Morphine inhibits the recruitment of Tie2+ monocytes to the tumor microenvironment

Of greatest interest the Tie-2+ expressing monocytes have been identified in both human blood and tumors. The neutralization of these Tie-2+ monocytes in various

experimental tumor models inhibits have shown to inhibit tumor angiogenesis. In mice, the circulating Tie2+CD45+ hematopoietic cells are mostly CD11b+ and Ly6G/Gr-1 (low/negative). The surface marker profile of Tie-2 expressing monocytes is similar to that of monocytes, including CD14, but distinct from the classical inflammatory monocytes and is thought to consist of precursors of tissue macrophages (Lewis CE, 2007).

In these experiments we also analyzed the expression of Tie2+/CD14+ expressing cells from a fraction of the total population of cells recruited into the tumor cell conditioned media containing PVA sponges. Tie-2 expressing monocytes can localize to and incorporate into the tumor blood vessels. They can also produce high levels of the proangiogenic factors, and matrix-remodeling proteins. They can function as "pathfinders" for activated endothelial cells to form provisional endothelium-like structures for blood vessel formation. (Lewis CE, 2007). As shown in **Figure 29**, on day 1 of bone marrow progenitor migration, on average 0.73% of the total cells recruited were Tie2+/CD14+ in samples taken from placebo treated mice. In the case of morphine treatment, on average 0.23% were Tie2+/CD14+on day 1, and this was significantly lower than placebo treatment ($p<0.01$).

On day 4 of the experiment, the number of Tie2+/CD14+ cells in placebo treated mice increased from day 1, on average greater than 14% of the total population. Compared to placebo, morphine treatment significantly reduced the amount of Tie2+/CD14+ expressing monocytes on day 4 ($p<0.005$), with only on average 1.01% of morphine treated samples expressing the cell surface markers Tie2+/CD14+ (**Figure 28**). Morphine treatment reduced recruitment of monocytes expressing the cell surface

markers Tie2+ and CD14+ towards the tumor microenvironment. These studies do not exclude the presence of another subset of tumor promoting cells, the myeloid derived suppressor cells that also have significant roles in the development of angiogenesis.

Considering that the recruitment of Tie2+endothelial progenitors were reduced in the presence of morphine and they contribute to vessel formation, we predicted that the amount CD31+ endothelial cells present within the PVA sponges would also be reduced after morphine treatment. Data from the FACS analysis showed that on average 4-9% of the total population of cell were positive for the endothelial cell marker CD31. As expected, the reduction in Tie2+/CD14+ expressing monocytes was accompanied with a significant reduction the amount CD31+ endothelial cells by 75% when compared to placebo ($p<0.000002$, **Figure 30**). These results further support the view that the effect of morphine on angiogenesis is partly mediated through multiple mechanisms involving hypoxic tumor cells, pro-inflammatory monocytes and endothelial cell precursors.

Discussion

Tumor angiogenesis is highly dependent on the chemotaxis and thus recruitment of pro-inflammatory cells into the tumor microenvironment. In models of inflammatory diseases, tissue macrophages sequentially recruit cells involved in the first line of defense, that includes neutrophils, followed by monocyte-macrophage like cells that also further contribute to tissue remodeling and tube formation. In the case of a growing tumor, frequently an excessive pro-inflammatory reaction results, and this creates a tumor microenvironment commonly described as a "non-healing wound". In the initial stages of tumor growth these cells are capable of rejecting tumor cells, but as the tumors grow and tumor cells down-regulate antigen expression, they escape immune surveillance and this disrupts the balance between tumor cell growth and death, such that tumor cell growth outweighs tumor cell death (Lamagna C, 2006). These experiments were designed to test the effect of morphine on the immune system's contribution to angiogenesis and thus the growth and progression of established tumors, in tumor-bearing mice.

In these models of experimental angiogenesis, both the placebo and morphine treated mice were implanted with matrigel plugs or PVA sponges containing tumor cell conditioned media. The recruitment pattern was characterized by first identifying the cells that were capable of migrating out of the blood and into the matrigel plugs that contained chemotactic factors derived from tumor cells. Even in a model, where the chemotactic gradients were similar in between treatment groups, *in vivo* morphine significantly inhibited: 1) the migration of bone marrow derived progenitors to tumor cell-derived chemokines and 2) the recruitment of inflammatory cells out of peripheral blood circulation and into the tumor microenvironment in mice when compared to

placebo (**Figures 23-24**). This inhibition in leukocyte recruitment pattern exerted by morphine into the matrigel plug containing tumor cell media both on day 1 and day 4 of the investigations may have simply resulted from reduced migration. Therefore, taking into consideration that the effects observed by morphine on recruitment may have been a direct consequence of morphine on cell migration; we tested the effects of morphine on bone marrow derived progenitor cell chemotaxis towards tumor cell media derived from normoxic and hypoxic tumor cells in an *in vitro* system. Using a standard chemotaxis double chamber system, we compared the migration of naïve cells, to morphine pre-treated bone marrow derived progenitors cells. We found that the migration response were similar between naïve and morphine pretreated cells towards tumor cell media taken from normoxic cells (**Figure 31**). In contrast, naive bone marrow derived progenitor cell migration was greater towards tumor cell media derived from hypoxic tumor cells than normoxic cells ($p<0.02$) and morphine pre-treatment did not affect this pattern of migration any further ($p=0.28$). These results suggested that in an isolated *in vitro* system, lacking an intact endothelial barrier, morphine has no direct effect on cell migration towards a chemotactic gradient. Additionally, the inhibition in cell migration seen *in vivo* may have resulted from effects on the interaction between the endothelial cell barrier and immune components involved in cell adhesion or tissue extravasation.

While signaling through the appropriate chemokine receptors aid in the migration and localization of leukocytes expressing these receptors towards specific chemokine gradients, adhesion and extravasation are also necessary steps in the recruitment inflammatory cells out of the blood and into most tissue environments (**Figure 10**). The concomitant decrease in cell recruitment observed with morphine treatment could have

resulted from changes in the adhesion properties of the immune cells or at the endothelial cell level. To this extent CD11b, is an important integrin molecule involved in the regulation of leukocyte (monocytes, granulocytes, macrophages and natural killer cells) adhesion, migration, phagocytosis, chemotaxis and cellular activation (Solovjov DA, 2005). FACS analysis for the characterization of CD11b+ cells in these studies showed that in placebo treated control mice, cells expressing this cell surface protein were recruited to the PVA sponges on day 1; and then further accumulated upto day 4. In contrast to placebo, morphine treatment was accompanied with a significant inhibition in the recruitment pattern of CD11b+ cells ($p<0.004$ on day 1 and $p<0.01$ on day 4). These results suggest that morphine treatment could have directly or indirectly altered the expression profile of these cells, reducing their ability to adhere to the activated endothelial cells after injection into the peritoneum; thereby preventing their extravasation into the blood for subsequent migration to the PVA sponges. The effects of morphine on cell recruitment seen *in vivo*, is most likely dependent on the interaction with the endothelium, and this was lacking in the *in vitro* system. Therefore further studies are necessary to address the exact mechanisms affected by morphine during leukocyte migration.

Another valid explanation for the observed reductions in the normal migration pattern towards the tumor microenvironment could have been due simply to a shift or delay in the normal migration pattern of inflammatory cells. In wound healing models, a sequential recruitment pattern of immune cells coincides with and is unique to the phase of remodeling (Park JE, 2004). At the initial injury, platelets come in during coagulation events, followed by neutrophils and macrophages in the inflammation stage and finally

during remodeling the fibroblasts and lymphocytes accumulates (Park JE, 2004). Several independent investigations inhibiting neutrophil migration, and recruitment, have positively confirmed the importance and significant contribution of neutrophils in tube formation (Noonan DM 2006; Shibuya M, 2006; Matsuo Y, 2009). The delay in the initial recruitment of neutrophils could have blunted the subsequent recruitment of inflammatory cells in particular, macrophages. Macrophages secrete many cytokines such as tumor necrosis factor-α, transforming growth factor-α and -β, platelet derived growth factor and insulin like growth factor, all shown to directly increase endothelial cell proliferation and collagen synthesis (Park JE, 2004). We hypothesize that morphine may play a role in disrupting this sequential recruitment pattern, it is this initial blunting that could have led to the observed overall reduction in recruitment. To this effect, it would be of great interest to see if the reconstitution of neutrophils in the presence of morphine would rescue the inhibition of bone marrow derived cell migration towards the tumor microenvironment and rescue tumor growth. In studies stimulating monocytes and peripheral blood mononuclear cells with peptidoglycan from *Staphylococcus aureus*; morphine significantly inhibited the production of cytokines such as TNF and IL-6 from monocytes; but in peripheral blood mononuclear cells morphine inhibited the TNF, but not the IL-6 production (Bonnet MP, 2009). Additionally, morphine can suppress the ability of human THP-1 monocytes to convert into a macrophage phenotype after Phorbol 12-myristate 13-acetate (PMA) treatment (Hatsukari I, 2006). In these studies, PMA conversion of monocytes to macrophages increased their adhesive properties and migration towards an MCP-1 chemokine gradient but was significantly reduced in the presence of morphine. These results suggest that the monocyte to macrophage conversion

is a prelude for adhesion and subsequent transmigration. Alternatively, the lower number of recruited cells could have resulted from direct effects of morphine on bone marrow cell survival, receptor expression and or cytokine secretion and these events should be investigated further.

The characterization of the cells recruited to the tumor microenvironment, confirmed the presence of neutrophils and macrophages, both inflammatory cells known to contribute significantly to blood vessel formation (Bingle L, 2001, Noonan DM 2008, Shibuya M, 2006). Therefore, selective purification and or replacement of these individual pro-inflammatory cell subpopulations into morphine treated mice should reverse the effects of morphine if the effect of morphine is primarily through that particular cell type. The sequential recruitment of the immune cells may be an important response disrupted after morphine treatment (comparing placebo). Any disruptions in the migration pattern of neutrophils, involved in the first line of defense can lead to additional deficits in the second phase of cell recruitment required for further support and maintenance of blood vessels within the tumor microenvironment. Similarly, morphine could have produced suppressive effects on the activation of tissue macrophages, which could have lead to a delay in the migration pattern to offset cell recruitment by a few days. Therefore, selectively purifying these individual populations and later replacing them singly into morphine treated mice should rescue the effects of morphine if the effect of morphine is primarily through deficits in activity of these particular cells.

Alternatively, the effects seen on leukocyte recruitment could have been due to changes in bone marrow mobilization, in particular on day 4. In these experiments, cells from donor mice were injected in the peritoneal cavity, but one cannot discount the

contribution of the host's own bone marrow cells especially since we did not irradiate the animals before adoptive transfer. While the initial leukocyte recruitment observed in recipient mice was primarily cells of the donor mice; at the later stage, on day 4 we were observing the recipient's own bone marrow mobilization response. The recruitment patterns observed by day 4 in placebo animals most likely involved the host's own bone marrow mobilization, and since this was reduced with morphine treatment, we speculate that morphine could also have effects on the ability of the spleen or bone marrow to release chemokines or myeloid progenitors that would normally contribute to tumor growth. The fact that the Tie2+ monocyte recruitment pattern was significantly compromised raises the question whether the effect of morphine in these studies stemmed from alterations in stem cell progenitor populations already known to contribute significantly to angiogenesis and tumor growth (Palmer MD, 2005; Lewis CE, 2007; Venneri MA, 2007). However, more studies are necessary to address these questions. In these experiments, even though the chemokine gradients were are equal in placebo and morphine treated mice, it was the host response to chemotaxis that was altered. Taken together, these results suggest that morphine is acting in multiple pathways to alter angiogenesis associated with tumor growth.

CHAPTER 3

CHRONIC MORPHINE INHIBITS MONOCYTE MIGRATION AND RECRUITMENT TO INHIBIT TUMOR INDUCED ANGIOGENESIS

Introduction

The tumor microenvironment is a rich source of endothelial cells, fibroblasts, inflammatory cells and extracellular matrix molecules. There are also cells from the immune system present in the tumor microenvironment since immune cells appear to have a dual function in tumor growth. Leukocytes are recruited to the tumor microenvironment and influence tumor cells, promoting tumor growth and tumor cell survival (Noonan DM, 2008). Scientific studies from transgenic mouse models and analysis of human tumor biopsies suggest that bone marrow-derived myeloid cells, such as macrophages, neutrophils, eosinophils, mast cells and dendritic cells, all contribute to the formation and maintenance of blood vessels in tumors (Murdoch C, 2008; Shibuya, 2006; Shojaei F, 2008).

The tumor microenvironment is often described as a highly pro-inflammatory environment. Here cells of the innate immunity suppress the adaptive immunity and have a reduced ability to destroy tumor cells. These pro-inflammatory cells are a significant source of vascular endothelial growth factor within the tumor microenvironment and have a multifaceted role in the development of angiogenesis (Shojaei F, 2008; Nyberg P, 2008). The hypoxic tumor cells may initiate the angiogenic process, but many other cells support and maintain blood vessel formation. Recruited stem cell-like endothelial progenitors and monocytes from the bone marrow differentiate and de-differentiate into mature endothelium or pro-inflammatory cells (Shibuya M, 2006).

Extensive work has already been done to identify infiltrating and recruited cells within the tumor microenvironment. The identification of and roles these cells play to either support or inhibit tumor growth is already well established. These cells have been positively identified through the expression of cell surface markers as: neutrophils, M2 polarized macrophages, Tie-2 expressing monocytes, and a subset of CD11b+/CD14+ myeloid derived suppressor cells (Murdoch C, 2008). Hypoxic areas within tumor sites stimulate the recruitment of inflammatory cells into the tumor microenvironment through the migration and differentiation of monocyte derived peripheral blood cells (Bosco MC, 2006). Current research strongly supports a role of mononuclear phagocytes at various differentiation stages as regulators of angiogenesis, pro-inflammatory cytokines, receptors and other inflammatory mediators, mediating tissue neo-vascularization and cell activation (Bosco MC, 2008).

Morphine is widely accepted as a highly immunosuppressive drug (Weinert CR, 2008). In humans morphine decreases the effectiveness of several immune responses involving both arms of the immune system, innate and acquired immunity (Sacerdote P, 2008). Morphine treatment leads to the impairment of monocyte and neutrophil function, as well as NK-cell-mediated cytotoxicity. Opioid receptors have been shown to modulate the activity of a distinct subset of immune cells, altering their susceptibility to various infectious agents and inhibiting the inflammatory response. Morphine can also regulate the immune function indirectly as studies show that morphine is capable of varying nitric oxide release, cell adhesion and even modulating stress hormone levels (McCarthy L, 2001; Sacerdote P, 1997; Schneemilch CE, 2004; Walters, 2003).

Considering the effects of morphine on immune responses and the involvement of immune cells in the development of angiogenesis, the following studies were designed to investigate the effects of morphine on bone marrow-derived progenitor cell migration and recruitment towards a tumor microenvironment. These studies also further characterized the leukocyte phenotypes attracted towards a lung cancer tumor-derived tumor microenvironment in the presence and absence of morphine treatment.

Materials and Methods

Morphine Treatment

Mice received morphine or placebo through the pellet implantation method as described previously (Roy S, 2001). Briefly, 75mg morphine pellets or placebo pellets (NIH/NIDA) were inserted in a small pocket created by a small incision on the animal's dorsal side, which was resealed using surgical wound clips (Stoelting, Wooddale, IL).

Matrigel Plug Tumor Conditioned Media Angiogenesis Assay

Mice received placebo or morphine by pellet implantation (anterior dorsal) method followed by subcutaneous injections of 500uL matrigel admixed 1:3 with tumor cell media on the posterior right flank. The tumor cell media was derived from long-term cultures of Lewis Lung Carcinoma in a 37^0C incubator in normal air.

Matrigel was purchased from Sigma, St. Louis, MO). After 7 days, the animals were sacrificed and the matrigel plugs were surgically removed. Plugs were fixed in10% formalin overnight and histological analysis was performed at the University of Minnesota, Fairview Clinical Pathology and Lab Services. Plugs were paraffin embedded and hematoxylin and eosin stained. In subsequent experiments, matrigel plugs were snap-frozen in liquid nitrogen and cryostat sections were used for morphometric analysis using CD31 immuno-fluorescent staining for blood vessel density.

Morphometric Analysis for Blood Vessel Density

Snap-frozen matrigel plugs were cryostat sectioned into 8-10μm sections. Matrigel plug sections were fixed in ice-cold acetone and non-specific binding was

blocked with 1% BSA in PBS. For CD31-staining (dilution 1:50), sections of matrigel plugs (n=5) per treatment group were used to determine blood vessel density as described previously (Wild R, 2000). Briefly, captured digital images were binarized and skeletonized using the Reindeer Plug In Functions for Adobe Photoshop. A toolkit was used to measure the average blood vessel density, branching and length.

COAT-A-COUNT Serum Morphine In-vitro Diagnostic Test Kit

On the day of termination of the experiments, blood was collected from experimental mice and serum was separated and stored at -80'C. The concentration of morphine in experimental mice serum was determined by Radio-Immuno-Absorbent Assay using equal volumes of serum samples (n=2) as directed by manufacturer (Diagnostic Products Corporation, Los Angeles CA). The serum concentration of morphine was expressed in ng/ml and the number of experimental animals tested was (n=5).

Bone Marrow Recruitment and Adoptive Transfer Model

C567BL6 male mice 7-8 weeks old were first treated with placebo or morphine through pellet implantation as described previously (Roy S, 2001). Bone marrow from sex and age-matched mice were isolated from the long bones of transgenic luciferase positive mice. The luciferase positive bone marrow was prepared into single cell suspension in hanks' buffered salt solution. Red blood cell lysis buffer (Sigma, St. Louis, MO) was used in red blood cell lysis. Trypan blue exclusion was used to count the number of live cells and 20 x 10^6 cells/500ul were injected into the peritoneal cavity of drug treated mice. An incision was used to make a small pocket at the contralateral side

of the pellets and mice were also implanted wih a $1mm^2$ PVA sponge that was presoked with tumor derived supernatant. The Lewis Lung carcinoma cells were cultured under normal room air for three days and this media was collected without cells and stored at -80^0C in aliquots. Experiemental mice were administered 100ul of a 15mg/ml Luciferin stock solution intra-peritoneally 15 miuntes prior to whole body imaging using the Xenogen Imaging System (Biomedical Processing and Inaging Lab, University of Minnesota). Mice bone-marrow recipients were imaged at 24 hours post-innoculation of luciferase positive donor bone marrow progenitors to monitor the migration of lucifrease positive bone marrow progenitors out of the peritoneal cavity and toward the chemokine gradient that was set up using the PVA sponge presoaked with tumor cell-conditioned media. After 1 and 4 days post innoculation, PVA sponges were removed and recruited cells, isolated and further characterized using Fluoresecent activated cell sorting.

Fluorescent Activated Cell Sorting and Analysis

To characterize the cells recruited into the Polyvinylalchol sponges, sponges were placed in a microfuge tube and spun for 10 minutes at 4^0C at 1500rpm. Sponges were then removed and placed in a fresh tube and 500ul of PBS was added. Using the tip of a 1000-P micropipettor, the sponge was squeezed to one side of the tube and the expelled fluid was immediately pipeted out and transferred to the previous tube. This was repeated with a fresh volume of 500ul of PBS. Cells were then spun down into a pellet and the supernatant stored at -80^0C. Cell pellets were washed in 1x PBS and then resuspended in 100*u*l 1xPBS, and fixed through the addition of 4% paraformaldehyde overnight at 4^0C. Cells were then washed and non-specifically blocked using 1% bovine serum albumin in

1X PBS. A fraction of the cells was then used to stain for cell surface markers present on cells of the bone marrow. Cells were diluted in 1% bovine serum albumin in 1X PBS and 1:200-1:1000 antibody dilutions were used for overnight staining at 4^0C. Stained cells were washed and immediately analyzed using the Guava Easy Cyte FACS system (Guava Technologies, USA). Stained cells were compared to non-stained cells. Guava Express plus was used to determine cell surface expression of markers. Machine settings were done using the non-stained cells to determine the background associated with cell auto-fluorescence.

Confocal Microscopy

Aliquots of stained cells prepared for FACS analysis were used to make cytospins for each antibody used. Cells were then visualized using a Confocal Microcope (40X) after being counter stained with the nuclear dye DAPI. Bright light and fluorescent images were captured and later merged using Adobe Photoshop.

Statistics

All numerical data are expressed as a mean ± SE. Differences of means between different treatment groups were compared using a one-tail Student's T-test; a value of $P < 0.05$ was considered statistically significant.

Results

Morphine Inhibits Recruitment of Leukocytes towards a Tumor Microenvironment

Morphine is well known to suppress numerous functions of the immune system and is therefore regarded as a highly immunosuppressive agent (Weinert CR, 2008). Pro-inflammatory monocytes contribute significantly to the formation and maintenance of angiogenesis (Noonan DM, 2008; Murdoch C, 2008). To test the effect of morphine on leukocyte recruitment towards the tumor microenvironment, mice were first treated with either placebo or morphine pellets through pellet implantation. Next, mice were injected subcutaneously with a 3:1 ratio of matrigel admixed with supernatant derived from long term cultures of Lewis lung carcinoma cells (CM). These tumor cells have a high basal level of chemokines. In this model, the matrigel plug created a chemotactic gradient stimulating the cell migration response towards a "tumor microenvironment". This experimental design was used to determine if the effect of morphine on tumor growth was solely through the effects on tumor cells or involved other host derived stromal cells.

Matrigel plugs containing tumor cell conditioned media was removed after 7 days and processed for hematoxylin and eosin staining. As shown in **Figure 23**, the undersurface of skin, atop of the matrigel developed strong, connected blood vessels in placebo mice (**Figure 23A**). In contrast to placebo, morphine mice displayed weaker, less connected vessels (**Figure 23D**). In **Figure 23B**, placebo treated mice showed more intense hematoxylin staining and thus cell infiltration within areas outside the host vessels, located at the periphery of the matrigel plugs. In contrast, as shown in **Figure 22E** morphine treatment resulted in a reduction in the hematoxylin staining and this was more reduced as we looked further away from the major blood vessels into the core of the

matrigel plugs. Examination of the sections towards the inner core of the matrigel plugs showed a reduced cell recruitment pattern and migration/infiltration into the plug containing tumor cell-derived conditioned media. As shown in **Figure 23C**, cells from placebo treated animals were capable of migrating into the core of the matrigel plug and accumulated as evidenced by the intense hematoxylin and eosin staining; in contrast, fewer cells migrated into matrigel plugs from morphine treated mice **(Figure 23F).** Lewis Lung carcinoma cells can secrete high basal levels of chemokines, sufficient to recruit host leukocytes to the tumor microenvironment. As we expected, this staining was reduced in sections analyzed from morphine treated mice. Comparison of placebo and morphine treated sections show leukocytes' infiltration out of the blood circulation and into the surrounding muscle tissue of experimental mice. These results suggest, in addition to effects on hypoxic tumor cells, that morphine treatment can inhibit host cell recruitment and migration towards the tumor microenvironment *in vivo*.

Clinical studies report that the dose required for analgesic effects of morphine vary between cancer patients. Patients that receive morphine orally at a dose of 40-4800 mg often result in serum levels around 1.0 -2106 ng/ml. Morphine administration through parenteral route of administration often occur within 10-9062 mg, and this result in serum levels ranging from 7- 21,730 ng/ml (Tiseo PJ, 1995). To ensure that this method of morphine administration achieved blood levels within analgesic range, mice blood serum samples were collected at the time of matrigel plug removal and tested for morphine using the Morphine Coat-A-Count Serum kit. The morphine serum levels from morphine treated wild type and MORKO mice show that this method of pellet implantation produced morphine blood levels between 200-400ng/ml. This concentration falls within

physiological levels, and is seen among cancer patients receiving morphine for pain management. Taken together, the data generated from these experiments suggest that morphine at doses used clinically for pain management is capable of inhibiting leukocyte infiltration towards a tumor microenvironment.

Morphine Inhibits the Migration of Myeloid Derived Bone Marrow Cells to the Tumor Microenvironment

The initial source of inflammatory cells in the tumor microenvironment is from the circulating peripheral blood pool. In contrast, the sustained migration of cells necessary for maintaining angiogenesis is primarily derived from bone marrow. Tumor and stromal cell expression of VEGF recruit bone marrow-derived progenitors that contribute to tumor growth by incorporating themselves into the developing blood vessels (Lee TH, 2006). To determine if morphine inhibited bone marrow migration to suppress angiogenesis, we performed the following experiment. Polyvinyl-alcohol sponges (PVA) presoaked with conditioned tumor cell media from a long-term culture of normoxic cells were implanted subcutaneously at the anterior-dorsal right side of experimental mice. Experimental animals also received placebo or morphine through pellet implantation at the anterior-dorsal left side. In these experiments, bone marrow-suspensions from naïve luciferase positive mice, approximately $40x10^6$ cells per 500*u*L per mice were injected into C57BL/6 recipient wild type mice. After 24 hours post intra-peritoneal injection of Luciferase+ bone marrow cells, animals were administered 100ul of a 15mg/ml Luciferin at the sponge site and xenogen images were captured after 10 minutes post Luciferin administration. As shown in **Figure 24A**, xenogen-captured images of two representative

mice, show high expression of luciferase-positive bone marrow cells at the sponge sites (see arrows) reflecting a greater migration of luciferase+ bone marrow cells and thus increased cell recruitment when compared to morphine (**Figure 24B**). In these experiments the migration of bone marrow cells from the site of injection, from the peritoneal cavity to the PVA-tumor conditioned media sponge site in morphine treated mice were blunted as evidenced from the reduction in luciferase signaling (**Figure 24A-B**). Taken together, these results suggested that the reduction in leukocyte recruitment to the tumor microenvironment is as a result of defects in migration.

Morphine inhibited the recruitment of myeloid derived bone marrow cells to the tumor microenvironment

To further confirm the effect of morphine on leukocyte recruitment to the tumor microenvironment and its effects on migration to the PVA sponges-containing tumor cell media were removed after 1 and 4 days after post intra-peritoneal injection of donor bone marrow cells. Experimental mice were sacrificed and the PVA sponges removed and the total number of infiltrating bone marrow cells were determined using Guava Technologies FACS system and Guava Express Plus program. PVA sponges were placed microfuge tubes, and cells were centrifuge out of the PVA sponges. As shown in **Figure 25A**, the total number of cells isolated from placebo treated animals was determined to be within the range 3.0-10.4 x10^7cells/ml. In contrast, morphine treatment through pellet implantation resulted in a significant decrease in cell recruitment ($p<0.00001$) into the PVA sponges containing conditioned tumor cell media. Guava express plus software determined the relative number of cells recruited into the PVA sponges derived from

morphine treated animals were within 1.2-2.8x10^7 cells/ml. These results further confirmed the inhibitory effect of morphine on cell migration to the tumor microenvironment. These results further support the view that morphine inhibits leukocyte recruitment to further inhibit angiogenesis and thus tumor growth *in vivo*.

Quantification of CD45+ Bone marrow derived progenitors in the PVA sponges

In this model we expected that the recruitment of cells, other than bone marrow cells, as many other cells types are required in the repair and regeneration processes. To further verify the presence of the bone marrow derived myeloid cells within the PVA sponges, we next quantified the relative number of CD45+ expressing cells between placebo and morphine treatment. The mean % values of CD45+ cells per 5000 cells examined after staining and FACS ranged from 28-47% of total cells infiltrated into the PVS sponges. As shown in **Figure 25B**, the relative number of CD45+ cells from PVA sponges taken after placebo treatment was approximately 2.3 x 10^7 cell/ml +/- 6 x 10^6. Morphine treatment of mice resulted in a significant reduction in the total number of bone marrow myeloid derived CD45+ cells ($p<0.0005$), of mean value 1.1 x 10^7 cell/ml +/- 3.0 x 10^6. Taken together, these results support the view that morphine inhibits the migration and recruitment of CD45+ bone marrow derived myeloid cells towards a chemotactic gradients and this can potentially reduced angiogenesis within the tumor microenvironment.

Characterization of cells recruited to PVA sponges containing conditioned tumor media

There is strong evidence linking bone marrow derived myeloid cells to enhanced tumor angiogenesis and growth (Noonan DM, 2008; Shibuya, 2006). In the rest of these studies, we further investigated the role of inflammatory cells in tumor angiogenesis. We further characterized the leukocytes recruited in response to tumor cell derived chemokines from the PVA sponges after 1 and 4 days post-implantation. The relative number of CD11b+ cells was determined through Fluorescent Activated cell sorting and staining with fluorescently conjugated antibodies (**Figure 26A**). CD11b+, a trans-membrane protein involved in the binding to CD31on quiescent endothelial cells mediating cell adhesion (Vainer B, 2000). CD11b+ expression is primarily found on a subset of blood derived hemangiocytes, tie2+ monocytes, M2 macrophages, and neutrophils (Shojaei F, 2008).

Blood derived hemangiocytes, tie2+ monocytes, M2 macrophages, and neutrophils contribute to angiogenesis and work together to increase tumor growth. Results from the fluorescent activated cell sorting analysis using CD11b-FITC conjugated antibodies show that CD11b+ cells made up approximately 0.7-5.66% of the total cells infiltrated into the PVA sponges containing conditioned tumor cell media. The relative number of CD11b+cells infiltrated into the sponges increased from day 1 to day 4 under placebo treatment, see **Figure 26A**. Similar to the pattern seen with placebo treatment, the number of infiltrating cells into the PVA sponges also increased from day 1 to day 4 in the presence of morphine. However, morphine treatment significantly

decreased the number of infiltrating cells expressing CD11b, when compared to placebo treatment on day 1 ($p<0.004$) and day 4 ($p<0.01$).

To further characterize the PVA sponge cells we next stained PVA cells with antibodies against CD14, the Toll-like receptor's co-receptor, a protein that bind the *E. coli* cell wall component lipopolysaccaride. CD14 is found predominantly on a subset of monocyte progenitors, tie2 expressing monocytes, M2 macrophages, and neutrophils (low). The results from the fluorescent activated cell sorting analysis, using CD14-FITC conjugated antibodies show that CD14+ cells made up approximately 1.02-33.56% of the total cells infiltrated into the PVA sponges containing conditioned tumor cell media. The relative number of CD14+cells infiltrated into the sponges on day 1 was similar to that for day 4 under placebo and morphine treatment, see **Figure 26B**. Similar to the patterns were observed with seen with morphine treatment. In addition, morphine treatment significantly decreased the number of infiltrating cells expressing CD14 monocytes when compared to placebo treatment on day 1 ($p<0.003$) and day 4 ($p<0.00001$). Taken together, these results suggest that morphine can reduce myeloid cell derived monocyte infiltration into the tumor microenvironment to suppress VEGF-induced angiogenesis required for tumor growth.

Morphine inhibits M2 monocyte-macrophage polarization/differentiation at the tumor microenvironment

Hypoxic areas within tumor sites stimulate the migration and differentiation of monocyte derived peripheral blood cells (Bosco MC, 2006). These mononuclear phagocytes or primary monocytes often accumulate in large numbers at hypoxic areas

where they terminally differentiate into inflammatory and tumor-associated macrophages. These cells further recruit monocytes and endothelial cell progenitors from the bone marrow (Bosco MC, 2006). To this effect, we next determined the relative number of M2 polarized macrophages through double staining for F480/CD14+ cells using a fraction of the total PVA sponge cell population. As shown in **Figure 27**, on day 4, the number of M2 macrophages, possibly differentiated from the monocytes, was doubled the amount on day 1. In addition, morphine treatment resulted in a significant reduction in the amount of double positive F4/80+; CD14+ M2 macrophages within the PVA sponge on day 1($p<0.002$) and day 4 ($p<0.005$).

Morphine treatment inhibited neutrophil recruitment to the tumor microenvironment.

To characterize the recruited leukocytes, another fraction of the total population of cells was analyzed for markers of neutrophils, namely Ly6G, and CXCR2. Ly6G are present on large number of neutrophils progenitors. PVA sponge cells were stained with anti-Ly6G-FITC conjugated antibodies and fluorescent activated cell sorting analysis showed that the number of cells expressing the Ly6G cell surface markers were greater in placebo than morphine treatment on day 1 by 29.4%. The relative number of Ly6G+ cells recruited towards the tumor microenvironment decreased by day 4 (**Figure 28A**). Also on day 4, the relative number of cells recruited to the PVA sponges was significantly less than morphine treatment ($p<0.00004$).

To further validate the effect of morphine on neutrophils, relative number of cells expressing the chemokine receptor CXCR2 found mostly on mature neutrophils with

segmented nuclei was determined using CXCR2-PerCP conjugated antibodies and FACS. As shown in **Figure 28B**, the recruitment of CXCR2+ cells increased from day 1 to day 4. Compared to placebo, morphine treatment resulted in a 35.5% decrease in CXCR2+ cells on day 1 but was insignificant. On day 4, however morphine treatment had a significantly lower number of CXCR2+ cells ($p<0.0009$) present within the PVA sponges.

To verify the FACS data for positive identification of neutrophils progenitors and mature cells, cytospin preparations of fluorescently labeled cells were examined under confocal microscopy. As shown in **Figure 28C**, cells had a granular extracellular surface reminiscent of neutrophils containing granules. Ly6G positive cells were visualized with the nuclear DAPI stain, and a merged image is shown in **Figure 28E**. These images show cells with segmented nuclei with strong cell surface expression of Ly6G proteins (**Figure 28E**). Also shown in **Figure 28F**, are merged images of cells expressing CXCR2, double labeled with Ly6G after DAPI visualization. In this particular frame, cells are double and single labeled for both markers, confirming the presence of both mature and immature neutrophils. Taken together these cells confirmed the presence of neutrophils and their reduced recruitment in the presence of morphine to the tumor microenvironment to potentially reduce angiogenesis *in vivo*.

Morphine inhibits the recruitment of Tie2+ monocytes to the tumor microenvironment

Of greatest interest the Tie-2+ expressing monocytes have been identified in both human blood and tumors. The neutralization of these Tie-2+ monocytes in various

experimental tumor models inhibits have shown to inhibit tumor angiogenesis. In mice, the circulating Tie2+CD45+ hematopoietic cells are mostly CD11b+ and Ly6G/Gr-1 (low/negative). The surface marker profile of Tie-2 expressing monocytes is similar to that of monocytes, including CD14, but distinct from the classical inflammatory monocytes and is thought to consist of precursors of tissue macrophages (Lewis CE, 2007).

In these experiments we also analyzed the expression of Tie2+/CD14+ expressing cells from a fraction of the total population of cells recruited into the tumor cell conditioned media containing PVA sponges. Tie-2 expressing monocytes can localize to and incorporate into the tumor blood vessels. They can also produce high levels of the proangiogenic factors, and matrix-remodeling proteins. They can function as "pathfinders" for activated endothelial cells to form provisional endothelium-like structures for blood vessel formation. (Lewis CE, 2007). As shown in **Figure 29**, on day 1 of bone marrow progenitor migration, on average 0.73% of the total cells recruited were Tie2+/CD14+ in samples taken from placebo treated mice. In the case of morphine treatment, on average 0.23% were Tie2+/CD14+on day 1, and this was significantly lower than placebo treatment ($p<0.01$).

On day 4 of the experiment, the number of Tie2+/CD14+ cells in placebo treated mice increased from day 1, on average greater than 14% of the total population. Compared to placebo, morphine treatment significantly reduced the amount of Tie2+/CD14+ expressing monocytes on day 4 ($p<0.005$), with only on average 1.01% of morphine treated samples expressing the cell surface markers Tie2+/CD14+ (**Figure 28**). Morphine treatment reduced recruitment of monocytes expressing the cell surface

markers Tie2+ and CD14+ towards the tumor microenvironment. These studies do not exclude the presence of another subset of tumor promoting cells, the myeloid derived suppressor cells that also have significant roles in the development of angiogenesis.

Considering that the recruitment of Tie2+endothelial progenitors were reduced in the presence of morphine and they contribute to vessel formation, we predicted that the amount CD31+ endothelial cells present within the PVA sponges would also be reduced after morphine treatment. Data from the FACS analysis showed that on average 4-9% of the total population of cell were positive for the endothelial cell marker CD31. As expected, the reduction in Tie2+/CD14+ expressing monocytes was accompanied with a significant reduction the amount CD31+ endothelial cells by 75% when compared to placebo ($p<0.000002$, **Figure 30**). These results further support the view that the effect of morphine on angiogenesis is partly mediated through multiple mechanisms involving hypoxic tumor cells, pro-inflammatory monocytes and endothelial cell precursors.

Discussion

Tumor angiogenesis is highly dependent on the chemotaxis and thus recruitment of pro-inflammatory cells into the tumor microenvironment. In models of inflammatory diseases, tissue macrophages sequentially recruit cells involved in the first line of defense, that includes neutrophils, followed by monocyte-macrophage like cells that also further contribute to tissue remodeling and tube formation. In the case of a growing tumor, frequently an excessive pro-inflammatory reaction results, and this creates a tumor microenvironment commonly described as a "non-healing wound". In the initial stages of tumor growth these cells are capable of rejecting tumor cells, but as the tumors grow and tumor cells down-regulate antigen expression, they escape immune surveillance and this disrupts the balance between tumor cell growth and death, such that tumor cell growth outweighs tumor cell death (Lamagna C, 2006). These experiments were designed to test the effect of morphine on the immune system's contribution to angiogenesis and thus the growth and progression of established tumors, in tumor-bearing mice.

In these models of experimental angiogenesis, both the placebo and morphine treated mice were implanted with matrigel plugs or PVA sponges containing tumor cell conditioned media. The recruitment pattern was characterized by first identifying the cells that were capable of migrating out of the blood and into the matrigel plugs that contained chemotactic factors derived from tumor cells. Even in a model, where the chemotactic gradients were similar in between treatment groups, *in vivo* morphine significantly inhibited: 1) the migration of bone marrow derived progenitors to tumor cell-derived chemokines and 2) the recruitment of inflammatory cells out of peripheral blood circulation and into the tumor microenvironment in mice when compared to

placebo (**Figures 23-24**). This inhibition in leukocyte recruitment pattern exerted by morphine into the matrigel plug containing tumor cell media both on day 1 and day 4 of the investigations may have simply resulted from reduced migration. Therefore, taking into consideration that the effects observed by morphine on recruitment may have been a direct consequence of morphine on cell migration; we tested the effects of morphine on bone marrow derived progenitor cell chemotaxis towards tumor cell media derived from normoxic and hypoxic tumor cells in an *in vitro* system. Using a standard chemotaxis double chamber system, we compared the migration of naïve cells, to morphine pre-treated bone marrow derived progenitors cells. We found that the migration response were similar between naïve and morphine pretreated cells towards tumor cell media taken from normoxic cells (**Figure 31**). In contrast, naive bone marrow derived progenitor cell migration was greater towards tumor cell media derived from hypoxic tumor cells than normoxic cells ($p<0.02$) and morphine pre-treatment did not affect this pattern of migration any further ($p=0.28$). These results suggested that in an isolated *in vitro* system, lacking an intact endothelial barrier, morphine has no direct effect on cell migration towards a chemotactic gradient. Additionally, the inhibition in cell migration seen *in vivo* may have resulted from effects on the interaction between the endothelial cell barrier and immune components involved in cell adhesion or tissue extravasation.

While signaling through the appropriate chemokine receptors aid in the migration and localization of leukocytes expressing these receptors towards specific chemokine gradients, adhesion and extravasation are also necessary steps in the recruitment inflammatory cells out of the blood and into most tissue environments (**Figure 10**). The concomitant decrease in cell recruitment observed with morphine treatment could have

resulted from changes in the adhesion properties of the immune cells or at the endothelial cell level. To this extent CD11b, is an important integrin molecule involved in the regulation of leukocyte (monocytes, granulocytes, macrophages and natural killer cells) adhesion, migration, phagocytosis, chemotaxis and cellular activation (Solovjov DA, 2005). FACS analysis for the characterization of CD11b+ cells in these studies showed that in placebo treated control mice, cells expressing this cell surface protein were recruited to the PVA sponges on day 1; and then further accumulated upto day 4. In contrast to placebo, morphine treatment was accompanied with a significant inhibition in the recruitment pattern of CD11b+ cells ($p<0.004$ on day 1 and $p<0.01$ on day 4). These results suggest that morphine treatment could have directly or indirectly altered the expression profile of these cells, reducing their ability to adhere to the activated endothelial cells after injection into the peritoneum; thereby preventing their extravasation into the blood for subsequent migration to the PVA sponges. The effects of morphine on cell recruitment seen *in vivo*, is most likely dependent on the interaction with the endothelium, and this was lacking in the *in vitro* system. Therefore further studies are necessary to address the exact mechanisms affected by morphine during leukocyte migration.

Another valid explanation for the observed reductions in the normal migration pattern towards the tumor microenvironment could have been due simply to a shift or delay in the normal migration pattern of inflammatory cells. In wound healing models, a sequential recruitment pattern of immune cells coincides with and is unique to the phase of remodeling (Park JE, 2004). At the initial injury, platelets come in during coagulation events, followed by neutrophils and macrophages in the inflammation stage and finally

during remodeling the fibroblasts and lymphocytes accumulates (Park JE, 2004). Several independent investigations inhibiting neutrophil migration, and recruitment, have positively confirmed the importance and significant contribution of neutrophils in tube formation (Noonan DM 2006; Shibuya M, 2006; Matsuo Y, 2009). The delay in the initial recruitment of neutrophils could have blunted the subsequent recruitment of inflammatory cells in particular, macrophages. Macrophages secrete many cytokines such as tumor necrosis factor-α, transforming growth factor-α and -β, platelet derived growth factor and insulin like growth factor, all shown to directly increase endothelial cell proliferation and collagen synthesis (Park JE, 2004). We hypothesize that morphine may play a role in disrupting this sequential recruitment pattern, it is this initial blunting that could have led to the observed overall reduction in recruitment. To this effect, it would be of great interest to see if the reconstitution of neutrophils in the presence of morphine would rescue the inhibition of bone marrow derived cell migration towards the tumor microenvironment and rescue tumor growth. In studies stimulating monocytes and peripheral blood mononuclear cells with peptidoglycan from *Staphylococcus aureus*; morphine significantly inhibited the production of cytokines such as TNF and IL-6 from monocytes; but in peripheral blood mononuclear cells morphine inhibited the TNF, but not the IL-6 production (Bonnet MP, 2009). Additionally, morphine can suppress the ability of human THP-1 monocytes to convert into a macrophage phenotype after Phorbol 12-myristate 13-acetate (PMA) treatment (Hatsukari I, 2006). In these studies, PMA conversion of monocytes to macrophages increased their adhesive properties and migration towards an MCP-1 chemokine gradient but was significantly reduced in the presence of morphine. These results suggest that the monocyte to macrophage conversion

is a prelude for adhesion and subsequent transmigration. Alternatively, the lower number of recruited cells could have resulted from direct effects of morphine on bone marrow cell survival, receptor expression and or cytokine secretion and these events should be investigated further.

The characterization of the cells recruited to the tumor microenvironment, confirmed the presence of neutrophils and macrophages, both inflammatory cells known to contribute significantly to blood vessel formation (Bingle L, 2001, Noonan DM 2008, Shibuya M, 2006). Therefore, selective purification and or replacement of these individual pro-inflammatory cell subpopulations into morphine treated mice should reverse the effects of morphine if the effect of morphine is primarily through that particular cell type. The sequential recruitment of the immune cells may be an important response disrupted after morphine treatment (comparing placebo). Any disruptions in the migration pattern of neutrophils, involved in the first line of defense can lead to additional deficits in the second phase of cell recruitment required for further support and maintenance of blood vessels within the tumor microenvironment. Similarly, morphine could have produced suppressive effects on the activation of tissue macrophages, which could have lead to a delay in the migration pattern to offset cell recruitment by a few days. Therefore, selectively purifying these individual populations and later replacing them singly into morphine treated mice should rescue the effects of morphine if the effect of morphine is primarily through deficits in activity of these particular cells.

Alternatively, the effects seen on leukocyte recruitment could have been due to changes in bone marrow mobilization, in particular on day 4. In these experiments, cells from donor mice were injected in the peritoneal cavity, but one cannot discount the

contribution of the host's own bone marrow cells especially since we did not irradiate the animals before adoptive transfer. While the initial leukocyte recruitment observed in recipient mice was primarily cells of the donor mice; at the later stage, on day 4 we were observing the recipient's own bone marrow mobilization response. The recruitment patterns observed by day 4 in placebo animals most likely involved the host's own bone marrow mobilization, and since this was reduced with morphine treatment, we speculate that morphine could also have effects on the ability of the spleen or bone marrow to release chemokines or myeloid progenitors that would normally contribute to tumor growth. The fact that the Tie2+ monocyte recruitment pattern was significantly compromised raises the question whether the effect of morphine in these studies stemmed from alterations in stem cell progenitor populations already known to contribute significantly to angiogenesis and tumor growth (Palmer MD, 2005; Lewis CE, 2007; Venneri MA, 2007). However, more studies are necessary to address these questions. In these experiments, even though the chemokine gradients were are equal in placebo and morphine treated mice, it was the host response to chemotaxis that was altered. Taken together, these results suggest that morphine is acting in multiple pathways to alter angiogenesis associated with tumor growth.

Figure 23(A-F)

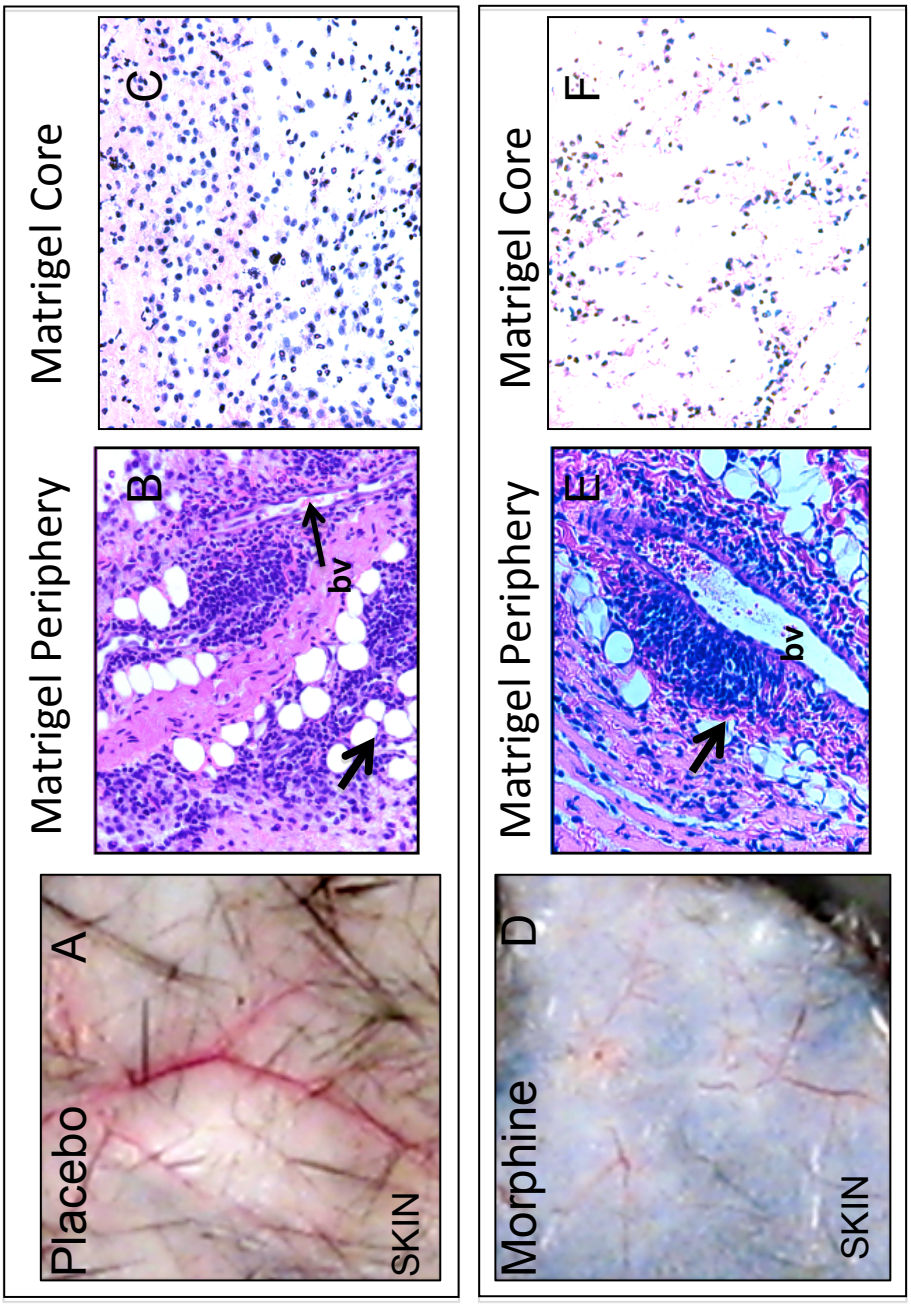
Matrigel Core
C
Matrigel Periphery
B
bv
A
Placebo
SKIN
Matrigel Core
F
Matrigel Periphery
E
bv
D
Morphine
SKIN

Figure 23(G-H)

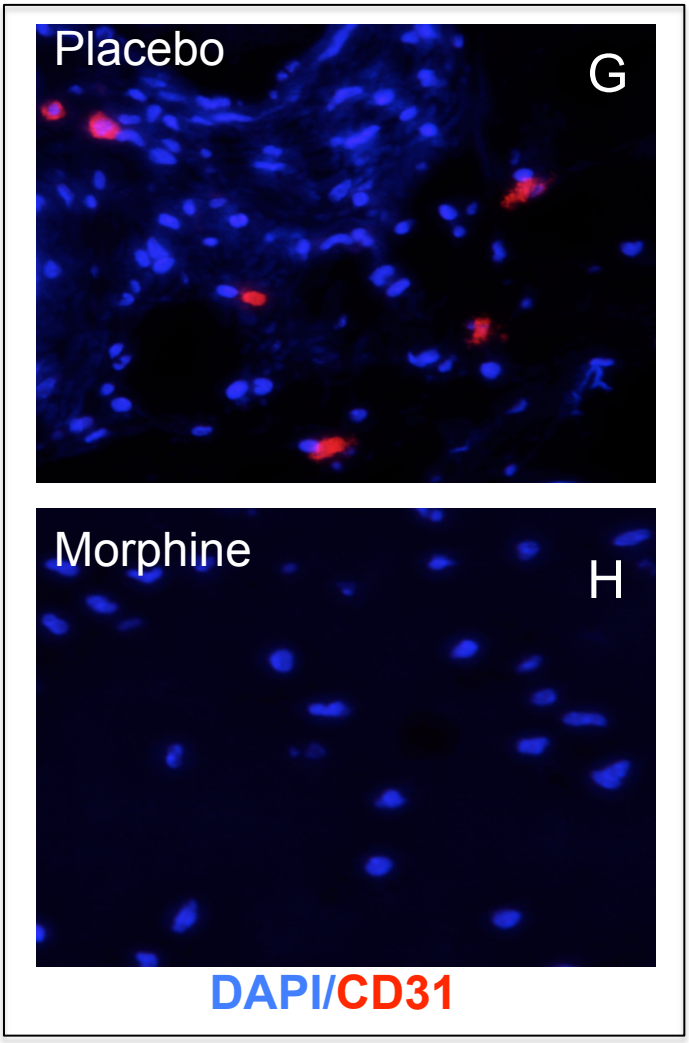

Figure 23: Morphine reduces the recruitment of leukocytes to the tumor microenvironment.

Tumor cell conditioned media from *in vitro* long term culture of Lewis lung carcinoma cells were admixed in matrigel and injected subcutaneous into placebo and morphine pelleted mice. Examination of skin above the plugs show stronger well interconnected vessels in placebo (A) compared to morphine mice (B). Hematoxylin and eosin stained sections from placebo mice (B) showed higher cell infiltration into the muscle from surrounding blood vessels (bv, arrows) at the matrigel plug periphery than sections analyzed from morphine treated mice (E). A similar pattern of cell density was observed deeper within the matrigel plugs; placebo plugs (C) contained qualitatively more infiltrating cells per field than sections examined from morphine treated mice (F). Parrafin embedded sections were used and infiltrated cells were also identified as CD31+ endothelial cells (G, H).

Figure 24

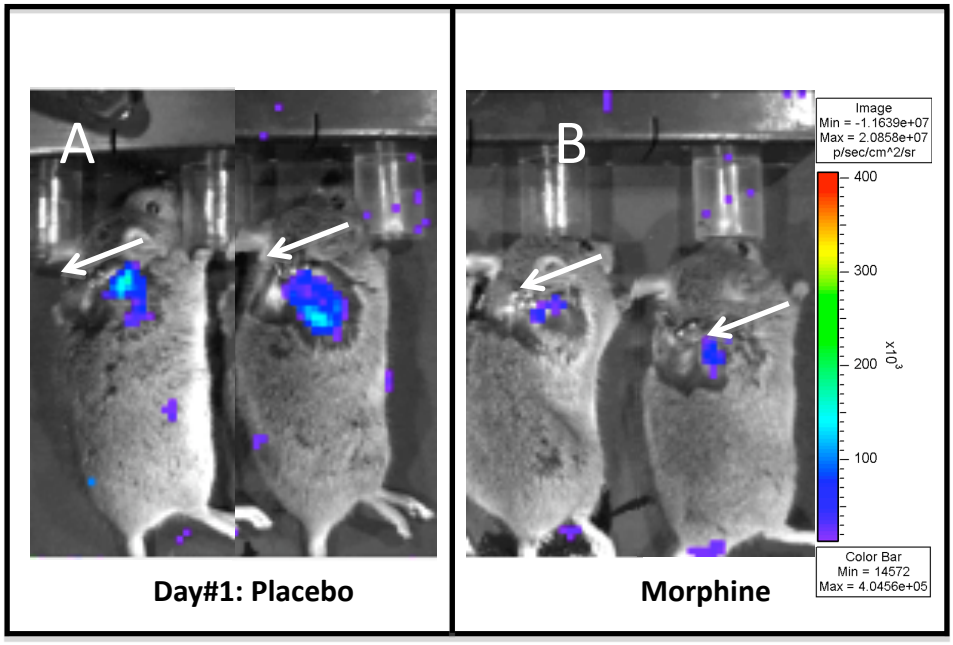

Figure 24: Morphine inhibited the migration of bone marrow progenitors from the peritoneum towards a tumor microenvironment

Mice were implanted with PVA sponges containing conditioned tumor cell media. Luciferase + bone marrow cells was adoptively transferred into wild-type mice receiving placebo or morphine through pellet implantation. After 24hrs, Luciferin was injected at the PVA sponge site and representative xenogen images are shown of placebo (A) and morphine treated mice (B).

Figure 25A

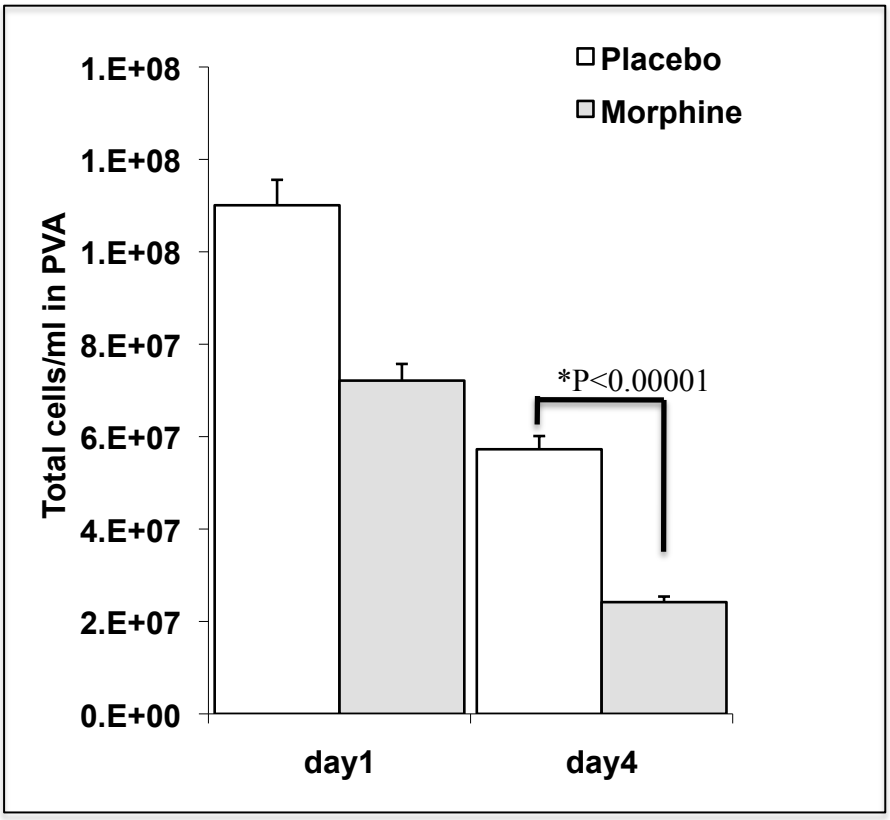

Figure 25A: Morphine inhibited total cell recruitment into the tumor microenvironment

In subsequent experiments, PVA sponges were removed at day 1 and 4 to quantify the number of infiltrating cells. PVA sponges were removed and cells were extracted as described in methods. Graph shows comparison of cell numbers between placebo and morphine treatment, determined using the Guava Express Plus software on the Guava Easy Cyte FACS system.

Figure 25B

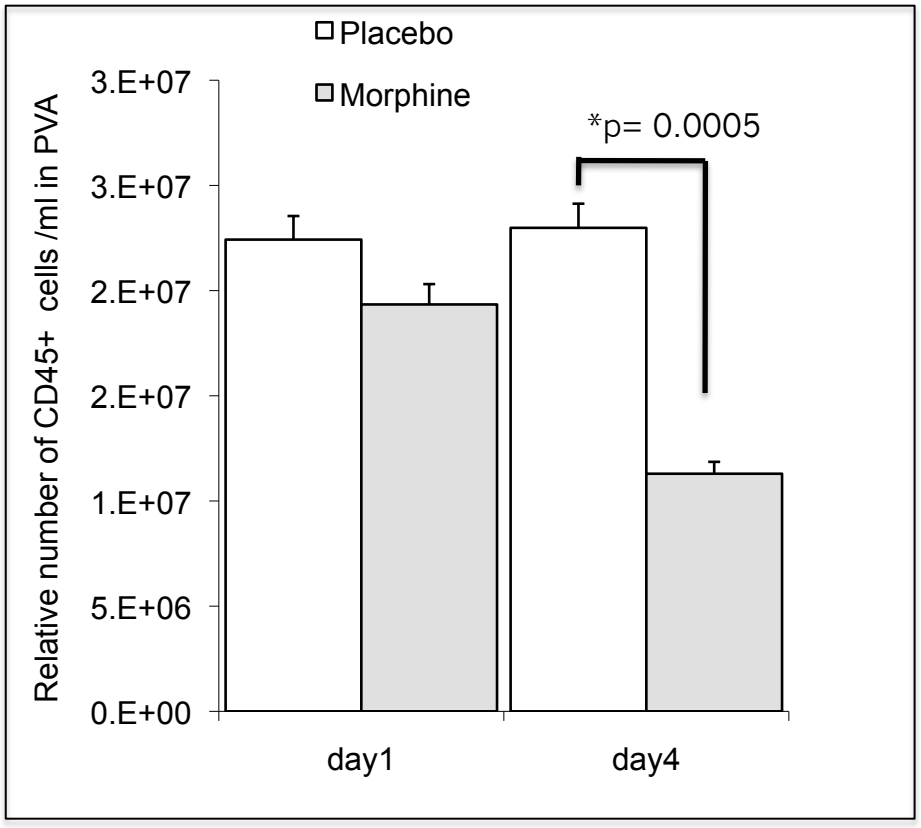
Placebo
Morphine
*p= 0.0005
Relative number of CD45+ cells /ml in PVA
3.E+07
3.E+07
2.E+07
2.E+07
1.E+07
5.E+06
0.E+00
day1
day4

Figure 25B: Morphine treatment concomitantly decreased CD45+ bone marrow derived myeloid cell recruitment

A fraction of the total cells isolated from the PVA sponges was stained for CD45 cell surface expression using CD45-PE conjugated fluorescent monoclonal antibodies. Cells were fixed, and non-specfically blocked before incubation with CD45 antibodies. Non-stained cells were used to adjust machine settings to account for cell auto-fluorescence. FACS analysis was performed on the Guava Easy Cyte System; data was collected using the Guava Express Plus software .

Figure 26A

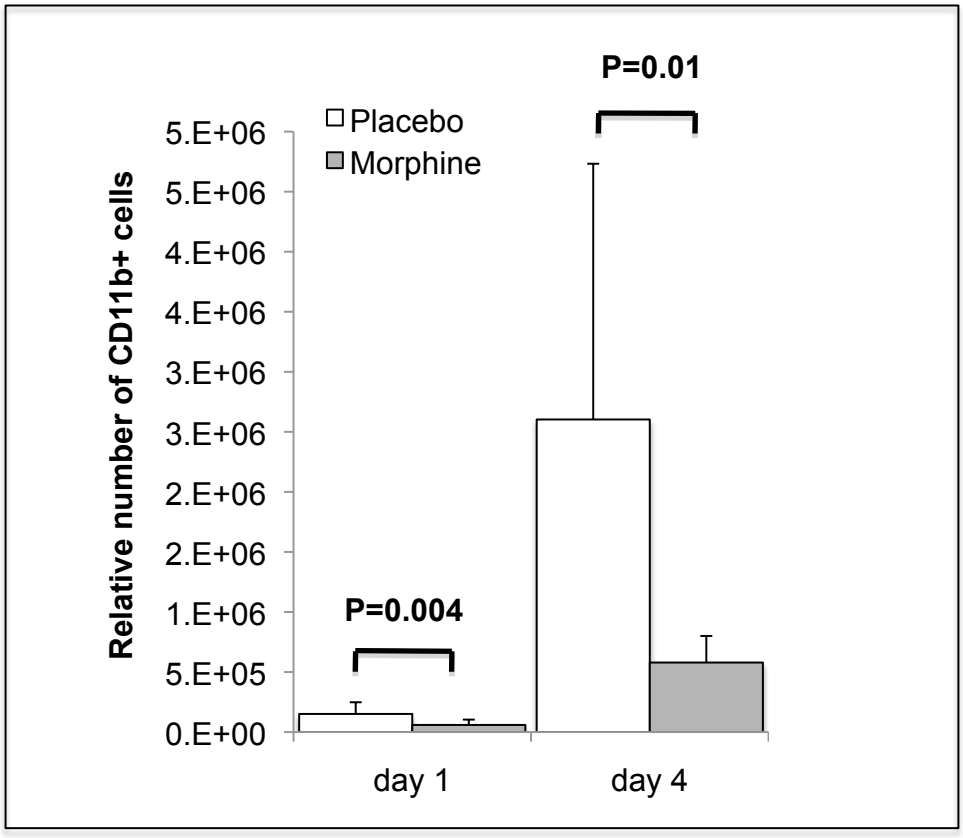
P=0.01
Placebo
Morphine
5.E+06
5.E+06
4.E+06
4.E+06
3.E+06
3.E+06
2.E+06
2.E+06
1.E+06
5.E+05
0.E+00
Relative number of CD11b+ cells
P=0.004
day 1
day 4

Figure 26A: Characterization of CD11b+ expressing monocytes isolated from tumor sites

A fraction of the total cells isolated from the PVA sponges was stained for CD11b cell surface expression using CD11b-FITC conjugated fluorescent monoclonal antibodies. Cells were fixed, and non-specfically blocked before incubation with CD11b antibodies. Non-stained cells were used to adjust machine settings to account for cell auto-fluorescence and FACS analysis was performed on the Guava Easy Cyte System; data was collected using the Guava Express Plus software .

Figure 26B

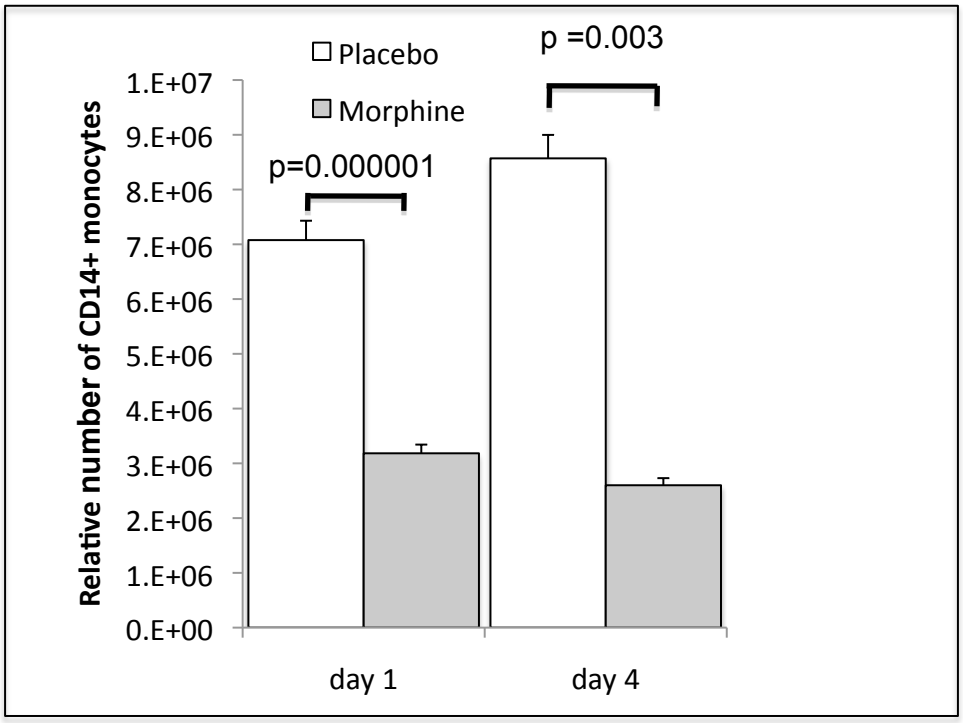

Figure 26B: Characterization of CD14+ expressing monocytes isolated from tumor sites

A fraction of the total cells isolated from the PVA sponges was stained for CD14 cell surface expression using CD14-PE conjugated fluorescent monoclonal antibodies. Cells were fixed, and non-specfically blocked before incubation with CD14 antibodies. Non-stained cells were used to adjust machine settings to account for cell auto-fluorescence and FACS analysis was performed on the Guava Easy Cyte System; data was collected using the Guava Express Plus software .

Figure 27

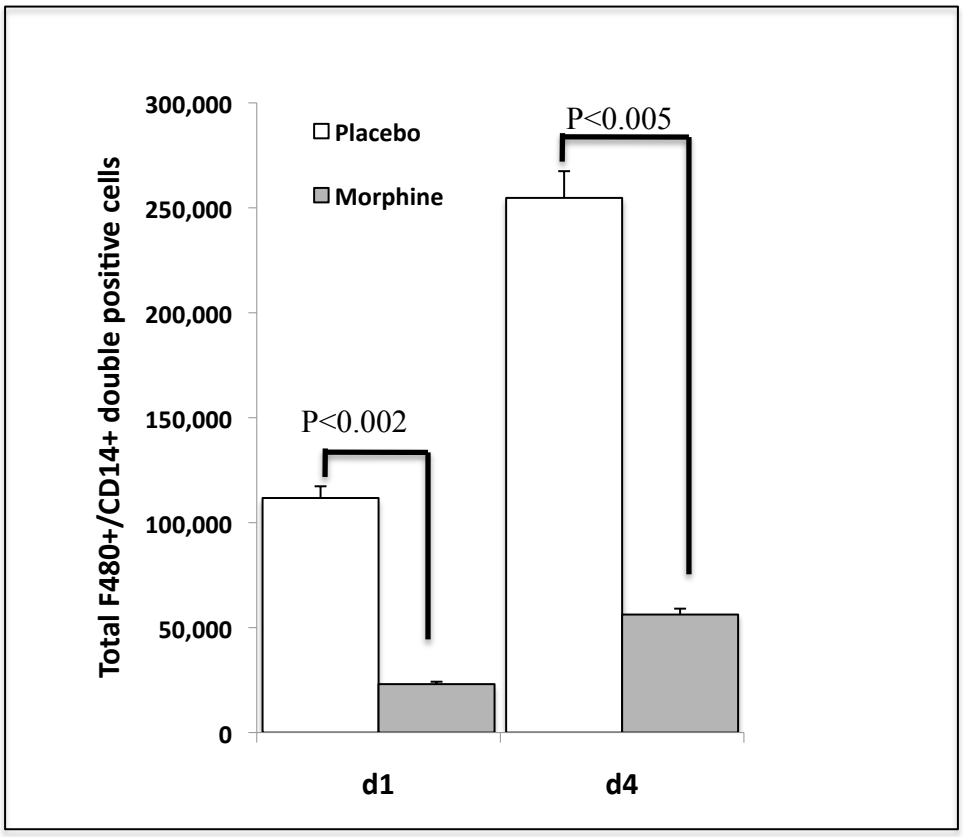
300,000
250,000
200,000
150,000
100,000
50,000
0
Total F480+/CD14+ double positive cells
Placebo
Morphine
P<0.005
P<0.002
d1
d4

Figure 27: Characterization of tumor promoting M2 polarized macrophages from tumor sites

A fraction of the total cells isolated from the PVA sponges was double stained with F480 and CD14 to determine the relative number of M2 polarized macrophages using F4/80-FITC and CD14-PE conjugated fluorescent monoclonal antibodies. Cells were fixed, and non-specfically blocked before incubation with antibodies. Non-stained cells were used to adjust machine settings to account for cell auto-fluorescence and FACS analysis was performed on the Guava Easy Cyte System; data was collected using the Guava Express Plus software .

Figure 28A

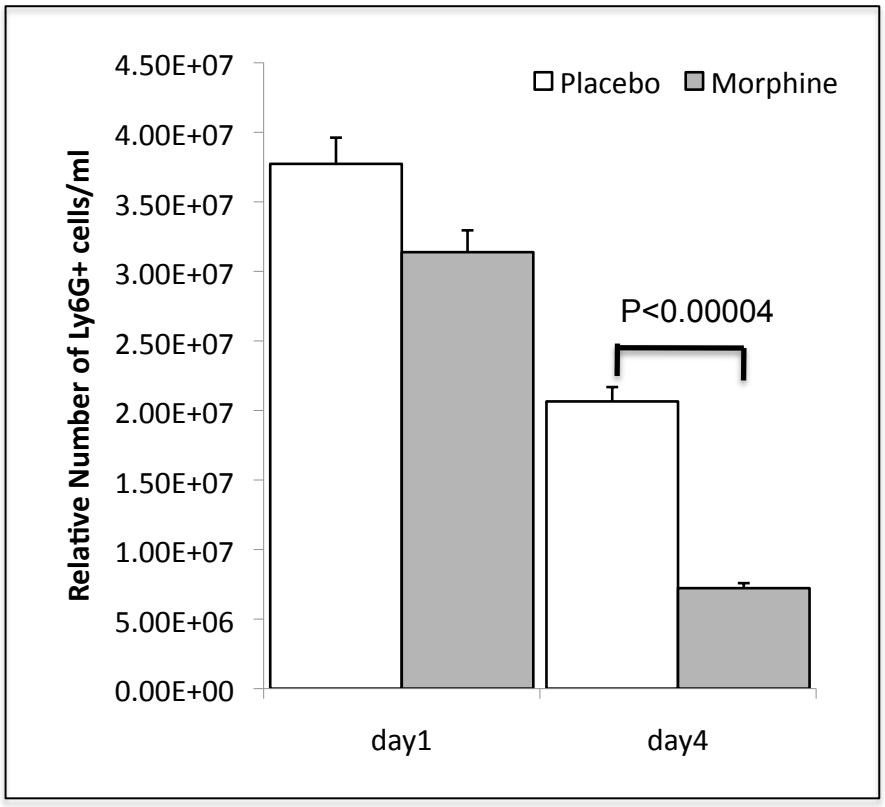
Placebo
Morphine
Relative Number of Ly6G+ cells/ml
4.50E+07
4.00E+07
3.50E+07
3.00E+07
2.50E+07
2.00E+07
1.50E+07
1.00E+07
5.00E+06
0.00E+00
P<0.00004
day1
day4

Figure 28A: Characterization of leukocytes from PVA-conditioned tumor sites

A fraction of the total cells isolated from the PVA sponges was stained with Ly6G-FITC antibodies to determine the relative number of neutrophils. Cells were fixed, and non-specfically blocked before incubation with antibodies. Non-stained cells were used to adjust machine settings to account for cell auto-fluorescence and FACS analysis was performed on the Guava Easy Cyte System; data was collected using the Guava Express Plus software .

Figure 28B

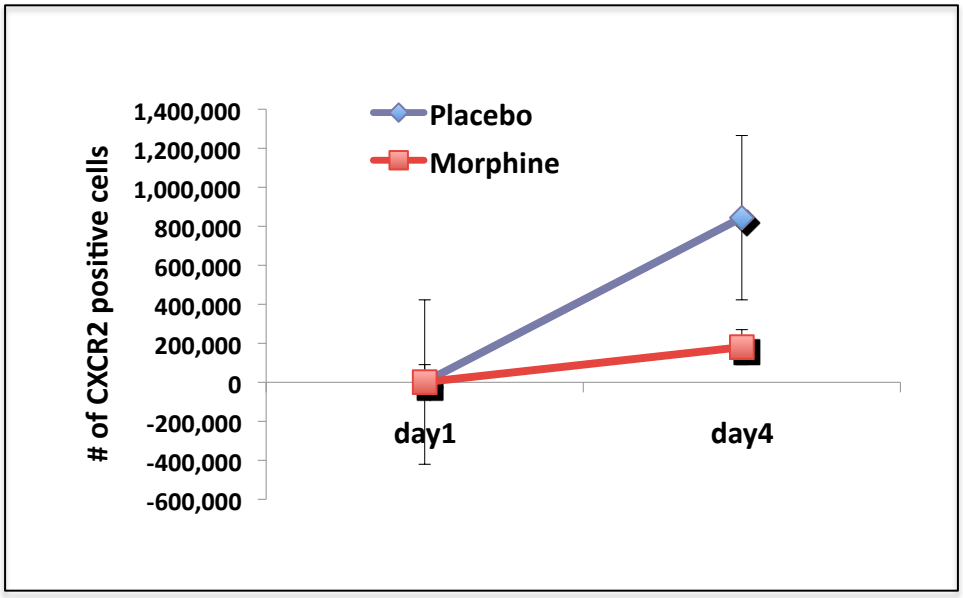

Figure 28B: Further characterization of leukocytes from tumor sites using neutrophil marker CXCR2.

A fraction of the total cells isolated from the PVA sponges was stained with CXCR2-Percp antibodies to determine the relative number of mature neutrophils. Cells were fixed, and non-specfically blocked before incubation with antibodies. Non-stained cells were used to adjust machine settings to account for cell auto-fluorescence and FACS analysis was performed on the Guava Easy Cyte System; data was collected using the Guava Express Plus software .

Figure 28C-E

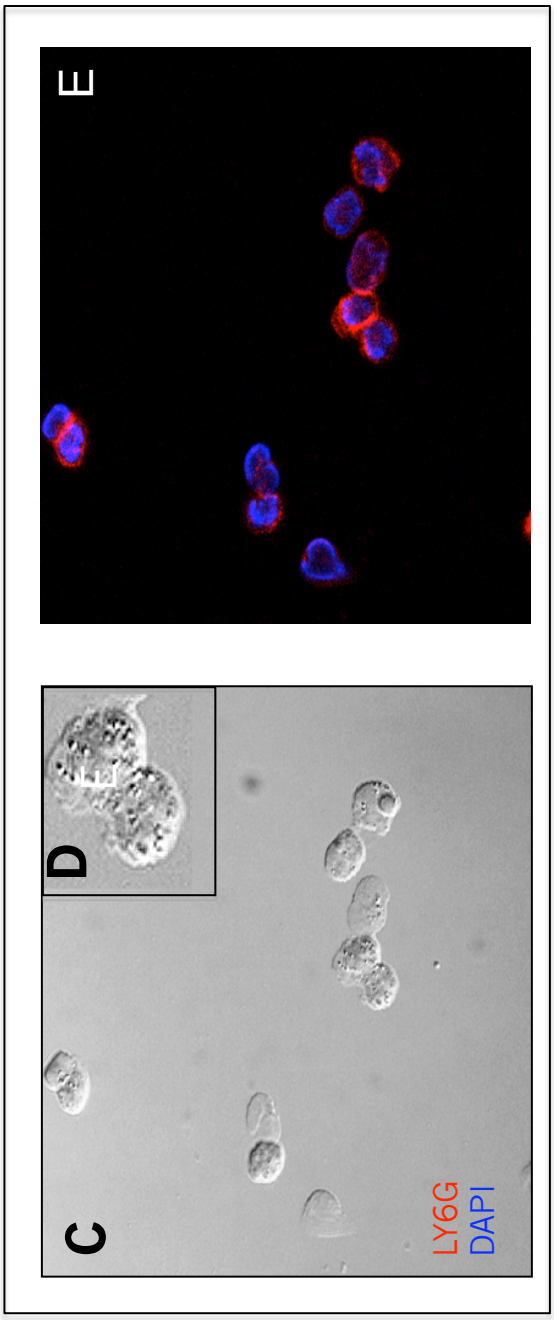

Figure 28F

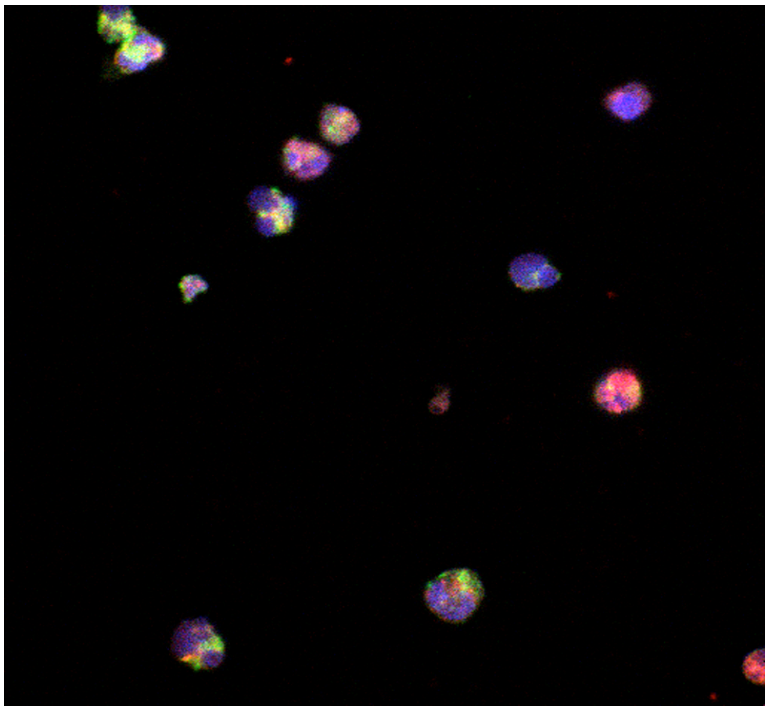

CXCR2
Ly6G
DAPI
Merged

Figure 28C-F: Positive identification of Ly6G+, CXCR2+ nuetrophils isolated from tumor sites

Cells were stained for FACS analysis and aliquots were used in cytopsin preparations. Stained slides were visualized in the presence of DAPI using confocal microscopy. The images were collected under bright-light (C) and magnified for cell granularity (D, inset). Fluorescent labels were collected in appropriate single color channels and Adobe Photoshop was used to merge the corresponding Ly6G-PE (red) with DAPI (nuclear stain, blue) (E). Double stained cells were collected in the appropriate single channels and Adobe Photoshop was used to merge the corresponding Ly6G-FITC (green) with CXCR2-PE (red) and DAPI (F) (40X).

Figure 29

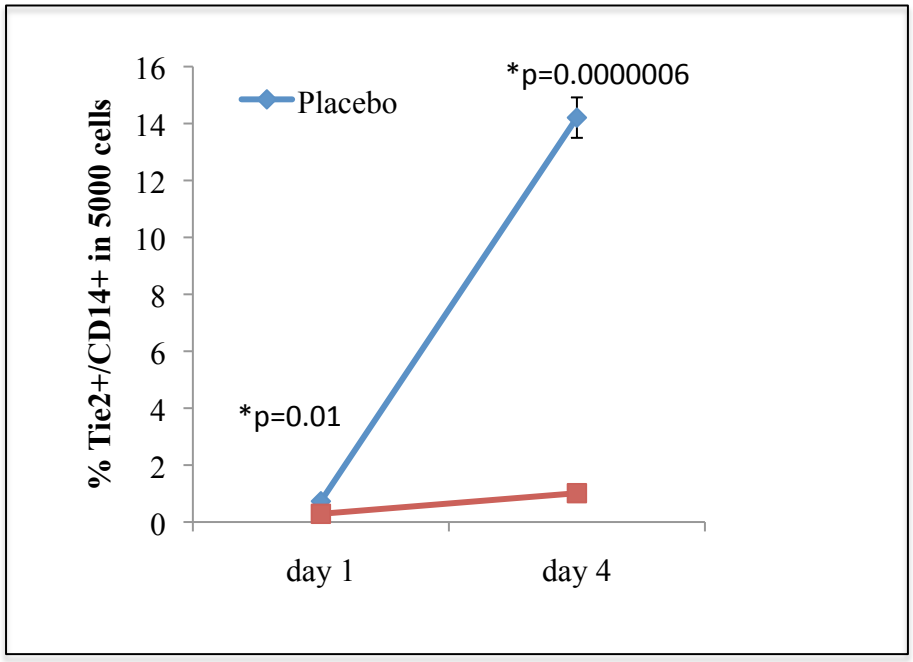

Figure 29: Characterization of tumor promoting Tie2 expressing monocytes from tumor sites

A fraction of the total cells isolated from the PVA sponges was stained with Tie2-PE and CD14-FITC conjugated antibodies to determine the relative number cells. Non-stained cells were used to adjust machine settings to account for cell auto-fluorescence and FACS analysis was performed on the Guava Easy Cyte System; data was collected using the Guava Express Plus software . Graph shows the % in 5000 double positive for Tie2+ and CD14+, an endothelial progenitor from a myeloid- monocytic lineage.

Figure 30

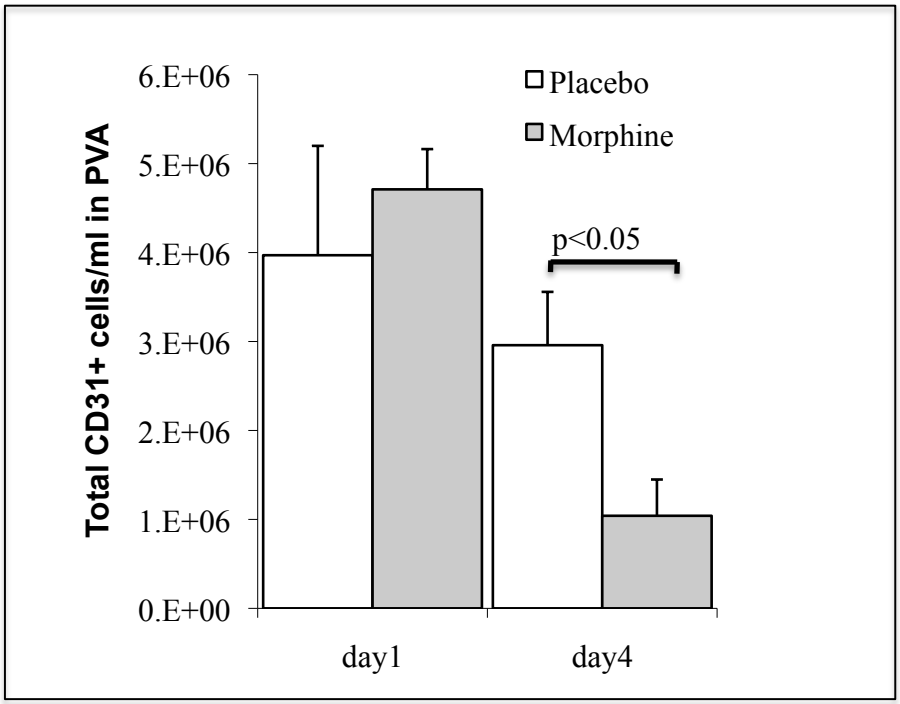

Figure 30: Quantification of CD31+ mature endothelial cells from tumor sites

A fraction of the total cells isolated from the PVA sponges was stained with CD31-PE conjugated antibodies to assess the status of mature endothelial cells that were recruited into the PVA as described. Non-stained cells were used to adjust machine settings to account for cell auto-fluorescence and FACS analysis was performed on the Guava Easy Cyte System; data was collected using the Guava Express Plus software . Graph shows the actual number of cells positive from the entire population of cells recruited into the PVA sponges.

Figure 31

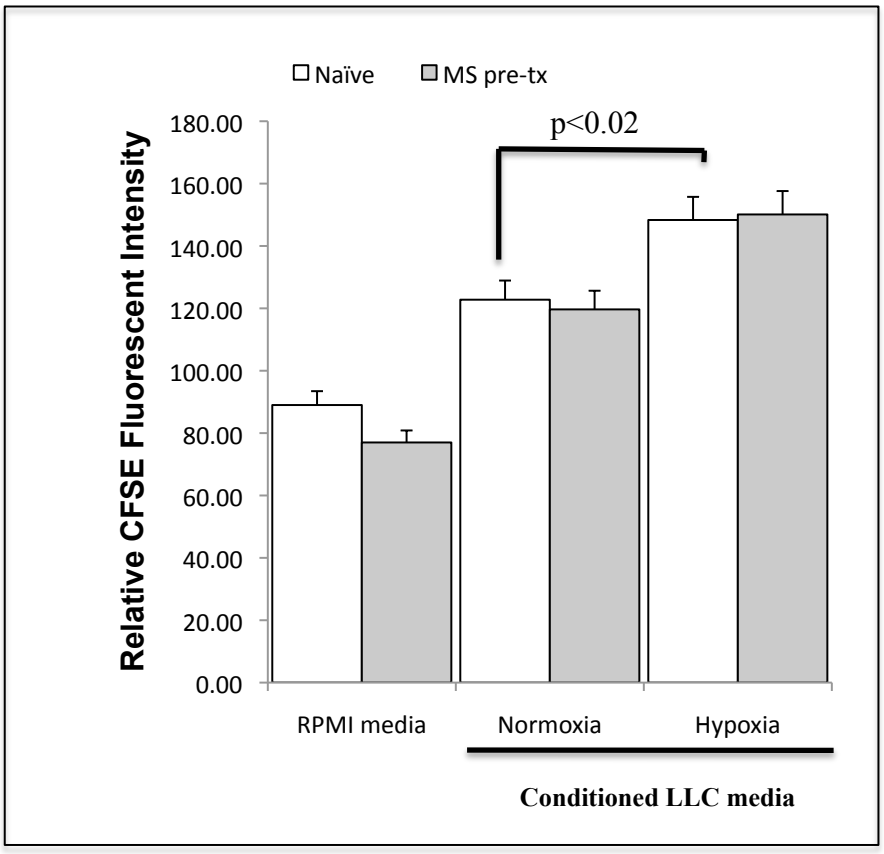
Naïve
MS pre-tx
p<0.02
Relative CFSE Fluorescent Intensity
180.00
160.00
140.00
120.00
100.00
80.00
60.00
40.00
20.00
0.00
RPMI media
Normoxia
Hypoxia
Conditioned LLC media

Figure 31: Effect of morphine on migration of bone marrow derived cells towards tumor cell derived chemokines *in vitro*.

Bone-marrow cells were isolated from 6-8week old mice. Equal numbers of naïve, or morphine treated CFSE label bone marrow cells were added to the top chamber and migration towards tumor cell media from normoxic or hypoxic cells assessed after 15 minutes. The top and bottom chambers were separated and CFSE expression was determined using a plate reader. Graph shows relative CFSE intensity after subtraction of background fluorescence and compared to cells allowed to migrate towards media only.

Figure 32

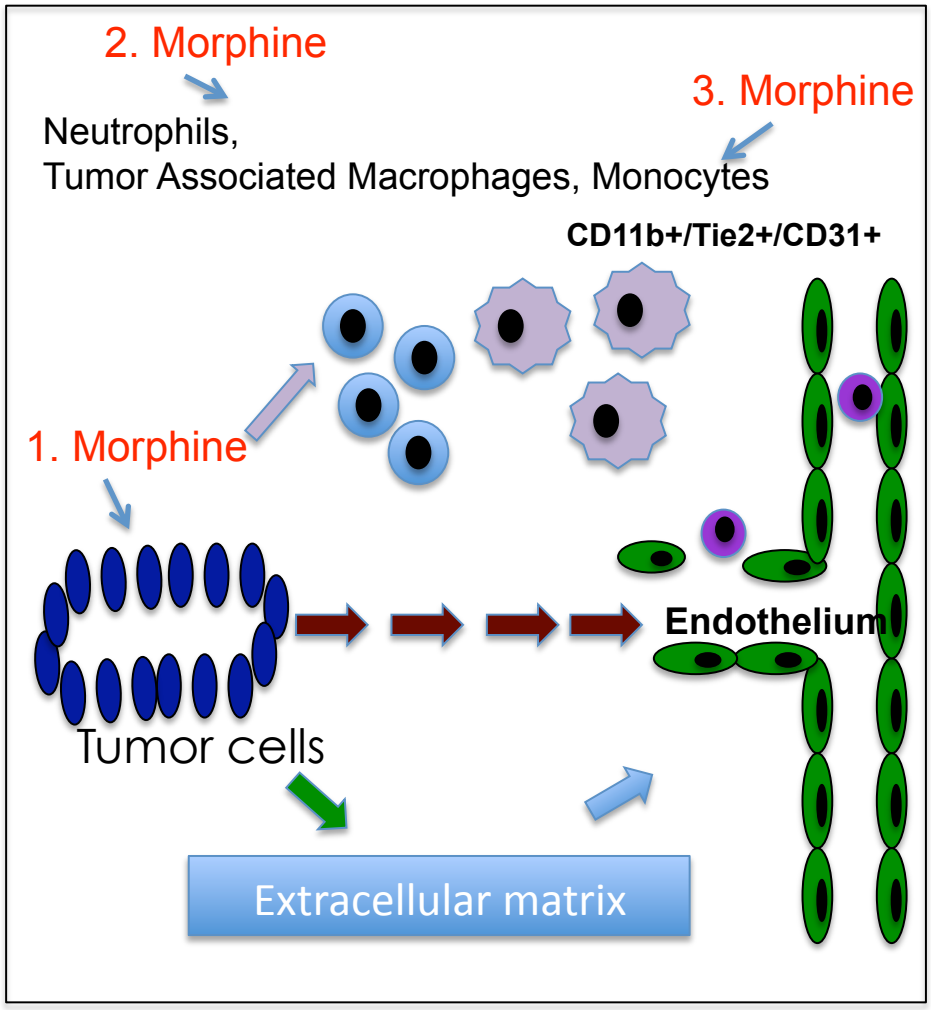
2. Morphine
3. Morphine
Neutrophils,
Tumor Associated Macrophages, Monocytes
CD11b+/Tie2+/CD31+
1. Morphine
Endothelium
Tumor cells
Extracellular matrix

Figure 32: Summary of results on the effects of morphine on tumor angiogenesis and growth

Morphine acted on hypoxic tumor cells to decrease proangiogenic factor secretion for angiogenesis. Morphine reduced leukocyte recruitment to conditioned tumor media and inhibited the chemotaxis of bone-marrow derived myeloid cells. Morphine treatment resulted in a concomitant decrease in neutrophil and monocyte migration to alter the differentiation of monocytes to tumor-promoting M2 macrophages and suppress the recruitment of Tie2+ EC progenitors that play a vital role in vessel formation. Taken together, morphine alters the host immune response to angiogenesis to decrease tumor growth

Conclusion

Given the prevalent use of morphine in cancer patients for pain management it is important to investigate the long-term use of morphine on tumor growth and progression. These studies have contributed to our current understanding of some of the essential elements contributing to tumor growth and progression. The balance between tumor growth and tumor cell death occurs through the development of angiogenesis and the action of pro- and anti-inflammatory cells. The exact mechanism by which tumor angiogenesis occurs has yet to be determined. Current evidence suggests in cases of both physiological and pathological angiogenesis, angiogenesis is partially dependent on the recruitment of endothelial stem-like progenitors from the bone marrow. Of equal importance to vessel formation and stabilization is the recruitment of peripheral blood monocytes, neutrophils and macrophages that further recruit inflammatory cells from spleen and bone marrow to support and maintain angiogenesis initiated by hypoxic cancer cells.

Taken together the investigations provided herein support the view that morphine acts on multiple mechanisms to inhibit tumor growth *in vivo* (**Figure 32**). Here we show that morphine inhibits the hypoxia-induced expression of proangiogenic factor, vascular endothelial growth factor from mouse lung and human ovarian cancer cells *in vitro*. Pathological examination of tumor tissues indicated that the effect of morphine treatment on VEGF was due to its ability to inhibit HIF-1 activation and gene regulation. *In vitro* studies further confirmed that morphine treatment resulted in a concomitant decrease in the hypoxic activation of p38 MAPK, and this inhibition of p38 MAPK under hypoxia prevented HIF-1alpha accumulation, and nuclear expression to reduce VEGF

transcription and secretion in lung and ovarian cancer cells. Additional *in vitro* studies assessing cell viability at concentrations used for pain management in vivo (~700ng/ml, 1.0uM MS) show that morphine does not produce any significant inhibitory effects at lower concentrations under normal conditions. However, at higher concentrations (>1mM) morphine directly reduced cell viability by over 50%. In our model, our method of morphine administration resulted in morphine blood serum levels at mean value of 300ng/ml (corresponds to approximately 2μM). Without, chronic treatment and at high doses, it may be very difficult to achieve blood levels above1mM *in vivo.* Since1.0μM morphine-sulfate was sufficient to inhibit VEGF *in vitro;* we concluded that morphine's inhibition of tumor growth is through affects on angiogenesis rather than through direct effects on the tumor cell apoptosis.

Morphine is highly immunosuppressive so we also investigated the effect of morphine on inflammatory cell migration and recruitment to the tumor microenvironment. Our data strongly supports the view that morphine suppresses the migration and recruitment of myeloid derived inflammatory cells towards a tumor-cell-derived chemotactic gradient reminiscent of the tumor microenvironment (**Figure 32).** These cells are the major contributors of angiogenesis in many disease states other than tumor growth. Angiogenesis is important in several physiological and pathological conditions, such as embryonic development and wound healing, diabetic retinopathy and rheumatoid arthritis to name a few. The studies presented herein support the use of morphine in cancer patients for pain management associated with cancer growth with little detrimental health consequence. In addition to its potent analgesic properties, morphine can act prevent solid tumor growth by suppressing angiogenesis through effects

on hypoxic tumor cells or inflammatory cell recruitment into the tumor microenvironment.

Literature Cited

Aherne, G.W., Piall, E.M., Twycross, R.G. (1979). Serum morphine concentration after oral administration of diamorphine hydrochloride and morphine sulphate. *Br J Clin Pharmacol*, 8, 577-80.

Balsubramanian, S., Ramakrishnan, S., Charboneau, R., Wang, J., Roy, S. (2001). Morphine sulfate inhibits hypoxia-induced vascular endothelial growth factor expression in endothelial cells and cardiac myocytes. *J Mol Cell Cardiol*, 33, 2179-87.

Bilton, R., Booker, G.W. (2003). The subtle side to hypoxia inducible factor (HIFα) regulation. *European Journal of Biochemistry.* 270 (5), 791 - 798.

Bingle, L., Brown, N.J., Lewis, C.E. (2002). The role of tumour-associated macrophages in tumour progression: implications for new anticancer therapies. *J Pathol.*, 196 (3), 254-65.

Blebea, J., Mazo, J.E., Kihara, T.K., Vu, J.H., McLaughlin, P.J., Atnip, R.G., Zagon, I.S. (2000). Opioid growth factor modulates angiogenesis. *J Vasc Surg*, 32, 364-73.

Bonnet, M.P., Beloeil, H., Benhamou, D., Mazoit, J.X., Asehnoune, K. (2009). The mu opioid receptor mediates morphine-induced tumor necrosis factor and interleukin-6 inhibition in toll-like receptor 2-stimulated monocytes. *Anesth Analg.* 106(4): 1142-9

Bosco, M.C., Puppo, M., Blengio, F., Fraone, T., Cappello, P., Giovarelli, M., Varesio, L. (2008). Monocytes and dendritic cells in a hypoxic environment: Spotlights on chemotaxis and migration. *Immunobiology* , 213 (9-10), 733-49.

Bosco, M.C., Puppo, M., Santangelo, C., Anfosso, L., Pfeffer, U., Fardin, P., Battaglia, F., Varesio, L. (2006). Hypoxia modifies the transcriptome of primary human monocytes: modulation of novel immune-related genes and identification of CC-chemokine ligand 20 as a new hypoxia-inducible gene. *J Immunology*, 177 (3), 1941-55.

Brancho, D., Tanaka, N., Jaeschke, A., Ventura J.J., Kelkar N., Tanaka Y., Kyuuma M., Takeshita, T., Flavell, R.A., Davis, R.J. (2003). Mechanism of p38 MAP kinase activation in vivo. *Genes Dev*., 17, 1969–1978.

Brekken, R.A, Thorpe, P.E. (2001). Vascular endothelial growth factor and vascular targeting of solid tumors. *Anticancer Res.*, 21 (6B), 4221-9.

Brooke, M.E., Leonidas, C.P., Black E. (2005). Mitochondrial reactive oxygen species activation of p38 mitogen-activated protein kinase is required for hypoxia signaling. *Mol Cell Biol*, 25 (12), 4853-62.

Cain, D.M., Wacnik, P.W., Eikmeier, L., Beitz, A., Wilcox, G., Simone, D. (2001). Functional Interactions Between Tumor and Peripheral Nerve in a Model of Cancer Pain in the Mouse. *Pain Medicine*, 2 (1), 15-23(9).

Cameron, I.L., Short, N., LuZhe Sun, and Hardman, W.E. (2005). Endothelial cell pseudopods and angiogenesis of breast cancer tumors. *Cancer Cell Int.*, 5, 17.

Chandel, N.S., McClintock, D.S., Feliciano, C.E. (2000). Oxygen Species Generated at Mitochondrial Complex III Stabilize Hypoxia-inducible Factor-1 during Hypoxia A mechanism of oxygen sensing. *J. Biol. Chem*, 275 (33), 25130-25138.

Conrad, P.W., Rust, R.T., Han J. (1999). Selective activation of p38alpha and p38gamma by hypoxia. *J Biol Chem*, 274, 23570-6.

Cotterell, S.E.J, Engwerda, C.R., Kaye, P.M. (2000). Enhanced Hematopoietic Activity Accompanies Parasite Expansion in the Spleen and Bone Marrow of Mice Infected with Leishmania donovani. *Infection and Immunity*, 68 (4), 1840-1848.

Cuenda, A., Rousseau, S. (2007). p38 MAPK-kinases pathway regulation, function and role in human diesease. *Biochimica et Biophysica Acta*, 1773, 1358-75.

D'Amore, P.A., Folkman, J., Patricia A. (1996). Blood Vessel Formation: What Is Its Molecular Basis? *Cell*, 87 (7), 1153-1155.

Dussault, A.A., Pouliot, M. (2006). Rapid and simple comparison of mRNA levels using real -time PCR. *Biol Proceed Online*, 8, 1-10.

Eguchi, Y., Shimizu, S., Tsujimoto, Y. (1997). Intracellular ATP levels determine cell death fate by apoptosis or necrosis. *Cancer Res.* 1835-40.

Eisenstein, T.K., Rahim, R.T., Feng, P., Thingalaya, N.K., Meissler, J.J. (2006). Effects of opioid tolerance and withdrawal on the immune system. . *J Neuroimmune Pharmacol*., 1 (3), 237-49.

Epstein, A.C., Gleadle, J.M., McNeill, L.A. (2001). C. elegans EGL-9 and mammalian homologs define a family of dioxygenases that regulate HIF by prolyl hydroxylation. *Cell,* 107, 43-54.

Eyers, P.A., Craxton, M., Morrice, N., Cohen, P., Goedert, M. (1998). Conversion of SB 203580-insensitive MAP kinase family members to drug-sensitive forms by a single amino-acid substitution. *Chem. Biol.,* 5, 321–328.

Ferrara N. (2004). Vascular Endothelial Growth Factor: Basic Science and Clinical Progress. *Endocrine Reviews*, 25 (4), 581-611.

Ferrara, N., Gerber, H.P., LeCouter, J. (2003). The biology of VEGF and its receptors. *Nature Medicine*, 9, 669-676.

Folkman, J., D'Amore, P.A., (1996). Blood vessel formation: what is its molecular basis? *Cell*, 87, 1153-5.

Folkman, J. (1971). Tumor angiogenesis: therapeutic implications. *New England Journal of Medicine*, 285, 1182-1186.

Forsythe, J.A., Jiang, B.H, Iyer, N.V. (1996). Activation of vascular endothelial growth factor gene transcription by hypoxia-inducible factor 1. *Mol Cell Biol,* 16, 4604-13.

Franchi, S., Panerai, A.E., Sacerdote, P. (2007). Buprenorphine ameliorates the effect of surgery on hypothalamus pituitary adrenal axis, natural killer cell activity and metastatic colonization in rats in comparison with morphine or fentanyl treatment. *Brain Behav Immun*, 21, 767-774.

Gardner, L.B., Corn, P.G. (2008). Hypoxic regulation of mRNA expression. *Cell Cycle*, 7 (13), 1916-24.

Gradin, K., Takasaki, C., Fujii-Kuriyama, Y., and Sogawa, K. (2002). The transcriptional activation function of the HIF-like factor requires phosphorylation at a conserved threonine. *J. Biol. Chem*., 277, 23508–23514.

Gum RJ, McLaughlin MM, Kumar S, Wang Z, Mower MJ, Lee JC, Adams JL, Livi GP, Goldsmith EJ, Young PR (1998). Acquisition of sensitivity of stress-activated protein kinases to the p38 inhibitor, SB 203580, by alteration of one or more amino acids within the ATP binding pocket. J. Biol. Chem. , 273, 15605–15610.

Gupta, K., Kshirsagar, S., Chang, L., Schwartz, R., Law, P.Y., Yee, D., Hebbel, R.P. (2002). Morphine stimulates angiogenesis by activating proangiogenic and survival-promoting signaling and promotes breast tumor growth. *Cancer Res*., 62 (15), 4491-8.

Hatsukari, I., Hitosugi, N., Dinda, A., Singhal, P.C. (2006) Morphine modulates monocyte-macrophage conversion phase. *Cell Immunol.* 239(1): 41-8.

Hicklin, D.J., Ellis, L.M. (2005). Role of the Vascular Endothelial Growth Factor Pathway in Tumor Growth and Angiogenesis . *Journal of Clinical Oncology,* 23 (5), 1011-1027.

Hirota, K., Semenza, G.L. (2005). Regulation of hypoxia-inducible factor 1 by prolyl and asparaginyl hydroxylases. *Biochem Biophys Res Commun*, 338, 610-6.

Hu, S., Sheng, W.S., Lokensgard, J.R. (2005). Morphine potentiates HIV-1 gp120-induced neuronal apoptosis. *J Infect Dis,* 191 (6), 886-9.

Kaluz, S., Kaluzová, M., Stanbridge, E.J. (2008). Does inhibition of degradation of hypoxia-inducible factor (HIF) alpha always lead to activation of HIF? Lessons learnt from the effect of proteasomal inhibition on HIF activity. *J Cell Biochem*., 104 (2), 536-44.

Kerber, M., Reiss, Y., Wickersheim, A., Jugold, M., Kiessling, F., Heil, M., Tchaikovski, V., Waltenberger, J., Shibuya, M., Plate, K.H., Machein, M.R. (2008). Flt-1 signaling in macrophages promotes glioma growth in vivo. *Cancer Res.*, 68 (18), 7342-51.

Khurana, A., Nakayama, K., Williams, S., Davis, R.J., Mustelin, T., Ronai, Z. (2006). Regulation of the ring finger E3 ligase Siah2 by p38 MAPK. *J Biol Chem.*, 281 (46), 35316-26.

Kulisz, A., Chen, N., Chandel, N.S., Shao, Z., Schumacker, P.T. (2002). Mitochondrial ROS initiate phosphorylation of p38 MAP kinase during hypoxia in cardiomyocytes. *Am J Physiol Lung Cell Mol Physiol*, 282, L1324-9.

Kuraishi, Y. (2001). Effects of morphine on cancer pain and tumor growth and metastasis. *Nippon Rinsho.,* Abstract 59 (9), 1669-74.

Laderoute, K.R., Mendonca, H.L., Calaoagan, J.M., Knapp, A.M., Giaccia, A.J., Stork, P.J. (1999) Mitogen-activated protein kinase phosphatase-1 (MKP-1) expression is

induced by low oxygen conditions found in solid tumor microenvironments. *J Biol Chem*, 2 (74), 12890-7.

Lam, C.F., Chang, P.J., Huang, Y.S., Sung, Y.H., Huang, C.C., Lin, M.W., Liu, Y.C., Tsai, Y.C. (2008). Prolonged use of high-dose morphine impairs angiogenesis and mobilization of endothelial progenitor cells in mice. *Anesth Analg*., 107 (2), 686-92.

Lamagna, C., Aurrand-Lions, M., Imhof, B.A. (2006). Dual role of macrophages in tumor growth and angiogenesis. *J Leukoc Biol*., 80 (4), 705-13.

Lee, T.H., Bolontrade, M.F., Worth, L.L., Guan, H., Ellis, L.M., Kleinerman, E.S. (2006). Production of VEGF165 by Ewing's sarcoma cells induces vasculogenesis and the incorporation of CD34+ stem cell into the expanding tumor vasculature. *Int J Cancer* , 119, 839–46.

Lewis, C.E., Palma, M.D., and Naldini, L. (2007). Tie2-Expressing Monocytes and Tumor Angiogenesis: Regulation by Hypoxia and Angiopoietin-2. *Cancer Research*, 67, 8429-8432.

Luger, N.M., Mach, D.B., Sevcik, M.A., Mantyh, P.W. (2005). Bone cancer pain: from model to mechanism to therapy. *J Pain Symptom Manage.*, 29 (5 Suppl), S32-46.

Mantovani, A. (1992). The origin and function of tumor associated macrophages. *Immunology Today*, 13, 265-270.

Martucci, C., Panerai, A.E., Sacerdote, P. (2004). Chronic fentanyl or buprenorphine infusion in the mouse: similar analgesic profile but different effects on immune responses. *Pain*, 110, 385-392.

Matsuo, Y., Ochi, N., Sawai, H., Yasuda, A., Takahashi, H., Funahashi, H., Takeyama, H., Tong, Z., Guha, S. (2009). CXCL8/IL-8 and CXCL12/SDF-1alpha co-operatively promote invasiveness and angiogenesis in pancreatic cancer. *Int J Cancer*., 124 (4), 853-61.

Maxwell, P.H., Wiesener, M.S., Chang, G.W., Clifford, S.C., Vaux, E.C., Cockman, M.E., Wykoff, C.C., Pugh, C.W., Maher, E.R., Ratcliffe, P.J. (1999). The tumour suppressor protein VHL targets hypoxia-inducible factors for oxygen-dependent proteolysis. *Nature*, 399 (6733), 271-5.

McCarthy, L., Wetzel, M., Sliker, J.K. (2001). Opioids, opioid receptors, and the immune response. *Drug Alcohol Depend*, 62, 111–123.

Micevych, P.E., Rissman, E.F., Gustafsson, J.A. (2003). Estrogen receptor-alpha is required for estrogen-induced mu-opioid receptor internalization. *J Neurosci Res*, 71, 802-10.

Minet, E., Arnould, T., Michel, G., Roland, I., Mottet, D., Raes, M., Remacle, J., Michiels, C. (2000). ERK activation upon hypoxia: involvement in HIF-1 activation. *FEBS Lett.*, 468, 53–5 .

Minet, E., Michel, G., Mottet, D. (2001). Transduction pathways involved in Hypoxia-Inducible Factor-1 phosphorylation and activation. *Free Radic Biol Med,* 31, 847-55.

Murdoch, C., Muthana, M., Coffelt, S.B., Lewis, C.E. (2008). The role of myeloid cells in the promotion of tumor angiogenesis. *Nature Reviews Cancer,* 8, 618.

Naldini, A., Carraro, F. (2005). Role of inflammatory mediators in angiogenesis. *Curr Drug Targets Inflamm Allergy,* 4 (1), 3-8.

Noonan, D.M., Barbaro, A.D.L., Vannini, N., Mortara, L., Albini, A. (2008). Inflammation, inflammtory cells and angiogenesis: decisions and indecisions. *Cancer Metastasis Review,* 27 (31), 40.

Nyberg, P., Salo, T., Kalluri, R. (2008). Tumor microenvironment and angiogenesis. *Front Biosci.*, 13, 6537-53.

Oztürk, T., Karadibak, K., Catal, D., Cakan, A., Tugsavul, F., Cirak, K. (2008). Comparison of TD-fentanyl with sustained-release morphine in the pain treatment of patients with lung cancer. *Agri.*, 20 (3), 20-5.

Palma, M.D., Venneri, M., Galli, R., Sergi, L., Politi, L., Sampaolesi, M., Naldini, L. (2005). Tie2 identifies a hematopoietic lineage of proangiogenic monocytes required for tumor vessel formation and a mesenchymal population of pericyte progenitors. *Cancer Cell*, 8 (3), 211-226.

Park JE, Barbul A. Understanding the role of immune regulation in wound healing. (2004) Am J Surg. 187(5A):11S-16S. Review.

Pasi, A., Qu, B.X., Steiner, R., Senn, H.J., Bär, W., Messiha, F.S. (1991). Angiogenesis: modulation with opioids. *Gen Pharmacol,* 22.

Pescador, N., Cuevas, Y., Naranjo, S., Alcaide, M., Villar, D., Landázuri, M.O., Del Peso, L. (2005). Identification of a functional hypoxia-responsive element that regulates the expression of the egl nine homologue 3 (egln3/phd3) gene. *Biochem J.*, 390 (Pt 1), 189-97.

Richard, D.E., Berra, E., Gothie, E., Roux, D., Pouyssegur, J. (1999) p42/p44 mitogen-activated protein kinases phosphorylate hypoxia-inducible factor 1α (HIF-1α) and enhance the transcriptional activity of HIF-1. *J. Biol. Chem.*, 274, 32631–32637 .

Rousseau, S., Dolado, I., Beardmore, V., Shpiro, N., Marquez, R., Nebreda, A.R., Arthur, J.S., Case, L.M., Tessier-Lavigne, M., Gaestel, M., Cuenda, A., Cohen, P. (2006).

CXCL12 and C5a trigger cell migration via a PAK1/2- p38alpha MAPK–MAPKAP-K2–HSP27 pathway. *Cell. Signal*, 18, 1897–1905.

Rousseau, S., Houle, F., Landry, J., Huot, J. (1997). p38 MAP kinase activation by vascular endothelial growth factor mediates actin reorganization and cell migration in human endothelial cells. *Oncogene,* 15, 2169–2177.

Roy S, Balasubramanian S, Wang J, Chandrashekhar Y, Charboneau R, Barke R. (2003). Morphine inhibits VEGF expression in myocardial ischemia. *Surgery*, 134, 336-44.

Roy, S., Wang, J.H., Balasubramanian, S., Sumandeep, M., Charboneau, R., Barke, R., Loh,

H.H. (2001). Role of hypothalamic-pituitary axis in morphine-induced alteration in thymic cell

distribution using mu-opioid receptor knockout mice. *J Neuroimmunol,* 116, 147-55.

Ryan, H.E., Lo, J., Johnson, R.S. (1998). HIF-1 is required for solid tumor formation and embryonic vascularization. *The EMBO Journal*, 17, 3005-15.

Sacerdote, P., Manfredi, B., Mantegazza, P., Panerai, A.E. (1997). Antinociceptive and immunosuppressive effects of opiate drugs: a structure-related activity study. *Br J Pharmacol*, 121, 834–840.

Sacerdote, P. (2008). Opioid-induced immunosuppression. *Curr Opin Support Palliat Care*, 2 (1), 14-18.

Sasamura, T., Nakamura, S., Iida, Y., Fujii, H., Murata, J., Saiki, I., Nojima, H., Kuraishi, Y. (2001). Morphine analgesia suppresses tumor growth and metastasis in a mouse model of cancer pain produced by orthotopic tumor inoculation. *Eur J Pharmacol*., 441 (3), 185-91.

Schneemilch, C.E., Schilling, T., Bank, U. (2004). Effects of general anaesthesia on inflammation. *Best Pract Res Clin Anaesthesiol*, 18, 493–507.

Seko, Y., Takahashi, N., Tobe, K. Kadowaki, T., Yazaki, Y. (1997). Hypoxia and hypoxia/reoxygenation activate p65PAK, p38 mitogen activated protein kinase (MAPK), and stress activated protein kinase (SAPK) in cultured rat cardiac myocytes. 239:840-4. *Biochem Biophys Res Commun*, 239, 840-4.

Semenza, G.L., Wang, G.L. (1992). A nuclear factor induced by hypoxia via de novo protein synthesis binds to the human erythropoietin gene enhancer at a site required for transcriptional activation. *Mol Cell Biol*, 12, 447–5454.

Semenza, G.L. (2002). HIF-1 and tumor progression: pathophysiology and therapeutics. *Trends Mol. Med.,* 8, S62–S67.

Shariftabrizi, A., Nifli, A.P., Ansari, M., Saadat, F., Ebrahimkhani, M.R., Alizadeh, N., Nasseh, A., Alexaki, V.I., Dehpour A.R., Castanas, E., Khorramizadeh, M.R. (2005). Matrix metalloproteinase 2 secretion in WEHI 164 fibrosarcoma cells is nitric oxide-related and modified by morphine. *Eur J Pharmacol.,* 530 (1-2), 33-9.

Shibuya, M. (2006). Differential roles of vascular endothelial growth factor receptor-1 and receptor-2 in angiogenesis. *J Biochem Mol Biol.,* 39 (5), 469-78.

Shojaei, F., Zhong, C., Wu, X., Yu, L., Ferrara, N. (2008). Role of meloid cells in tumor growth and angiogenesis. *Trends in Cell Biology*, 18 (8), 372.

Sica, A., Larghi, P., Mancino, A., Rubino, L., Porta, C., Totaro, M.G., Rimoldi, M., Biswas, S.K., Allavena, P., Mantovani, A. (2008). Macrophage polarization in tumour progression. *Semin Cancer Biol*., 18 (5), 349-55.

Singleton, P.A., Lingen, M.W., Fekete, M.J., Garcia, J.G., Moss, J. (2006). Methylnaltrexone inhibits opiate and VEGF-induced angiogenesis: role of receptor transactivation. *Microvasc Res.,* 72 (1-2), 3-11.

Sodhi, A., Montaner, S., Patel, V., Zohar, M., Bais, C., Mesri, E.A., Gutkind, J.S. (2000). The Kaposi's sarcoma-associated herpes virus G protein-coupled receptor up-regulates vascular endothelial growth factor expression and secretion through mitogen-activated

protein kinase and p38 pathways acting on hypoxia-inducible factor 1α. *Cancer Res.*, 60, 4873–4880.

Tegeder, I., Grösch, S., Schmidtko, A. (2003). G protein-independent G1 cell cycle block and apoptosis with morphine in adenocarcinoma cells: involvement of p53 phosphorylation. *Cancer Res*, 63, 1846-52.

Terasawa, M., Nagata, K., Kobayashi, Y. (2008). Neutrophils and monocytes transport tumor cell antigens from the peritoneal cavity to secondary lymphpoid tissues. *Biochemical and Bioresearch Communications,*12;377(2): 589-94.

Tiseo, P.J., Thaler, H.T., Lapin, J., Inturrisi, C.E., Portenoy, R.K. and Foley, K.M. (1995). Morphine-6-glucuronide concentrations and opioid-related side effects: a survey in cancer patients. 61(1), 47-54.

Vainer, B., Nielsen, O.H., Horn, T. (2000). Comparative studies of the colonic in situ expression of intercellular adhesion molecules (ICAM-1, -2, and -3), beta2 integrins (LFA-1, Mac-1, and p150,95), and PECAM-1 in ulcerative colitis and Crohn's disease. *Am J Surg Pathol.,* 24 (8), 1115-24.

Vaupel, P., Mayer, A., Höckel, M. (2006). Impact of Hemoglobin Levels on Tumor Oxygenation: the Higher, the Better? *Strahlentherapie und Onkologie,* Abstract, 182 (2), 63-71.

Venneri, M.A., De Palma, M., Ponzoni M., Pucci F., Scielzo C., Zonari E., Mazzieri R., Doglioni C., and Naldini, L. (2007). Identification of proangiogenic TIE2-expressing monocytes (TEMs) in human peripheral blood and cancer. *Blood*, 109 (12), 5276-5285.

Walsh, D., Perin, M.L. (2006). Parenteral Morphine Prescribing Patterns Among Inpatients With Pain From Advanced Cancer: A Prospective Survey of Intravenous and Subcutaneous Use. *Am. Jour. of Hospice and Palliative Medicine*, 23 (5), 353-359.

Walters, I. (2003). Opioids and immunosuppression: clinical relevance. *Der Anaesthetist*, 52:442–452 , 52, 442–452.

Weinert, C.R., Kethireddy, S., Roy, S. (2008). Opioids and infections in the intensive care unit should clinicians and patients be concerned? *J Neuroimmune Pharmacol.*, 3 (4), 218-29.

Wiffen, P.J, McQuay, H.J. (2007). Oral morphine for cancer pain. *Cochrane Database of Systematic Reviews* 2007 (3), 1-51.

Wild, R., Ramakrishnan, S., Sedgewick, J. (2000). Quantitative assessment of angiogenesis and tumor vessel architecture by computer-assisted digital image analysis:

effects of VEGF-toxin conjugate on tumor microvessel density. *Microvasc Res,* 59, 368-76.

World Health Organization. (1983). Cancer Pain Relief.

Xin, L., Qing, L., Wand, Y.J. (2007). Morphine inhibits doxorubicin-induced reactive oxygen species generation and nuclear factor-kappaB transcriptional activation in neuroblastoma SH-SY5Y cells. *Biochem J.*, 406 (2), 215-21 .

Yin, D., Woodruff, M., Zhang, Y., Whaley, S., Miao, J., Ferslew, K., Zhao, J., Stuart, C. (2006). Morphine promotes Jurkat cell apoptosis through pro-apoptotic FADD/P53 and anti-apoptotic PI3K/Akt/NF-kappaB pathways. *J Neuroimmunol*., 174 (1-2), 101-7.

Yokoyama, Y., Ramakrishnan, S. (2004). Improved biological activity of a mutant endostatin containing a single amino-acid substitution. *Experimental Therapeutics*, 90, 1627-35.